

MITIGATING THE EFFECT OF SOFT-LIMITING FOR OFDM PEAK REDUCTION

A THESIS SUBMITTED TO THE UNIVERSITY OF MANCHESTER
FOR THE DEGREE OF DOCTOR OF PHILOSOPHY
IN THE FACULTY OF ENGINEERING AND PHYSICAL SCIENCES

2014

By
Nargis Bibi
School of Computer Science

Contents

Abstract	11
Declaration	13
Copyright	14
Acknowledgements	15
1 Introduction	16
1.1 Motivation	18
1.2 Research Hypothesis	19
1.3 Aims and Objectives	19
1.4 Research Contribution	20
1.4.1 Inverted Wrap-Around (IWRAP) limiting	20
1.4.2 The Equation-Method	20
1.4.3 Equation-Method with AWGN	22
1.4.4 HARQ for Clipping	22
1.4.5 ‘HARQ for Clipping’ with the Equation-Method	22
1.5 Thesis Outline	22
2 Background and Related Work	24
2.1 WiMAX and LTE	24
2.2 Orthogonal Frequency Division Multiplexing (OFDM)	25
2.2.1 OFDM Transmitter	26
2.2.2 OFDM Receiver	27
2.3 Orthogonal Frequency Division Multiple Access (OFDMA)	28
2.3.1 Subcarrier Allocation Mode	28

2.4	Single Carrier-Frequency Division Multiple Access (SC-FDMA) . . .	29
2.4.1	IEEE 802.11 Standard Specifications for OFDM	31
2.5	Advantages of OFDM	32
2.5.1	Multipath Effects	32
2.5.2	Spectral Efficiency	33
2.6	Disadvantages of OFDM	33
2.7	Peak to Average Power Ratio (PAPR)	33
2.7.1	Distribution of PAPR	34
2.8	Factors affecting PAPR	35
2.8.1	Number of subcarriers	36
2.8.2	Modulation scheme	36
2.9	PAPR reduction Techniques	37
2.10	PAPR reduction with Distortion	38
2.10.1	Soft-clipping and Filtering	38
2.10.2	Companding	41
2.11	PAPR Reduction with Distortionless Techniques	41
2.11.1	Coding	41
2.11.2	Partial Transmit sequence (PTS)	43
2.11.3	Selected Mapping Scheme	44
2.11.4	Active Constellation Extension Technique	45
2.11.5	Interleaving	46
2.11.6	Tone reservation	47
2.11.7	Tone injection	47
2.12	Hybrid Automatic Repeat reQuest	47
2.12.1	HARQ Type I	48
2.12.2	HARQ Type II	48
2.12.3	HARQ Type III	48
2.13	Discussion	49
2.14	Conclusions	49
3	Iterative receivers based on statistics of memoryless distortion	51
3.1	Clipping	51
3.1.1	Clipping Nyquist sampled Signals	52
3.1.2	Clipping Oversampled Signals	54
3.1.3	Busgang theorem for memoryless non-linearities	55
3.1.4	Signal to Clipping noise ratio	56

3.2	Clipping noise mitigation techniques	57
3.2.1	Busgang Noise Cancellation Receiver (BNC)	57
3.2.2	Evaluation of BNC algorithm with different levels of AWGN .	59
3.2.3	Finding the best value of α	61
3.2.4	Decision Aided Reconstruction	64
3.2.5	Results and Discussion	66
3.3	Comparison of the BNC and DAR receivers	67
3.4	Inverted Wrap-Around (IWRAP) limiting	68
3.5	Evaluating Parameters for limiting	70
3.5.1	BER Analysis	70
3.5.2	Power Spectral Density (PSD)	71
3.5.3	PAPR Reduction and Peaks Re-growth	71
3.6	Conclusions	73
4	Equation-Method	75
4.1	Problem Formulation	75
4.1.1	Effect of Clipping on Constellation Symbols	76
4.1.2	Effect of clipping with no bit-error correction	78
4.2	The Equation-Method	80
4.2.1	Equal number of Equations and unknowns	82
4.2.2	Overdetermined number of equations	84
4.2.3	The Naive approach	86
4.2.4	Results and Discussion	87
4.2.5	Snapping Threshold Strategy	87
4.2.6	Results using Optimized Snapping Threshold	89
4.3	Dither and Recursion strategy	89
4.3.1	Dither	90
4.3.2	Recursion	91
4.3.3	Results	92
4.4	Selective Dither and recursion	93
4.4.1	Results and Discussion	94
4.4.2	Bit-error Probability for the Equation-Method	94
4.4.3	Equation-Method in comparison to other approaches	95
4.5	Conclusions	97

5	Equation-Method in additive white Gaussian noise (AWGN)	98
5.1	Analysis of Equation-Method with Noise	98
5.1.1	Effect of noise on Naive Method	100
5.1.2	Effect of noise on Snapping Threshold Method	103
5.1.3	Effect of noise on Dither and Recursion Method	105
5.1.4	Effect of noise on Selective Dither and Recursion Method	108
5.1.5	Conclusions for analysis of the methods with noise	110
5.2	Strategies for reducing the effect of AWGN on the Equation-Method	110
5.2.1	Margin Factor Threshold	111
5.2.2	MFT with naive method	113
5.2.3	Margin factor with ST method	114
5.2.4	Margin factor with Dither and Recursion Method	115
5.2.5	Margin factor with Selective Dither and Recursion	116
5.3	Conclusions	117
6	Hybrid ARQ for Clipping	118
6.1	HARQ	119
6.2	Performance of HARQ- Chase Combining	119
6.2.1	Chase Combining Algorithm	120
6.2.2	Errors due to AWGN	121
6.2.3	Errors due to Clipping	122
6.3	HARQ for Clipping	123
6.3.1	Soft Decisions	123
6.3.2	Combining to correct bit-errors caused by clipping	128
6.3.3	First Transmission:	128
6.3.4	Re-transmission	128
6.3.5	‘HARQ for Clipping’ Soft Combining	129
6.4	Simulation Results	130
6.5	‘HARQ for Clipping’ with the Equation-Method	131
6.6	Comparison to other approaches	133
6.7	Conclusions	134
7	Conclusions	136
7.1	Future Work	138
	Bibliography	140

A	Deriving non-linear distortion factor Alpha for limiting	148
A.1	Introduction	148
A.1.1	Alpha for Clipping	148
A.1.2	Alpha for IWRAP Limiting	152
B	Calculating output power of IWRAP limiter	154

List of Tables

2.1	Comparison of PAPR reduction techniques	50
3.1	Notations of clipping distortion factor used for tests	61
4.1	Estimate of Clipped Samples before Error-Correction	81
5.1	Simulation parameters for the experiments	100
6.1	Constellation mapping for 16-QAM	124

List of Figures

2.1	OFDM Transmitter	26
2.2	Cyclic Prefix	27
2.3	OFDM Receiver	28
2.4	Subcarrier distribution	29
2.5	Probability $PAPR > PAPR_0$ for OFDMA and SC-FDMA symbols . .	30
2.6	Probability that $PAPR > PAPR_o$ with different number of subcarriers	36
2.7	Maximum PAPR (dB) of an OFDM symbol against the number of subcarriers	37
2.8	Block diagram of an OFDM system with Clipping and Filtering . . .	38
2.9	Recursive clipping and filtering using bounded control, reproduced from [1]	39
2.10	Block Diagram of RBPR-SBS	42
2.11	Partial Transmit Sequences	43
2.12	Selected Mapping	45
2.13	Active constellation extension with 16-QAM mapping. The shaded regions represent the corner point extension areas whereas dotted arrows represent the extension paths for side points.	46
3.1	Clipping at Nyquist sampling	52
3.2	Clipping and filtering an oversampled signal	54
3.3	BNC Process	58
3.4	Comparison of BNC results	60
3.5	Probability of Bits in error using the three distortion factors	62
3.6	The difference of α_t and α_{te}	63
3.7	The difference of α_t and α_{bg}	64
3.8	BEP against SNR using all three distortion factors with the BNC receiver	65
3.9	DAR Process	65
3.10	Comparison of modified DAR with original DAR	67

3.11	DAR with multiple iterations	68
3.12	Comparison of DAR and BNC	69
3.13	Iwrap Limiting	69
3.14	BEP of clipped 16-QAM mapped OFDM signal in AWGN channel . .	71
3.15	IWRAP and soft-clipping with BNC	72
3.16	PSD for clipping and IWRAP	72
3.17	Probability of $PAPR > PAPR_o$ for soft-clipping and IWRAP limiting .	73
4.1	Decision boundaries for snapping	77
4.2	An example of constellation snapping	78
4.3	Distribution of N_{cs} with no symbol-error correction	79
4.4	OFDM symbol error probability without correction	80
4.5	Powers of the exponential function P for N=4	83
4.6	OFDM symbol error probability using Naive approach	88
4.7	Best Snapping thresholds against Clipping thresholds	89
4.8	OFDM symbol error probability using ST strategy	90
4.9	Symbol error Probability using Equation-Method with Dither and Re- cursion	93
4.10	Symbol error Probability using the Equation-Method with Selective Dither and Recursion	95
4.11	Bit error Probability using Equation-Method	96
4.12	Comparison of the Equation-Method with BNC	96
5.1	Bit-error Probability against SNR using Naive method Experiment 1 .	101
5.2	OFDM Bit-error Probability against SNR using Naive method Experi- ment 2	102
5.3	OFDM Bit-error Probability against SNR using ST method Experi- ment 1	104
5.4	OFDM Bit-error Probability against SNR using ST method Experi- ment 2	105
5.5	OFDM Bit-error Probability against SNR using Dither and Recursion method Experiment 1	106
5.6	OFDM Bit-error Probability against SNR using Dither and Recursion method Experiment 2	107
5.7	OFDM Bit-error Probability against SNR using Selective Dither and recursion method Experiment 1	108

5.8	OFDM Bit-error Probability against SNR using Selective Dither and recursion method Experiment 2	109
5.9	Margin Factor Threshold	111
5.10	MFT algorithm block diagram	112
5.11	OFDM Bit-error Probability against SNR using Naive method with MFT	113
5.12	OFDM Bit-error Probability against SNR using ST with MFT	114
5.13	OFDM Bit-error Probability against SNR using Dither & Recursion with MFT	115
5.14	OFDM Bit-error Probability against SNR using Selective Dither & Recursion with MFT	116
6.1	Chase Combining	120
6.2	OFDM Bit-error Probability against SNR using Combining without clipping	121
6.3	OFDM Bit-error Probability against SNR using Combining at $A = 0.40$	122
6.4	OFDM Bit-error Probability against SNR using Combining at $A = 0.60$	123
6.5	A Grey-coded 16-QAM Constellation	124
6.6	Decision regions for soft bits	126
6.7	OFDM Bit-error Probability against SNR using 'HARQ for Clipping' at $A=0.6$ and $A=0.40$	131
6.8	OFDM Bit-error Probability against SNR using 'HARQ for Clipping' with EM-Selective Dither at $A = 0.6$	132
6.9	Comparison of BEP for 'HARQ for Clipping' with/without Equation-Method (EM) with clipping at $A = 0.6$	133
6.10	Comparison of BEP for 'HARQ for Clipping' with the Equation-Method to BNC receiver, clipping at $A = 0.6$	134

Abstract

Digital communication systems which use Orthogonal Frequency Division Multiplexing (OFDM) are now widely used and have many advantages. The main disadvantage is the requirement for highly linear analogue electronics including the high power amplifier (HPA). This requirement cannot be met in all circumstances because of the occurrence of symbols with high peak to average power ratio (PAPR). Such symbols may be non-linearly distorted by limiting. Approaches to solve this problem have been either to reduce the PAPR at the transmitter or to try to mitigate the effect of the non-linearity at the receiver. Soft-limiting, i.e. applying limiting in software prior to the HPA is a simple way to reduce the PAPR. It produces non-linear distortion which will cause an increase in the bit-error-rate (BER) at the receiver. This thesis surveys existing alternatives ways of reducing the effect of non-linearity and proposes some new ones. Two iterative receiver techniques, based on statistical analysis of the nature of the non-linearity, have been implemented and investigated. These are the ‘Busgang Noise Cancellation’ (BNC) technique and the ‘Decision Aided Reconstruction’ (DAR) techniques. As these techniques are valid for any memory-less nonlinearity, an alternative form of limiting, named as Inverted-Wraparound (IWRAP) has been included in the BNC investigation.

A new method is proposed which is capable of correcting the received time-domain samples that are clipped, once they have been identified. This is named the ‘Equation-Method’ and it works by identifying constellation symbols that are likely to be correct at the receiver. If there are a sufficient number of these and they are correctly identified, the FFT may be partitioned to produce a set of equations that may be solved for the clipped time-domain samples. The thesis proposes four enhancements to this new method which improve its effectiveness. It is shown that the best form of this method outperforms conventional techniques especially for severe clipping levels. The performance of these four enhancements is evaluated over channels with additive white Gaussian noise (AWGN) in addition to clipping distortion. A technique based on a ‘margin factor’ is designed to make these methods work more effectively in the presence of AWGN noise. A new combining algorithm referred as ‘HARQ for Clipping’ is presented where soft bit decisions are combined from multiple transmissions. ‘HARQ for Clipping’ has been combined with the best version of the Equation-Method, and the performance of this approach is evaluated in terms of the BER with different levels of AWGN. It has been compared to other approaches from the literature and was

found to out-perform the BNC iterative receiver by 3dB at signal to noise ratios around 10dB. Without HARQ, the best version of the Equation-Method performs better than the BNC receiver, at signal-to-noise ratios above about 17dB.

Declaration

No portion of the work referred to in this thesis has been submitted in support of an application for another degree or qualification of this or any other university or other institute of learning.

Copyright

- i. The author of this thesis (including any appendices and/or schedules to this thesis) owns certain copyright or related rights in it (the “Copyright”) and s/he has given The University of Manchester certain rights to use such Copyright, including for administrative purposes.
- ii. Copies of this thesis, either in full or in extracts and whether in hard or electronic copy, may be made **only** in accordance with the Copyright, Designs and Patents Act 1988 (as amended) and regulations issued under it or, where appropriate, in accordance with licensing agreements which the University has from time to time. This page must form part of any such copies made.
- iii. The ownership of certain Copyright, patents, designs, trade marks and other intellectual property (the “Intellectual Property”) and any reproductions of copyright works in the thesis, for example graphs and tables (“Reproductions”), which may be described in this thesis, may not be owned by the author and may be owned by third parties. Such Intellectual Property and Reproductions cannot and must not be made available for use without the prior written permission of the owner(s) of the relevant Intellectual Property and/or Reproductions.
- iv. Further information on the conditions under which disclosure, publication and commercialisation of this thesis, the Copyright and any Intellectual Property and/or Reproductions described in it may take place is available in the University IP Policy (see <http://documents.manchester.ac.uk/DocuInfo.aspx?DocID=487>), in any relevant Thesis restriction declarations deposited in the University Library, The University Library’s regulations (see <http://www.manchester.ac.uk/library/aboutus/regulations>) and in The University’s policy on presentation of Theses

Acknowledgements

In the name of Almighty Allah who gave me courage and blessed me to complete the research work presented in this thesis.

I want to thank my parent university 'Fatima Jinnah Women University, Pakistan' for awarding me PhD scholarship and giving me opportunity to study at such pretigious institute.

This thesis would not have been possible without my supervisor Barry Cheetham's continuous support, kind attention and able advice throughout the research period.

I would like to say thanks to Nick Filer for his kind support and encouragement at every stage of my research.

I will extend my gratitude to Anthony Kleerekoper for his valuable ideas and suggestions related to my research work.

Thanks to my advisor Prof. Jim Miles for his guidance and support throughout my PhD.

I am very thankful to all my colleagues and friends in IT301 who always gave me the best moments to enjoy and work.

Thanks to my dear husband for his great understanding, continuous support, love and encouragement.

I would love to say thanks to my lovely and caring son, Hamza, who always prayed for me, cheered me up at times of sadness, loved me unconditionally, encouraged me like elders and always made me proud of himself.

I would like to say thanks to my parents for their utmost love and care, without them I would not be what I am now.

My sincere thanks to my dear brothers and loving sisters, and whole family who always prayed and encouraged me.

My sincere thanks to Mr. & Mrs. Irfan Nawaz, Shamaila, Aameena and Saima for their moral support and help during our stay in Manchester.

Chapter 1

Introduction

The rapid evolution of wireless communications systems has increased the demand for efficient broadband service on mobile devices with high data rates and better quality of service.

The next mobile communication system with high data rate transmission, fourth generation (4G) is expected to satisfy the increasing demand of users for wireless broadband service. New 4G mobile telephony uses Orthogonal Frequency Division Multiplexing (OFDM) on its physical layer.

OFDM has significant advantages over conventional single carrier modulation techniques that make it the desired modulation technique for all future wireless communication systems. OFDM splits a high rate single carrier into multiple lower rate narrowband subcarriers. Over the time-window of each OFDM symbol, all these subcarriers are orthogonal to each other so they can transmit and receive data simultaneously without interference. The idea has been taken from frequency division multiplexing in which there are guard intervals in between the subcarriers to avoid interference. In OFDM, because of the orthogonality there is no need to add guard intervals between carrier frequencies. The orthogonality eliminates inter sub-carrier interference (ICI) and is achieved by the power of digital signal processing (DSP) techniques, in particular, by the use of the fast Fourier transform (FFT) and its inverse.

The transmitted signal reflects off numerous objects before being received, which causes multiple delayed copies of the same signal to arrive at the receiver. This can result in inter symbol interference (ISI) due to multipath delay spread. Achieving high data rates in wireless networks using single carrier modulation is limited by multipath delay spread. OFDM overcomes this problem in a very efficient way with the use of a cyclic prefix. Dividing the carrier into multiple carriers increases the OFDM symbol

duration. This, along with the addition of a cyclic prefix, reduces the effect of multipath delay spread.

All the subcarriers are modulated by conventional single carrier modulation techniques such as Binary Phase Shift Keying (BPSK), Quadrature Phase Shift Keying (QPSK) and Quadrature Amplitude Modulation (QAM). The Inverse-FFT achieves the multicarrier modulation at the transmitter in a highly elegant and efficient way. These modulated subcarriers are summed up by using the IFFT and then transmitted on the channel. At the receiver side an FFT is applied to get back the modulated subcarriers.

OFDM has been deployed successfully in Digital Audio Broadcasting (DAB), Digital Video Broadcasting (DVB), IEEE 802.11 Wifi, IEEE 802.16 WiMAX and 3GPP Long term Evolution (LTE). OFDM allows only one user at a certain time to transmit and receive on all the subcarriers. In order to accommodate multiple users, OFDM is extended to Orthogonal Frequency Division Multiple Access (OFDMA). OFDMA is a multi-user and multi-carrier modulation technique which is used in 4G mobile telephony. It distributes sub-carriers among several users so that they can share one channel to transmit and receive simultaneously. Each user is allocated a subset of subcarriers to use at a certain time. OFDMA inherits all the advantages and disadvantages of OFDM.

OFDM is the key transmission technology for the most recently evolved 4G mobile systems [2, 3]. LTE uses OFDMA on its downlink physical layer and a new modulation technique called Single Carrier Frequency Division Multiple Access (SC-FDMA) for its uplink transmissions. The SC-FDMA scheme combines the lower peak to average power ratio (PAPR) characteristics of single carrier systems along with the frequency-domain equalization from OFDM systems. SC-FDMA is also called DFT-spread OFDMA, because time-domain data symbols are converted to the frequency-domain by applying a DFT before the OFDMA modulation.

SC-FDMA has lower PAPR values as compared to the OFDM and OFDMA modulation schemes, which is very important for mobile terminals [4]. However, the PAPR of SC-FDMA increases after pulse shape filtering at the transmitter, which makes PAPR still a problem for SC-FDMA. There is some work in the literature for reducing the PAPR by designing efficient pulse shaping filters [5]. SC-FDMA is not being proposed for downlink transmissions with LTE because of the extra computation involved [6]. The effects of high PAPR are not as serious a problem for a base-station as for battery powered mobiles.

1.1 Motivation

Despite all its advantages, OFDM and its variations have the major drawback of having a non-constant signal envelope with high peak to average power ratios (PAPR). The high peaks can produce serious in-band nonlinear distortion when applied to a High Power Amplifier (HPA) with non-linearities. A highly linear amplifier with a wide dynamic range must be used to minimize distortion. Linear amplifiers may be effectively used at the base-station, where power consumption is not a serious issue. However for user equipment this is likely to make inefficient use of the limited battery power of mobile devices [7].

Many approaches have been proposed to reduce high PAPR levels or mitigating non-linear distortion such as soft-clipping [8, 9, 10], coding [11, 12], partial transmit sequences [13, 14], selected mapping [15, 16] and Active Constellation Extension (ACE) [17]. A simple way of reducing the PAPR is to limit the high amplitude peaks of a signal before it is passed to the HPA. This soft-limiting introduces out-of-band and in-band distortions in the signal resulting in an increase in the bit error rate (BER).

Transmitting packets on wireless networks is very expensive in terms of energy and bandwidth. Therefore, Forward Error Correction (FEC) codes are used as an error control mechanism, which avoids frequent ARQ retransmissions. FEC adds extra redundant bits at the transmitter side so that, at the receiver, error bits can sometimes be corrected. A combination of FEC and ARQ is often called Hybrid ARQ (HARQ). Other forms of HARQ enable the receiver to recover from bit-errors by storing corrupted packets at the receiver rather than discarding them. It can make a good packet from a combination of bad ones in the case where retransmitted packets have errors. LTE and WiMAX use HARQ on their Medium access control (MAC) layer for retransmissions.

This project is motivated by the BER control problem in 4G mobile telephony particularly for WiMAX which uses OFDMA as the modulation technique for both uplink and downlink. The bit-errors caused by soft-limiting performed to eliminate the possibilities of amplifier non-linearities, can be differentiated from those produced by additive white Gaussian channel noise (AWGN).

This research will focus on the effects of non-linear distortion produced for OFDM symbols having high PAPR with deliberate clipping. A method of correcting the bit-errors that result from the distorted signal will be presented.

1.2 Research Hypothesis

The research hypothesis of this project is that the bit-errors that occur due to the soft-limiting of the high peaks of OFDMA symbols can be controlled more efficiently, than by conventional methods which treat limiting errors and channel noise errors all in the same way.

1.3 Aims and Objectives

The aim of this research is to efficiently control the bit-errors that are caused by non-linear distortion in OFDM systems. Soft-limiting (e.g. clipping performed in software) is used as the PAPR reduction technique at the transmitter. More specifically, the objectives are:

1. To observe and analyze the effects of soft-limiting on BER at different levels of clipping threshold.
2. To analyze the effects of soft-limiting on received frequency-domain symbols.
3. To analyze the effect of soft-limiting on the BER obtained with OFDM transmissions, and to explore two possible approaches for mitigating the effect of this ‘memory-less’ non-linear distortion. The approaches are the ‘decision aided reconstruction’ (DAR) method and the ‘Busgang noise cancellation’ (BNC) receiver.
4. To formulate a methodology for recognizing the clipped time-domain samples at the receiver, and then for using the non-clipped time-domain samples and the resulting frequency-domain symbols to correct the clipped time-domain samples, thus eliminating the effect of the clipping. This methodology will be referred to as the ‘Equation Method’. It will first be formulated for a noise-free channel, and then modified to cater for the effect of additive white Gaussian noise (AWGN).
5. To evaluate the Equation Method as a way of reducing the BER of OFDM transmissions over a range of operating conditions, and to refine the method by introducing a number of improvements.
6. To design and implement a set of methods using hybrid ARQ (HARQ) combining strategies in order to try to further mitigate the effect of the limiting distortion.

7. To analyze the combined effect of the Equation Method and the new form of HARQ over a range of channel conditions and AWGN levels. This effect is to be compared with results in the literature.

1.4 Research Contribution

In spite of much research towards PAPR reduction of OFDM systems, until now no definitive solution has been proposed. Some of the approaches are too heavy in terms of computational complexity to adapt for mobile devices. Telecommunication companies are still looking for some better solution in terms of complexity, BER and power consumption. The areas outlined in the following sections were made the focus of this research.

1.4.1 Inverted Wrap-Around (IWRAP) limiting

This technique is similar to the wrap-around mechanism that occurs naturally with non-saturation mode fixed point digital arithmetic, where samples which exceed the allowed threshold are not hard limited, but instead wrap around to samples of the opposite sign. Instead of discarding the high peaks as occurs in conventional clipping (hard limiting or saturation), the high peaks will be, in a sense, preserved. The advantages and disadvantages of using IWRAP in place of conventional soft-clipping are explored and evaluated.

1.4.2 The Equation-Method

With knowledge of clipping levels at the transmitter, it will be seen that a new method, known as the Equation-Method can generate an unclipped form of the received clipped signal, from ‘reliable’ constellation symbols, which are those that are received correctly after quantisation. A big problem is to identify ‘reliable’ constellation symbols at the receiver. To address this problem, we have invented four approaches which are as follows:

Naive Approach

This is a simple approach for which all the received constellation symbols are taken as ‘reliable’ even if they are not. This makes number of equations that must be solved

for all transmitted OFDM symbols equal to the number of subcarriers. This approach works well in low distortion because the majority of the received constellation symbols are correctly received and they dominate the effect of those which are wrongly received.

Snapping Threshold Strategy

With this strategy, the constellation symbols which move least during the quantisation or ‘snapping’ process are taken as reliable. The snapping process is where received frequency-domain symbols are quantized to the defined constellation points. e.g, those for 16-QAM or 64-QAM. A new snapping threshold (ST) term is defined and symbols which move less than the ST are considered as ‘reliable’. This strategy improves the results obtained from the naive approach and performs better even at severe clipping thresholds.

Dither and Recursion

This technique introduces a mirror of the receiver at the transmitter to allow feedback. The mirrored receiver can identify which constellation symbols are likely to be reliable at the real receiver and which of them will be correctly identified. It introduces ‘dither’ which makes small randomized changes in the original constellation symbols. It tries to make the Snapping Threshold method work better by modifying the original input symbols slightly. If these original symbols are not exactly on the constellation points, it does not matter because they will be snapped to the constellation points at the receiver. Various examples of dither are tried and the mirrored receiver is used to test the effectiveness of each example. Eventually, the most effective dither is applied to the transmission.

Selective Dither and Recursion

This technique reduces the overhead of applying dither to all the constellation symbols and selects only those constellation symbols which have been wrongly chosen as reliable by the mirrored receiver in the first iteration. This is an iterative process and it runs for a finite number of iterations to try to find the best dither. The receiver uses a certain snapping threshold to decide the reliability of the received constellation symbols.

1.4.3 Equation-Method with AWGN

Being affected by clipping, the received signal will also be affected by AWGN. This noise will effect the decisions as to which time-domain samples have been clipped and also the snapped constellation symbols. Its effect will also cause the behavior of the mirrored receiver at the transmitter to differ from that of the real receiver. Ways of dealing with these problems are presented in this thesis.

1.4.4 HARQ for Clipping

This technique is appropriate to the use of multiple re-transmissions of packets that are received in error. If each transmission is identical, clipping noise will remain the same in every retransmission. In traditional ARQ incorrect packets are simply discarded whereas, with more advanced forms of HARQ, damaged packets are combined to produce a good packet. We have investigated a way of changing the re-transmissions in such a way that the effect of the soft-clipping is different for each transmission and re-transmission. We have used soft bit decisions for the received bits to combine multiple transmsions. The technique is referred as ‘HARQ for Clipping’. The performance of the proposed system has been evaluated in the presence of the AWGN.

1.4.5 ‘HARQ for Clipping’ with the Equation-Method

‘HARQ for Clipping’ may be combined with the best version of the Equation-Method i.e. Selective Dither and Recursion. In all the re-transmissions, the OFDM symbols go through the Selective Dither and Recursion process at the transmitter. The receiver uses the Equation-Method at the receiver to try to find the true values of the clipped samples. The multiple re-transmissions are soft-combined at bit-level. The BER significantly decreases when using both these methods in combination.

1.5 Thesis Outline

Chapter 2 explains the main structure of OFDM and its adaptation to OFDMA and SC-FDMA. It considers the likely statistical distribution of PAPR values over many transmitted OFDM symbols, and also the factors that affect this distribution. It discusses the most prominent and recent PAPR reduction techniques that have been published in the research literature.

Chapter 3 further examines the effects of soft-limiting when applied to base-band OFDM signals. It considers two cases: (a) where the limiting is applied directly at the normal sampling frequency and (b) where the limiting is applied to an over-sampled version of the OFDM signal which allows some of the higher frequency ‘out-of band’ components of the distortion to be filtered out before it becomes in-band (aliased) distortion. This chapter also discusses two iterative receivers for mitigating the ‘memory-less’ effects of clipping distortion. These are the ‘decision aided reconstruction’ (DAR) method and the Busgang noise cancellation (BNC) receiver. Both receivers are simulated in MATLAB. The performances of these receivers are evaluated and discussed in terms of bit-error probability. A new form of limiting is presented in this chapter which may be combined with other techniques to reduce the distortion it produces to the signal.

Chapter 4 presents the Equation-Method, which works with soft-clipping at the transmitter. It explores many different aspects of the proposed method and four strategies for improving its performance. Results are presented showing the effect of the various forms of the Equation-Method on the OFDM symbol error probability and bit-error probability.

Chapter 5 extends the Equation-Method to channels affected by various degrees of AWGN. The effect of the AWGN on the clipping decisions and the reliability of the frequency-domain symbols have been investigated through experiments. A new ‘margin factor threshold’ method is introduced for dealing with the effects of AWGN on the Equation Method. BER estimates, obtained using MATLAB simulations, are presented for different levels of AWGN for each version of the Equation-Method.

Chapter 6 presents a new way using Hybrid ARQ to mitigate the effects of clipping and AWGN at the receiver. HARQ is designed to work with AWGN but it can be adapted to soft-clipping. A new algorithm is designed using multiple re-transmissions and soft-combining at the receiver referred as ‘HARQ for Clipping’. The Selective Dither and Recursion strategy of the Equation-Method is combined with the ‘HARQ for Clipping’.

Chapter 7 gives an overview of this research along with the other possibilities to be explored in respect to the proposed methods.

Chapter 2

Background and Related Work

Mobile phone history is divided into generations to mark the technology change over time. The first generation (1G) radio systems used analogue cellular systems like Advanced Mobile Phone Service (AMPS) and the Nordic Mobile Telephone (NMT) system. The second generation (2G) mobile phone systems started using digital communications systems such as Global Systems for Mobile Communications (GSM), digital-AMPS, Time Division Multiple Access (TDMA) and Code Division Multiple Access (CDMA). The third generation (3G) mobile systems used three major air interfaces, Wideband CDMA (WCDMA), CDMA2000 and Time Division Synchronous (TD-SCDMA) [18]. WiMax IEEE 806.16e, DAB, DVB-T are some of the new emerging standards that use OFDM. The basic principle and function of OFDM, OFDMA and SC-FDMA has been explained. This chapter gives background and details of related work to PAPR reduction and mitigation techniques. HARQ strategies are also discussed.

2.1 WiMAX and LTE

Two technologies are competing for future adoption by mobile companies. WiMAX standardized by IEEE, was first developed to give broadband access to stationary devices and later enhanced for mobile devices. The other emerging technology is Long Term Evolution (LTE) standardized by the Third Generation Partnership Project (3GPP). WiMAX and LTE both use OFDMA for transmission from base station (BS) to mobile station (MS). For uplink transmission, WiMAX uses OFDMA whereas LTE

uses Single Carrier-FDMA (SC-FDMA) [6]. SC-FDMA, having single carrier characteristics, has low PAPR as compared to OFDMA but at the cost of increased computational complexity at the mobile and base station [6]. OFDM, OFDMA and SC-FDMA are explained below.

2.2 Orthogonal Frequency Division Multiplexing (OFDM)

OFDM is an example of a hybrid multiplexing technique which combines TDMA and frequency division multiple access (FDMA). TDMA is a medium access method in which each user is allocated a time slot in the spectrum to send and receive.

OFDM splits a high rate single carrier into multiple lower rate narrow spaced subcarriers. For each OFDM symbol, these multiple subcarriers are time limited by the duration of the symbol and are made orthogonal to each other over this duration.

An OFDM symbol is a sum of N time-windowed subcarriers which are modulated with data in the frequency-domain. The frequencies of the N subcarriers over a bandwidth of B Hz are separated by a $\Delta f = B/N$ Hz spacing. The continuous-time base-band representation for an OFDM symbol of duration T with N subcarriers is written as:

$$x(t) = \sum_{k=0}^{N-1} X_k e^{j \frac{2\pi k \Delta f t}{T}} \quad 0 \leq t < T \quad (2.1)$$

where $T = 1/\Delta f$ is the symbol period and X_k are the complex constellation symbols drawn from a known finite constellation, e.g. QPSK or 16-QAM.

In practice, the base-band modulation is done in the digital domain. The discrete-time representation for the OFDM symbol can be obtained by sampling the continuous signal as represented in Equation 2.1. For $\Delta f = 1/T$, if $x(t)$ is sampled at $t = T/N$, then Equation 2.1 becomes as follows:

$$x(n) = \sum_{k=0}^{N-1} X_k e^{j \frac{2\pi k n}{N}} \quad 0 \leq n < N-1 \quad (2.2)$$

where n indexes discrete sampling points. In this representation the real and imaginary parts of the signal will correspond to the in-phase and quadrature components of the OFDM signal when it is modulated onto its high frequency carrier. The N subcarriers are required to be orthogonal, when they are time-windowed to a duration T seconds. It can be arranged that the peak of each subcarrier in the frequency-domain coincides

with the zero-crossings of all the other time-windowed subcarriers. This is called the orthogonality condition and it may be achieved by keeping the adjacent subcarriers $1/T$ Hz apart. In order to avoid inter-symbol interference, OFDM time-domain symbols are augmented with a cyclic prefix (CP). The length of the CP is decided in such a way that it is greater than or equal to the maximum anticipated delay spread of the channel response.

OFDM is implemented using an Inverse fast Fourier transform (IFFT) at the transmitter and a fast Fourier transform (FFT) at the receiver.

2.2.1 OFDM Transmitter

Figure 2.1 is a block diagram of an OFDM transmitter. The input bit-stream is sent to the constellation mapping which feeds an IFFT with N complex symbols. The bit-stream is modulated onto each subcarrier using an appropriate modulation scheme such as PSK or M-QAM. The IFFT of these N complex symbols is used to create the base-band discrete-time OFDM symbol. Next the symbol is extended in time by the cyclic prefix. For the cyclic prefix, the last part of each OFDM symbol is copied at the start of the symbol. Figure 2.2 illustrates the introduction of a cyclic prefix.

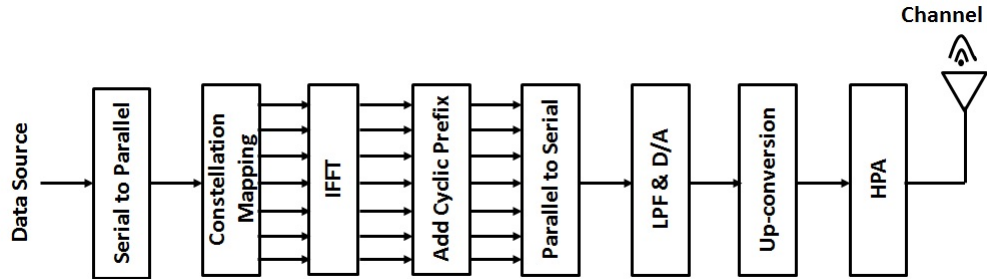


Figure 2.1: OFDM Transmitter

Next the base-band symbol is up-sampled and used to modulate a high frequency carrier with frequency f_c . The real and imaginary parts of each OFDM symbol have to be multiplied by the cosine and sine of the desired carrier frequency, and the real part is taken to get a segment of final OFDM signal. The process is repeated for successive OFDM symbols.

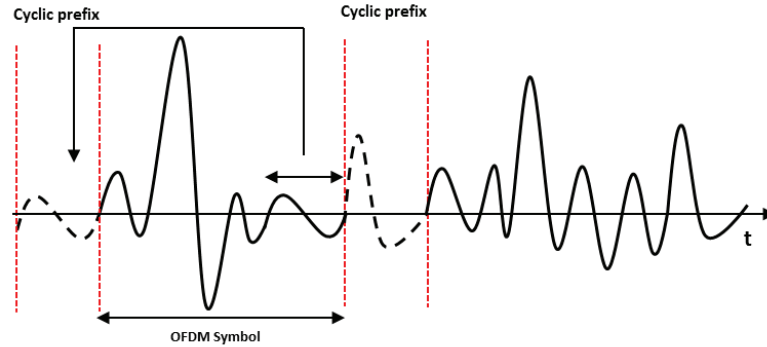


Figure 2.2: Cyclic Prefix

2.2.2 OFDM Receiver

At the receiver, the in-phase and quadrature components of the received signal are coherently detected and down-converted from the channel. A complex valued LPF is applied to eliminate out of band components. The received symbols are converted to a parallel stream and the CP is removed from each OFDM symbol. An FFT is applied to convert the time-domain samples to frequency-domain constellation symbols. Frequency selective fading due to multipath propagation introduced by the channel may be removed by applying an equalizer to the output of the FFT. The received bits are demapped from the constellation and converted to a serial bit-stream.

For each symbol the OFDM subcarriers are used in three ways: as data carriers, pilot carriers or null carriers. Pilot carriers are to provide channel estimation and synchronization information. There will be differences between the frequencies and phases of local oscillators at the transmitter and the receiver. These frequency offsets can destroy the orthogonality of subcarriers. Using some of the narrowband subcarriers as pilot carriers can solve this problem by helping receivers to generate a closely matched frequency reference to that of the transmitter. Null subcarriers are placed at the edges of the allotted bandwidth and are unmodulated to avoid leakage to adjacent channels. Data carriers are modulated by QPSK or some form of QAM to convey the required bit-stream.

OFDM allows only one user at a time to use all the subcarriers. There is an enhanced version of OFDM which gives access to multiple users. It is called Orthogonal Frequency Division Multiple Access (OFDMA).

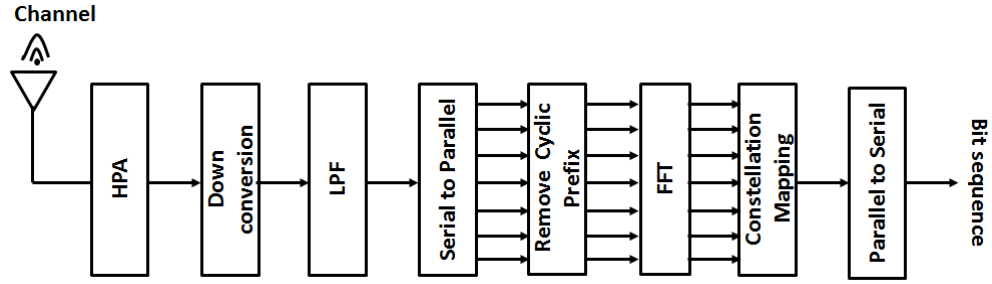


Figure 2.3: OFDM Receiver

2.3 Orthogonal Frequency Division Multiple Access (OFDMA)

OFDMA is a multiple access multiplexing scheme which can provide a multiplexing operation of data streams from multiple users for downlink and uplink data transmissions. It allows multiple users access to the channel at the same time. It distributes the subcarriers into subsets. Each subset is called a sub-channel. These sub-channels are allocated to users according to their requirements. In this way it works like FDMA. However, OFDMA avoids the guard bands that are necessary in FDMA to separate different user streams.

A user close to the base-station would normally be assigned a large number of subcarriers with a high capacity modulation scheme such as 64-QAM (quadrature amplitude modulation) to deliver a high data throughput for that user. Users farther away are dynamically assigned to fewer subcarriers. However, the power allotted to each sub-channel is raised. The modulation scheme may change from 16-QAM to Quaternary Phase Shift Keying (QPSK) and even binary phase shift keying (BPSK) at longer ranges. The data throughput drops as the channel capacity and modulation change, but the link maintains its strength.

OFDMA supports Time Division Duplexing (TDD) and Frequency Division Duplexing (FDD) [19]. In FDD, the uplink and downlink frames are transmitted simultaneously on different carrier frequencies, while in TDD uplink and downlink frames are transmitted using the same carrier frequency at different times.

2.3.1 Subcarrier Allocation Mode

An OFDMA symbol can be divided into several sub-channels by grouping its subcarriers. There are two traditional methods for subcarrier allocation in OFDMA: interleaved

and localized subcarrier allocation. For localized distribution, a sub-channel is formed by assigning a contiguous set of subcarriers. In interleaved, the subcarriers of each user are uniformly spaced over the bandwidth of the signal at a uniform distance from each other. The current trend of OFDMA favors a more flexible scheme in which users can select their best subcarriers, which is called random distribution. Figure 2.4 shows an example of subcarrier distributions for four users.

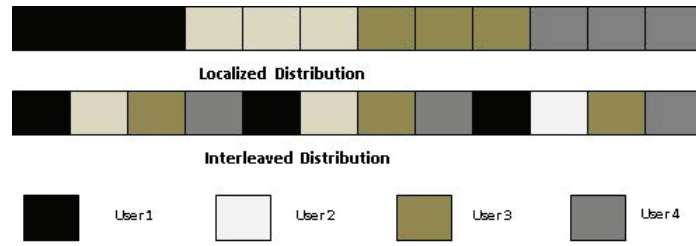


Figure 2.4: Subcarrier distribution

2.4 Single Carrier-Frequency Division Multiple Access (SC-FDMA)

SC-FDMA systems are also called DFT-spread OFDMA systems because time-domain symbols are transformed into the frequency-domain by applying a DFT before the OFDMA modulation. At the transmitter side, bit-mapping to the complex symbols is done in the time-domain. A SC-FDMA transmitter first groups N constellation symbols and applies a N -point DFT on them to produce a frequency-domain representation of the input symbols. Then each of the outputs of the DFT is mapped to one of the subcarriers from M , where $M > N$. The subcarrier mapping is achieved by using the same techniques which are applied in OFDMA systems as illustrated in Figure 2.4. As in OFDMA, an M -point IFFT is applied to transform the subcarrier amplitudes to a complex time-domain signal. The cyclic prefix is then appended and pulse shape filtering is performed.

The receiver transforms the received signal to the frequency-domain by applying it to a FFT, demaps the subcarriers and then performs frequency-domain equalization. The equalized symbols are transformed to the time-domain by applying an IFFT and detection and decoding takes place.

SC-FDMA is called single-carrier because of the sequential transmission of the modulated data symbols over a single frequency carrier, whereas, OFDM transmits

the data symbols in parallel. This is the reason why SC-FDMA systems have lower PAPR as compared to OFDMA systems. Figure 2.5 shows a comparison of the probability of different levels of PAPR for OFDMA and SC-FDMA. The probabilities have been calculated by randomly generating 10,000 OFDMA and SC-FDMA symbols and modulating 12 subcarriers. In the case of SC-FDMA, the parameters are $N = 12$, and $M = 64$. For OFDMA twelve subcarriers are modulated with data and the others are padded with zeros. We take an IFFT of 64 frequency-domain samples.

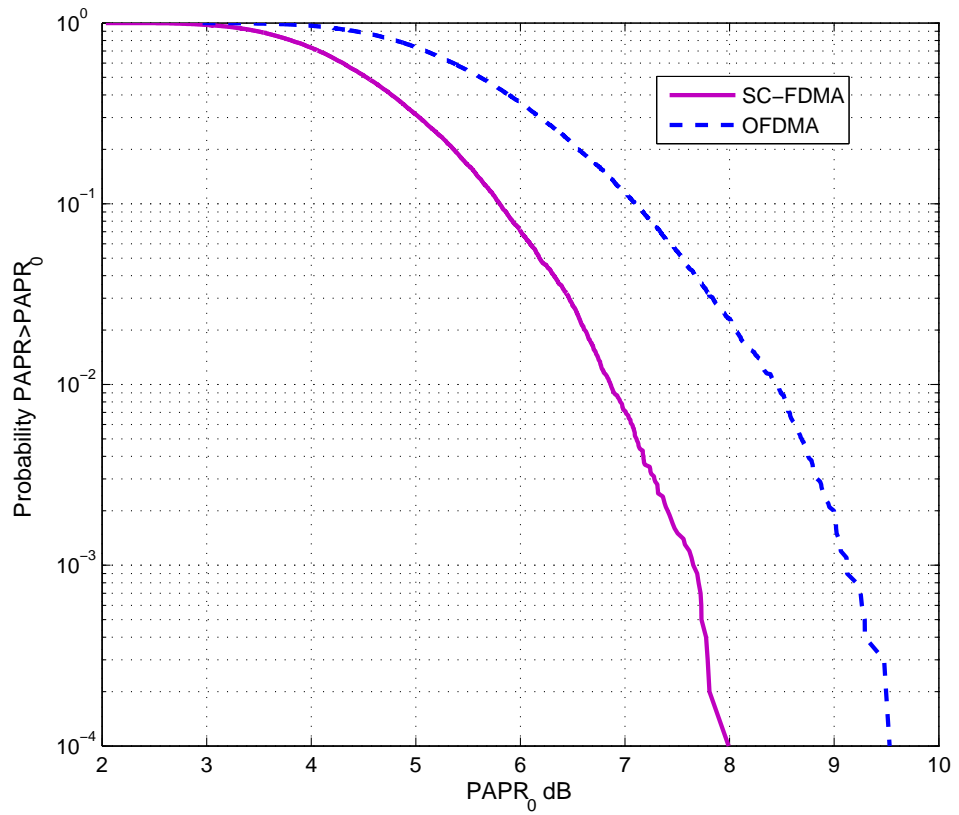


Figure 2.5: Probability $PAPR > PAPR_0$ for OFDMA and SC-FDMA symbols

The probability of getting a PAPR of 6dB or higher is seen to be 0.06 with SC-FDMA and 0.4 for OFDMA. The symbols with higher PAPR are more likely to suffer non-linear distortion by the HPA of the transmitter. It may be concluded that if the symbols with higher PAPR are not taken care of, they may be affected by nonlinearities, the effect of which can not be removed. More recently a lot of work has been done to reduce the PAPR of the SC-FDMA systems. The same techniques which

have been proposed for OFDM PAPR reduction have been modified to work with SC-FDMA systems. A companding technique and selected mapping techniques as applied to SC-FDMA will be explained in further sections [20], [21], [22].

2.4.1 IEEE 802.11 Standard Specifications for OFDM

The IEEE 802.11 OFDM specification provides a WLAN with data payload communication capabilities at 6, 9, 12, 18, 24, 36, 48 and 54Mb/s [23]. The support of transmitting and receiving at data rates of 6, 12 and 24Mb/s is mandatory. The system uses 52 subcarriers that are modulated using BPSK, QPSK, 16-QAM or 64-QAM. FEC is used with a coding rate of $1/2$, $2/3$ or $3/4$. These details are for 20MHz channel spacing. The OFDM specification also supports 20MHz, 10MHz and 5MHz channel spacing. The encoding process of the physical layer protocol data unit (PPDU) frame is as follows:

1. Specify the number of data bits per OFDM symbol (NDBPS), the number of coded bits per symbol (NCBPS), the number of bits per subcarrier (NBPSK) and the coding rate (R).
2. Extend the bit-string with at least 6 zero bits so that the resulting length is a multiple of NDBPS. This gives the DATA part of the packet.
3. Initiate the scrambler with a pseudo-random nonzero seed, generate a scrambling sequence and XOR it with the extended data string obtained in step 2.
4. Replace the 6 scrambled zero bits with zeros, these bits will return the convolutional encoder to zero state.
5. Encode the scrambled data string with a convolutional encoder of rate $R = 1/2$, $2/3$, $3/4$. The convolutional encoder uses the industry standard generator polynomials (133,171). Puncturing may be applied to achieve higher data rates.
6. Divide the encoded bit strings into groups of NCBPS bits. Within each group, perform an interleaving of the bits according to the specified rules.
7. Divide the resulting coded and interleaved data string into groups of NBPSK. Map each of the bit groups to complex numbers according to the modulation schemes available.

8. Divide the complex number strings into groups of 48 complex numbers. Each group is associated to one OFDM symbol. Each group of complex numbers is numbered as 0 to 47 and hereafter mapped into OFDM subcarriers.
9. Four pilot subcarriers and 12 null subcarriers are inserted into each OFDM symbol at specified positions according to the standard. The total number of subcarriers is 64.
10. For each group of 64 subcarriers, convert them to the time-domain using an IFFT. Append a cyclic prefix equivalent to 16 time-domain samples and set the boundaries of OFDM symbols by multiplying with a time-domain windowing function.
11. Append the OFDM symbols one after another.
12. Up-convert the complex base-band waveform to RF according to the central frequency of the desired channel and transmit.

2.5 Advantages of OFDM

The advantages of multi-carrier modulation and more specifically OFDM systems, are explained below.

2.5.1 Multipath Effects

The transmitted signal does not only have a direct path to the receiver in a wireless channel. The transmitted signal reflects off numerous objects before arriving which causes multiple delayed copies of the same signal to arrive at the receiver. This can result in inter symbol interference (ISI) which will increase the BER. This effect of signal communication is called multipath delay spread. For a longer delay of the paths, the ISI will also be higher. It is this effect which makes it difficult for single carrier systems to achieve high data rates. Dividing the available bandwidth into multiple subcarriers increases the symbol duration which reduces the effect of multipath delay spread.

2.5.2 Spectral Efficiency

One key point in OFDM systems is that the subcarrier transmissions are allowed to overlap in the frequency-domain just as single carrier transmissions are allowed to overlap in the time-domain (using sinc or raised cosine pulse shaping). The overlapping is acceptable as long as the amplitude of each time windowed subcarrier transmission is zero at the frequency of every other time windowed subcarrier. Then the windowed subcarrier transmissions are said to be orthogonal. The N equally spaced subcarriers will be orthogonal if the frequency-domain separation between the subcarriers is $\Delta f = 1/T$, where $N \cdot T$ is the symbol duration. This allows an efficient use of the spectrum.

In theory, the spectral efficiency of an OFDM system is identical to that of a single carrier system. However, in practice, it is feasible to engineer tolerances and other practical details to achieve higher spectral efficiency with OFDM.

2.6 Disadvantages of OFDM

The disadvantages of OFDM systems are mainly the complexity of the time and frequency synchronization required and the high PAPR values that will occasionally be produced. As PAPR is considered to be the major problem with OFDM systems, therefore, the focus of the next sections is PAPR and how to solve the problem of having high PAPR values.

2.7 Peak to Average Power Ratio (PAPR)

The PAPR of the OFDM symbol $x(n)$ is defined as the ratio between the maximum amplitude squared and the average power estimate of the symbol [24].

$$PAPR(x(n)) = \frac{\max_{0 \leq n < N-1} |x(n)|^2}{E\{|x(n)|^2\}} \quad (2.3)$$

where $\max_{0 \leq n < N-1} |x(n)|^2$ is often referred to as the maximum instantaneous power and $E\{|x(n)|^2\}$ denotes the average power estimate of the OFDM symbol. Moreover, $x(n)$ may be replaced by the continuous time signal $x(t)$; in that case the PAPR will be evaluated over the interval $t \in T$. Throughout this thesis, the PAPR will be referred to as the base-band PAPR, whereas, PAPR for the passband signal may be calculated

after modulating the signal to a high frequency carrier f_c . If $s(t)$ is represented as the passband signal, it may be written as:

$$s(t) = \text{Re} \left\{ x(t) e^{j2\pi f_c t} \right\} \quad (2.4)$$

The addition of the cyclic prefix does not make any difference to the PAPR, because the additional samples are a replica of the final samples of the symbol. OFDM uses an IFFT at the transmitter to modulate the signal. In the IFFT operation, all the subcarriers are summed after being amplitude and phase modulated. If all the modulated subcarriers add coherently, the addition may result in high peaks. The effects of these high peaks are analysed below and justify the need to find the ways of reducing the peaks. The cost of the transmitter/receiver hardware components rely on the dynamic range of the signals. The high PAPR of multicarrier systems requires operating with significant back off levels to handle the peaks of the transmitted signal and thus having linear amplification at RF. The average power is likely to be much lower than the peak power values. This leads to power inefficient amplification.

2.7.1 Distribution of PAPR

According to the central limit theorem, for large numbers of subcarriers N , the real and imaginary parts of a time-domain signal samples can be assumed to approach Gaussian distributions each with a mean of zero. Therefore the amplitude of an OFDM signal has a Raleigh distribution. The cumulative distribution function (CDF) of the PAPR can be used to evaluate the performance of PAPR reduction techniques.

For an OFDM system, the maximum power occurs when all the subcarrier components have identical phases i.e. $\arg \{X_{k=0}^N\} = \arg \{X_k^N\}, k = 0, 1, \dots, N-1$, where X_k^N are the complex constellation symbols. The higher the number of subcarriers the higher the PAPR can become. The PAPR of an OFDM system is usually expressed in terms of the complementary cumulative distribution function (CCDF). The CCDF of the PAPR denotes the probability that the PAPR of an OFDM symbol exceeds a given threshold. Rayleigh random variables normalized with the average power have the following probability distribution function (PDF)

$$Pdf(x) = \frac{2x}{\sigma^2} e^{-\frac{x^2}{\sigma^2}} = 2xe^{-x^2} \quad (2.5)$$

The probability that a sample from x_n is less than a predefined limit x_m is

$$P(x_n < x_m) = \int_0^{x_m} P d f(x_n) dx \quad n = 0, 1, \dots, N-1 \quad (2.6)$$

$$= 1 - e^{-x_m^2} \quad (2.7)$$

The joint probability that the PAPR of an OFDM symbol having N samples is less than x_m

$$P(x_n < x_m) = P(x_0 < x_m) \cdot P(x_1 < x_m) \dots P(x_{N-1} < x_m) \quad (2.8)$$

$$= (1 - e^{-x_m^2})^N \quad (2.9)$$

The Complementary CDF (CCDF) of the PAPR exceeding x_m is defined as

$$P(\text{PAPR}(x_n) > x_m) = 1 - P(\text{PAPR}(x_n) < x_m) \quad (2.10)$$

$$= 1 - (1 - e^{-x_m^2})^N \quad (2.11)$$

Equation-2.10 is derived assuming that N samples are independent and sampled at the Nyquist rate. This derivation does not hold for oversampled OFDM signals. In the case of oversampling the condition of uncorrelated samples does not remain true. It is difficult to derive CCDF for oversampled signals, therefore an approximation has been presented for oversampled signals by adding a certain number of uncorrelated samples to approximate the effect of oversampling [25]. The CCDF of an oversampled OFDM symbol can be expressed as

$$P(\text{PAPR}(x_n) > x_m) = 1 - (1 - e^{-x_m^2})^{\alpha N} \quad (2.12)$$

It has been shown by simulations that $\alpha = 2.8$ is a good approximation for oversampled signals [25]. Figure 2.6 shows the CCDF for a range of subcarriers like $N = 64, 256, 512$.

2.8 Factors affecting PAPR

The factors affecting the PAPR are discussed in the following sub-sections.

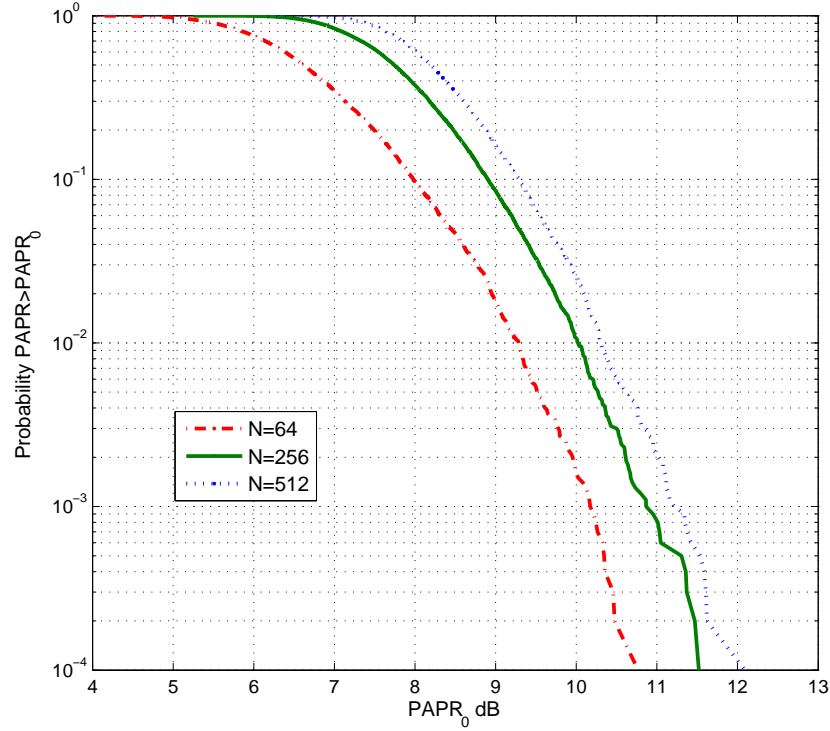


Figure 2.6: Probability that $PAPR > PAP_0$ with different number of subcarriers

2.8.1 Number of subcarriers

The PAPR in OFDM systems increases linearly with the increasing number of subcarriers. Figure 2.7 shows a plot which has been generated by running an OFDM simulation in MATLAB. It shows how the maximum possible PAPR increases as the number of subcarriers increases. The simulation is conducted on OFDM symbols having maximum PAPR, i.e. where all the constellation symbols have the same phases.

2.8.2 Modulation scheme

High rate data transmission is achieved in OFDM systems by using high order modulations on subcarriers, for example 16-QAM, 64-QAM and 256-QAM. For QAM schemes, information is encoded in the amplitudes as well as with phases, therefore the mapped signals have variations in the amplitudes. Hereby these modulation schemes will have larger variations and have high peaks. With the increasing order of modulation, the PAPR increases but the probability of getting high PAPR in signals is low.

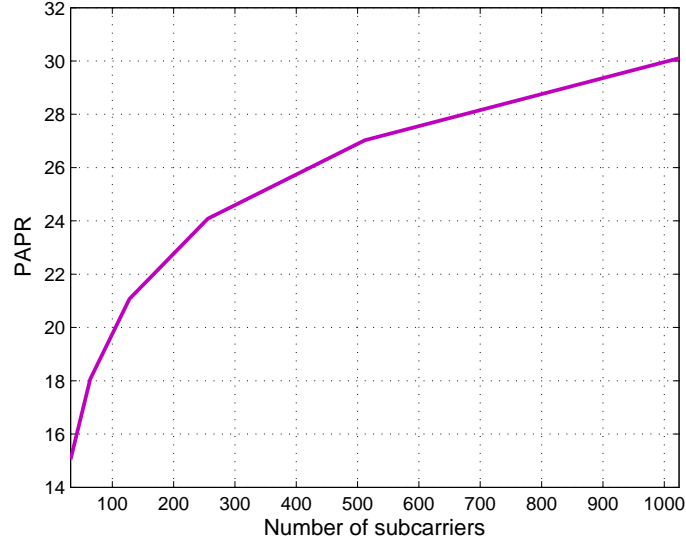


Figure 2.7: Maximum PAPR (dB) of an OFDM symbol against the number of subcarriers

Moreover, in OFDM systems, it is defined in the standards that subcarriers can have different modulation schemes on the basis of the channel conditions, so the PAPR of combined OFDM symbols may be difficult to predict.

2.9 PAPR reduction Techniques

Several PAPR reduction techniques have been proposed since the mid 1990's. Commonly, these techniques are classified in two categories. The first category comprises signal distortion techniques, which reduce the high peaks by non-linearly distorting the OFDM signal around the peaks. These techniques increase the bit-error rate (BER) at the receiver and are explained in Section 2.10. The second category comprises distortionless techniques which reduce the PAPR prior to the non-linear device (HPA) at the expense of reduced data rate but with no degradation in the BER. These types of techniques are explained in Section 2.11.

2.10 PAPR reduction with Distortion

2.10.1 Soft-clipping and Filtering

Soft-clipping is the simplest way of reducing high PAPR levels by limiting the high amplitudes to some predefined threshold value. For amplitude clipping [26], the soft-clipped complex valued signal is:

$$x_c(n) = \begin{cases} x(n), & \text{if } |x(n)| \leq A \\ A \cdot e^{j\theta(n)}, & \text{if } |x(n)| > A \end{cases} \quad (2.13)$$

where A is a predefined threshold value which is a positive real number and $\theta(n)$ is the argument of $x(n)$.

Since clipping is a nonlinear process, it produces distortion which increases the bit-error-rate. In theory, non-linear distortion such as clipping produces distortion of infinite bandwidth. If soft-clipping is applied directly to a base-band digital signal, sampled at F_s Hz say, the distortion will effectively produce components above $F_s/2$ Hz which are aliased back to the frequency range 0 to $F_s/2$. All the distortion produced is then said to be in-band distortion [26]. If, however, the signal is oversampled to increase the sampling frequency before the non-linear distortion is applied, much of the distortion will not be aliased back to the 0 to $F_s/2$ in-band frequency range. Now we have both in-band and out of band components and there is the possibility of filtering out the out-of-band distortion components [9].

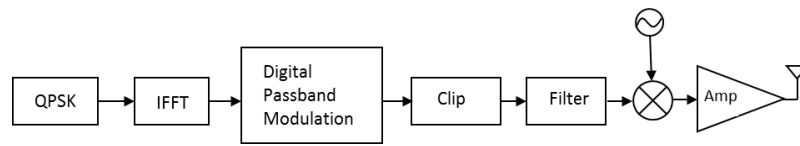


Figure 2.8: Block diagram of an OFDM system with Clipping and Filtering

Figure 2.8 shows the block diagram of an OFDM system with clipping and filtering. This technique is simple and requires little computational effort at the transmitter for a large number of subcarriers.

Results in [27] show that clipping an OFDM signal sampled at the Nyquist rate returns poorer peak reduction capability as compared to clipping a signal which is oversampled by a factor of J . It has been shown that the peak re-growth occurs in the case of Nyquist rate clipping, when the signal is up-sampled to allow it to modulate the carrier. Peaks that effectively lie between Nyquist rate sampling points will not

be clipped and will appear due to the interpolation that occurs with up-sampling. This peak re-growth may be more severe than for the oversampled case because of the phase differences, which will tend to be uniformly distributed with Nyquist sampling. For efficient peak power reduction, clipping is best applied to an oversampled signal.

In order to avoid signal peak re-growth after clipping, [28] has proposed applying clipping to an oversampled signal followed by a frequency-domain filtering. Frequency domain filtering is applied after clipping to reduce out of band power. The filter consists of an FFT and IFFT. Forward FFT is applied on the clipped signal to convert the signal to the frequency-domain. The in-band frequency components are passed unchanged to the inputs of an IFFT, whereas out of band components are nulled.

The filter is designed to remove the out of band noise produced by clipping without disturbing the in-band components.

Repeated clipping and filtering

To solve the problem of re-growth of peaks after filtering, repeated clipping and filtering is proposed [8].

The problem of peak re-growth can be solved by repeated clipping and filtering. However, as the number of repetitions of clipping and filtering increases, there is an increase in the BER. The increased BER is due to an increase in the in-band clipping noise. Another strategy is to use repeated clipping and filtering with bounded distortion (BD) to reduce the PAPR [1]. The idea of constellation perturbation has been used to disturb the signal points on all subcarriers under the predefined constraint of bound. Figure 2.9 shows the operations of recursive clipping and filtering using bounded distortion control.

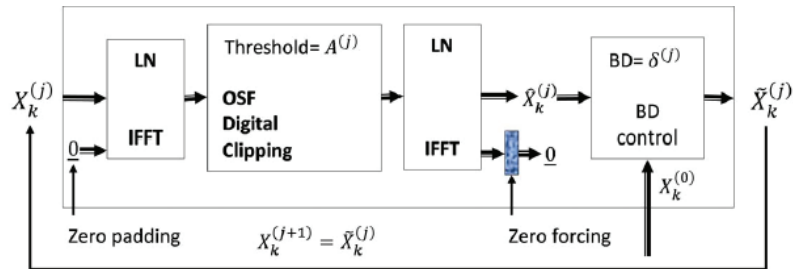


Figure 2.9: Recursive clipping and filtering using bounded control, reproduced from [1]

It has added a block of BD control to the previous system of oversampled clipping and filtering. The $(X_0, X_1, \dots, X_{N-1})$ are the input symbols to the IFFT block. The

output of the clipping and filtering block is $(\hat{X}_0, \hat{X}_1, \dots, \hat{X}_{N-1})$. The block of BD control is taking $(\hat{X}_0, \hat{X}_1, \dots, \hat{X}_{N-1})$ as input and gives output $(\tilde{X}_0, \tilde{X}_1, \dots, \tilde{X}_{N-1})$ with reference to the input $(X_0, X_1, \dots, X_{N-1})$ and distortion bound δ . The purpose of BD control is to adjust the value of each $\tilde{X}_k, k = 0, 1, \dots, N-1$. Each time after clipping the values of the output symbols are adjusted according to the input to reduce in-band distortion. This scheme reduces PAPR while keeping the distortion of the data under control [1].

There is another possibility of combining the interleaving and recursive clipping with filtering. The matrix interleaver is used to find W different ways of interleaving data and then the symbol with the lowest PAPR out of W is selected. The performance is actually dependent upon number of operations of the ineterleaver. If the data is interleaved many times, a significant PAPR reduction is achieved but increases the complexity [29].

Clipping in combination with other methods

A combination of adaptive symbol selection with Nyquist rate clipping is proposed in [30]. The random interleaver is applied to the data to get multiple symbols having same data. Theoretical analysis has shown that without any FEC as well as erroneous symbol selection may lead to severe BER degradation. However, if FEC codes are used with this scheme, then it might be a good selection for PAPR reduction.

There is another technique which proposes a kind of variable soft clipping with filtering [7]. It has start and end regions of clipping. Variable soft clipping reduces the PAPR to the medium level between the two hard clipping thresholds. It results in moderate BER performance. It reduces peak re-growth, however. The BER degradation is similar to that with conventional soft-clipping. Another method of PAPR reduction is to combine the simplified clipping and filtering with bounded distortion (SCFBD) and partial transmit sequences (PTS). The method is proposed in [31]. The results show a reduction in PAPR and lower BER as compared to the individual use of these schemes. [32] proposed to use clipping with side information, which need to be transmitted to the receiver. Therefore, the receiver, by knowing which time-domain samples were clipped, can recover the unclipped form of the OFDM symbols. Large peaks occur with a very low probability so clipping could be an effective solution to reduce PAPR.

2.10.2 Companding

Companding has been proposed for reducing the PAPR using a compressor at the transmitter and an expander at the receiver. The time-domain signal at the transmitter after the IFFT is passed through a compressor to compress the high peaks considering the low probability of high peaks occurrences. The receiver after converting the signal to the time-domain applies an expander to get the original signal. The technique reduces the PAPR sufficiently but the BER increases at the receiver in the process of expanding [33]. It also increases the noise in the signal. An enhanced version using an exponential companding technique for OFDM systems has been presented in [34]. It improves the PAPR reduction and the BER at the receiver. By choosing the transform parameters efficiently, an improvement in the PAPR reduction may be achieved. This has been proved by the results published in [35].

2.11 PAPR Reduction with Distortionless Techniques

These methods reduce the PAPR before the signal is applied to the HPA.

2.11.1 Coding

Coding schemes are attractive for PAPR reduction because of their error control capability. A simple idea of block coding is proposed in [36]. The method is to find out all possible codewords and then select those codewords that have less PAPR. In this technique a 3/4 rate block code has been implemented, which maps a 3-bit data word onto a 4-bit codeword such that it does not contain the sequences with high PAPR. The 4th bit is the odd parity bit to reduce PAPR. It has been shown that the PAPR of the signal can be reduced from 6.02dB to 2.48dB using this scheme. For N subcarriers, the total number of possible codewords is 2^N . The practical implementation of this approach will be difficult for a large number of N . This technique has two limitations. First, finding the best suitable codeword having low PAPR requires an exhaustive search. Second, it requires us to store large lookup tables. This is also called Systematic Odd Parity Checking (SOPC) code. There is another technique of cyclic coding introduced in [11] which uses a 3/4 rate code. It shows the same results as those with block codes in [36].

A similar approach has been presented in [12]. In this method, a redundant bit is chosen as the inverse of one of the bits present in the same frame. Based on the

results and simulations in [37], it is concluded that SOPC and the block code method presented in [12] are not very effective when the number of frames or N is large.

However the PAPR for a large value of N can be reduced by using Sub Block Coding (SBC) as proposed in [38]. The idea is to divide the long frame into several sub blocks and then encode them all using SOPC. Another extension to this scheme could be to find the best position of the odd parity bit. Optimizing the position of the parity bit can further reduce the PAPR; this is called Redundant Bit Location Optimized Sub-Block Coding (RBLO-SBS) [38]. In the case of RBLO-SBS, for a higher number of N , PAPR reduction starts decreasing, because it has fixed positions for odd parity bits.

A novel coding scheme has been introduced in [39] by using SBS with variable positions of the parity bit. It finds all the codewords with different positions of the parity bit by rotation, and then combines all those code words to select the one with the lowest PAPR. It requires $4^{N/4}$ comparisons to find best codeword. This is termed as Redundant Bit Position Rotation Sub-Block Coding (RBPR-SBS). Figure 2.10 shows the block diagram of this scheme. As the Figure shows, the Bit Position Rotation Encoder is used to rotate the redundant bit, as a result multiple codewords are produced. The PAPR calculator calculates the PAPR for each of codeword C , and then the Code Word Selector finds the best codeword with lowest PAPR. Redundant Bit Position information is transmitted with the codeword as side information.

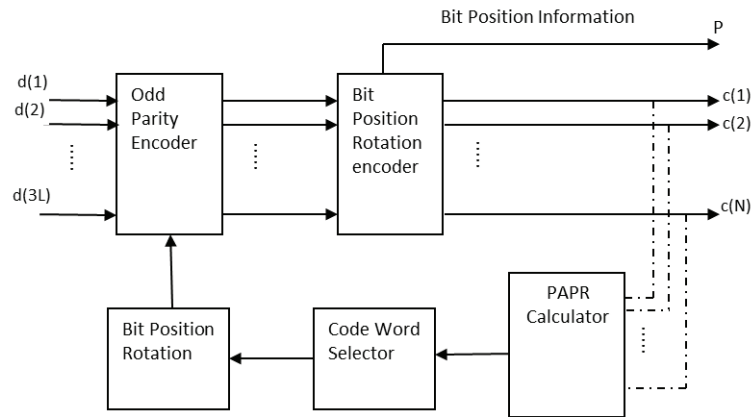


Figure 2.10: Block Diagram of RBPR-SBS

It is not possible to find the best code until all the $4^{N/4}$ comparisons has been done, which is not efficient. To reduce the complexity, a threshold PAPR is defined, so if a codeword is found with a value lower than the threshold value, it will stop searching and select that codeword [39]. These approaches do not address the problem

of error correction at the receiver. To implement coding scheme, large lookup tables are required at the transmitter and receiver which in turn will result in exhaustive search for best codes. The usefulness of these techniques is limited for multicarrier systems with small numbers of subcarriers. Therefore, the actual benefits of coding for PAPR reduction of OFDM systems are limited.

2.11.2 Partial Transmit sequence (PTS)

The PTS is a distortionless PAPR reduction technique. In this technique the input data block of N symbols is partitioned into small disjoint sub-blocks [40]. Here it is assumed that sub-blocks consist of contiguous sets of subcarriers having equal size. Figure 2.11 shows a block diagram of PTS. The idea is to form a weighted combination of all sub-blocks [13].

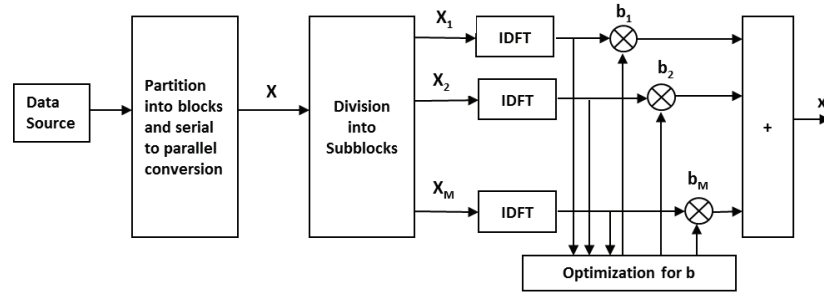


Figure 2.11: Partial Transmit Sequences

The subcarriers of each block are weighted by a phase factor. Let X be the set of data, $X_n, n = 0, 1, \dots, N-1$, as a vector $[X = X_0 \ X_1 \ \dots X_{N-1}]^T$. Then partition block X into M disjoint sub-blocks $X_m, m = 1, 2, \dots, M$, such that:

$$X = \sum_{m=1}^M X_m \quad (2.14)$$

All the sub-blocks are combined to reduce PAPR in the time-domain. The L-times oversampled time domain signal is denoted by $x_m = [x_{m,0}, x_{m,1}, \dots, x_{m,NL-1}]^T$. x_m is obtained by applying an IDFT of length NL on X_m padded with $(L-1)N$ zeros. These are called the partial transmit sequences. After that, complex phase factors $b_m, m = 1, 2, \dots, M$ are introduced to combine the PTS. The time-domain signal after combining with phase rotations is given by

$$x' = \sum_{m=1}^M b_m x_m \quad (2.15)$$

The actual components are phase factors which help to reduce the PAPR. The objective of this scheme is to find a set of phase rotations which minimize PAPR. The transmitter in PTS must have knowledge of the phase factors used to generate each OFDM symbol. Therefore phase rotations must be sent as side information along with PTS, which is an overhead and the cause of some loss of efficiency.

One rotation factor can be fixed by setting the value of $b_1 = 1$, then there is a need to find $M - 1$ phase factors [14]. There is no requirement of actual multiplication of PTS and phase factors. It is shown in [14] that using 128 subcarriers, with 4 sub-blocks and phase factors limited to the set of $\{\pm 1, \pm j\}$, 1% redundancy is used to achieve a significant 4dB PAPR reduction. The PTS scheme uses an N-point IDFT of all sub-blocks, If the large fraction of input values is kept zero, then the complexity of PTS can be reduced.

Another factor which can affect the PTS scheme for PAPR reduction is the sub-block partitioning. There are three types of partitioning schemes: adjacent, interleaved and pseudo-random partitioning [41]. Among these, the pseudo-random technique has been found to be the best choice. With an ordinary PTS scheme, an exhaustive search from all combinations of allowed phase factors is required. The search complexity for phase factors increases exponentially with the increase in the number of sub-blocks. To reduce complexity, various techniques have been suggested [42], [43].

2.11.3 Selected Mapping Scheme

In the Selected Mapping Scheme (SLM), the transmitter generates a different set of data blocks representing the same information as the original data. The most favorable with the lowest PAPR is selected for transmission [44]. Fig 2.12 shows the block diagram for the SLM scheme. U individual phase sequences are generated each of length N , $B^{(u)} = [b_{u,0}, b_{u,1}, \dots, b_{u,N-1}]^T$, $u = 1, 2, \dots, U$. After mapping data onto subcarriers, each subcarrier symbol is to be multiplied with the $B^{(u)}$ sequence, thus generating U different frames with components. One of the alternative subcarrier vectors could be the unchanged original one [45]. All these U frames X_1, X_2, \dots, X_U are transformed to the time-domain by applying an IDFT on each frame. Among the modified data blocks, the one with the lowest PAPR is selected to transmit. The receiver must have knowledge about the OFDM generation signal, so information about the selected phase

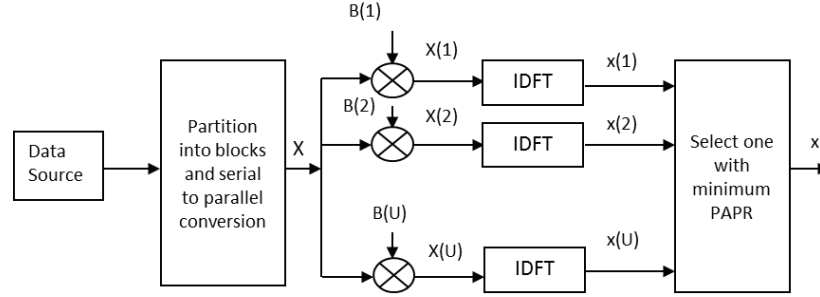


Figure 2.12: Selected Mapping

sequence will be transmitted as side information. There is no restriction on the type of modulation or number of subcarriers. There is only a slight overhead of the redundancy which has to be transmitted for the receiver.

The amount of PAPR reduction is based upon the number and design of phase sequences. To reduce the overhead of side information another approach using the SLM scheme has been proposed in [46]. This scheme presented SLM with scrambling. The idea of inserting labels $b^{(u)}$, $0 \leq u < U$ as prefix to the information word q has been used. These labels are U different binary vectors of length $\lceil \log_2 U \rceil$. The scrambler is a shift register with a feedback branch only. After scrambling the information word q , the output will be fed to an encoder and interleaver. An IDFT will be performed, and the transmit sequence with the lowest PAPR will be transmitted. At the receiver there will be a descrambler, decoder and deinterleaver. The results show that 1 and 2dB can be saved in backoff with 4 bits of redundancy per OFDM symbol. The main drawback of the SLM scheme is its computational complexity due to several IFFT operations. To reduce complexity in [47], [15], [16], [48], [49], SLM has been proposed with some modifications to the conventional SLM.

2.11.4 Active Constellation Extension Technique

This class of PAPR reduction methods introduces a new constellation to reduce large peaks. Rather than assigning each symbol to a certain constellation point, it is assigned a set of constellation points [17]. This is called Active Constellation Extension (ACE). It uses non-bijective constellations to reduce PAPR by appropriately encoding the data symbols [50]. The idea can be easily explained by taking the special case of OFDM with QPSK constellation. In each subcarrier there are four possible constellation points that lie in each quadrant in the complex plane and are equidistant from the real and imaginary axis. Any point that is farther from the decision boundaries than the

nominal constellation point will offer an increased margin which guarantees a lower BER. Therefore, constellation points can be modified within the quarter plane outside of the nominal constellation point with no degradation in performance. Figure 2.13 represents the active constellation extension for 16-QAM mapping scheme.

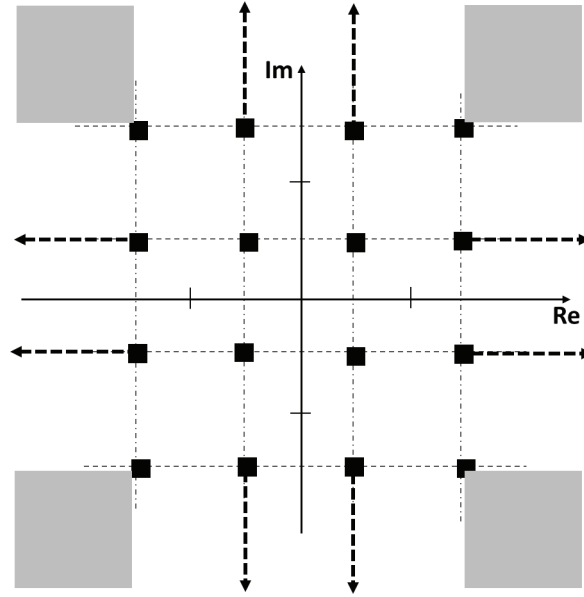


Figure 2.13: Active constellation extension with 16-QAM mapping. The shaded regions represent the corner point extension areas whereas dotted arrows represent the extension paths for side points.

2.11.5 Interleaving

An OFDM signal generates high PAPR if the data repeats patterns or the auto-correlation of the data gives high values at some delays including zero. Hence the PAPR can be reduced if we are able to break down the long correlation patterns. It utilizes data randomization techniques to reduce PAPR. Adaptive interleaving is proposed to reduce the complexity [51]. The concept of this technique is to find an early terminating threshold. Hence the technique does not search all the possible interleaved sequences but stops if it finds a sequence with PAPR value below this threshold. The results using this technique are comparable to PTS and the complexity for the interleaving technique remains less than that of PTS.

2.11.6 Tone reservation

This method reserves a small set of subcarriers to reduce the high PAPR. These reserved subcarriers are not used to send useful information and they are called peak reduction tones. They are randomly distributed across the signal bandwidth. The performance of the technique depends upon the number of reserved tones and the location of these tones. Increasing the number of reserved tones improves the capability of PAPR reduction at the prices of reduction in throughput because of reduction in data bearing subcarriers. In general there is a trade-off between these requirements by carefully selecting the number of reserved tones. The advantages of tone reservation are that it includes no side information and no special receiver oriented operation. The shortcomings are a decrease in the data rate and difficulties in finding the location for reserved tones.

2.11.7 Tone injection

This is to improve the data rate loss of tone reservation. It reduces the PAPR without compromising the data rate. The basic idea is to send information over all subcarriers by increasing the size of the constellation. Then each constellation symbol may be mapped to a set of equivalent constellation points in the extended constellation. It uses a set of equivalent constellation points for every constellation symbol in the original constellation. There is no effect on the BER and no data rate loss. However, tone injection reduces the PAPR at the expense of a little increase in total transmission power. This method needs side information for decoding the signal at the receiver and causes an extra IFFT operation at the transmitter, making it complex.

2.12 Hybrid Automatic Repeat reQuest

Automatic Repeat reQuest (ARQ) is an error control mechanism which is simple and provides high reliability for wired systems. However in wireless communication systems, which may have much higher bit-error rates than wired systems, its efficiency falls rapidly. Hybrid ARQ is a combination of forward error correction codes and ARQ using error detection. The transmitter appends redundant information with the message, so that the receiver can try to correct the message and then detect the existence of any remaining bit-errors. Despite its overhead of extra information it is widely used for wireless networks. Its purpose is to reduce the frequency of retransmission

which are much more costly and resource consuming on wireless systems than they would be on wired systems.

2.12.1 HARQ Type I

HARQ Type I uses a FEC code with the data and an error detecting code as mentioned above. The FEC code can be used to try to correct any bit-errors. If the decoder is unable to correct the errors, then it will discard the packet and request for retransmission. After receiving the second transmission, the receiver again tries to correct the packet, if it fails again, it rejects the packet and requests a further retransmission. This error correction and retransmission process continues in theory until the desired packet is received and decoded correctly. In practice, a maximum number of retransmission is allowed after which the packet is declared as lost. The disadvantage of Type I is that when the code rate is fixed for communication, then the FEC information will be transmitted even if it is not required. Also the discarding of erroneous packets when they may contain partially correct information is clearly inefficient.

2.12.2 HARQ Type II

HARQ Type II often refers to a strategy by Chase [52] who introduced a simple form of code combining. The packets in error are not discarded at the receiver after retransmission requests, and instead are saved. The saved packets are used along any retransmitted packet in an attempt to correct the errors. This is called Chase Combining. WiMAX supports a multi-channel ‘stop and wait’ HARQ scheme using Chase combining. Each data burst has to be re-transmitted until successful transmission is achieved using the same channel.

2.12.3 HARQ Type III

Type III HARQ generally means incremental redundancy, though the terminology is not consistent in the literature. With incremental redundancy the transmitter encodes the message bits for a lower FEC code rate and punctures this differently for each transmission or retransmission. When the receiver detects a bit-error, it saves the erroneous packet in its buffer, and requests a retransmission. The transmitter sends a different punctured version of the coded bits which is combined at the receiver with the older transmission. Every retransmission lowers the combined code rate of the combined

signal at the receiver. LTE uses HARQ Type III with 1/3 turbo encoders [19].

2.13 Discussion

The capability of the PAPR reduction for any method can not be predicted theoretically unless a simulation has been accomplished for all the methods. The main features for PAPR reduction methods may be defined in terms of the PAPR reduction capability, data rate loss, power increase, distortionless, any side information required to transmit, processing at the receiver. Table 2.1 shows a summary of all the PAPR reduction approaches mentioned in this chapter together with a mention of their main features.

2.14 Conclusions

Many different views about the impact of PAPR on OFDM signals have been presented in the literature, and a wide range of techniques for minimizing this impact have been proposed over passing years. Since the occurrences of high peaks in OFDM signals are events with non-negligible probability, effective PAPR mitigation techniques are essential to enable the efficient use of non-linear power amplifiers. A comparison of all the techniques has been presented which leads us to conclude that every presented method has some drawbacks. Although a lot of work has been done in this area, still there is space for research to come up with new ideas. The next chapter studies the effect of clipping and introduces further clipping noise mitigation techniques based on a statistical analysis of the nature of memoryless distortion. Chapter 4,5 and 6 describe new methods of clipping noise mitigation.

Table 2.1: Comparison of PAPR reduction techniques

PAPR Reduction techniques	Distortionless	Data rate loss	Power increase	Transmitter processing	Receiver processing
Clipping	No	No	No	Clipping function	Clipping noise mitigation techniques are required
Companding	No	No	No	Compress function	Expander
Coding	Yes	Yes	No	Coding or lookup tables	Decoding or lookup tables
PTS	Yes	Yes	No	Multiple IDFT operations	Side information
SLM	Yes	Yes	No	Multiple IDFT operations	Side information
ACE	Yes	No	Yes	Projection on to shaded region	None
Interleaving	Yes	Yes	No	Multiple IDFT operations	Side information
TR	Yes	Yes	Yes	Find appropriate sub-carriers to reserve	Identify and Ignore null data carriers
TI	Yes	No	Yes	IFFT,	Modulo operation

Chapter 3

Iterative receivers based on statistics of memoryless distortion

Limiting the peaks of OFDM symbols causes memoryless non-linear distortion that becomes in-band distortion with Nyquist sampling and both in-band and out-of-band distortion when the sampling frequency is increased by oversampling. This chapter further studies the effect of soft limiting (e.g. soft-clipping) as applied to base-band and oversampled time-domain signals to eliminate the possibility of high peak amplifier clipping. There is much research in the literature on this topic and many techniques for reducing the effect of limiting based purely on the statistical analysis of memory-less distortion. The performance of iterative receivers with limiting at the transmitter are studied in this chapter. The use of a different form of limiting is also investigated and evaluated in terms of PAPR reduction after filtering. We have evaluated the proposed technique through PAPR reduction and peak re-growth and have derived the distortion factor for this particular kind of limiting . The limiting technique is Inverted Wrap-around (IWRAP).

3.1 Clipping

Soft-clipping truncates the amplitudes of time-domain samples to a predefined threshold before amplification. The clipping is a non-linear process and produces distortion in an OFDM signal which generally degrades the bit-error rate (BER) at the receiver. Clipping at the Nyquist sampling rate causes all the clipping distortion to fall in-band. Unfortunately, significant peak-regrowth can occur after digital to analog conversion (D/A) because of the upsampling process and the nature of the interpolation between

Nyquist rate samples [27]. Clipping an oversampled signal reduces peak regrowth because the interpolation has already been done before the limiting. But it produces out-of-band (OOB) distortion which is called spectral regrowth [9]. The OOB may be removed by frequency-domain filtering as proposed by [28], though, unfortunately again, this filtering can also re-introduce some time-domain peaks. Ultimately the remaining in-band distortion can be compensated at the receiver as is the theme of this thesis.

The clipping could be applied to signals at different stages of processing. The possibilities are either to clip the discrete samples at the output of the IFFT, or to clip the continuous signal at the output of the RF modulator. In this thesis, we have described and used base-band clipping which is applied after the IFFT. A baseband OFDM signal is expressed as:

$$x(n) = \frac{1}{\sqrt{N}} \sum_{k=0}^{N-1} X_k e^{j\frac{2\pi nk}{N}} \quad 0 \leq n < N-1 \quad (3.1)$$

where N is the number of subcarriers and X_k for $k = 0, 1, \dots, N-1$ are the complex modulated data symbols.

3.1.1 Clipping Nyquist sampled Signals

An OFDM symbol in the time-domain may be expressed in polar form as

$$x(n) = |x(n)| \cdot e^{j\theta(n)} = x_I(n) + jx_Q(n) \quad (3.2)$$

where $x_I(n)$ and $x_Q(n)$ are the in-phase and quadrature components of the complex envelope in discrete form, respectively. The clipping process is described by the fol-

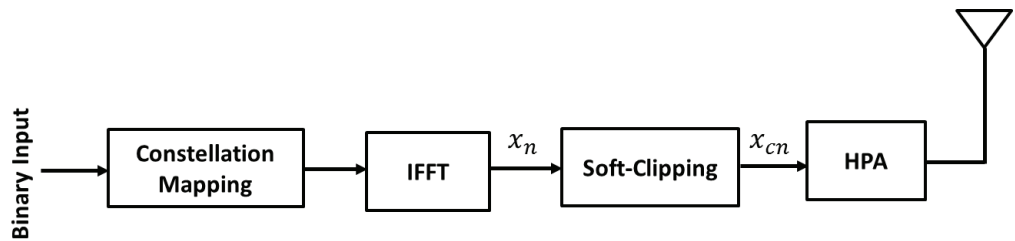


Figure 3.1: Clipping at Nyquist sampling

lowing expression:

$$x_c(n) = \begin{cases} x(n), & \text{if } |x(n)| \leq A \\ e^{j\theta(n)} A & \text{if } |x(n)| > A \end{cases} \quad (3.3)$$

The amplitudes of the time-domain samples are limited to A, keeping the phases unchanged. The clipping ratio (CR) is defined as:

$$\gamma = \frac{A}{\sqrt{P_{in}}} \quad (3.4)$$

where P_{in} is the average energy of the OFDM signal before clipping. When γ is high, there is no distortion in the signal. When γ reduces, clipping distortion increases. In deciBel form,

$$\gamma = 20 \log_{10} \left(\frac{A}{\sqrt{P_{in}}} \right) \text{dB} \quad (3.5)$$

The power spectral density (PSD) of a clipped analogue signal has a theoretically infinite bandwidth. For a signal sampled at the Nyquist rate aliasing will cause the spectral components of the clipping distortion above half the sampling frequency to be folded back into the signal bandwidth. This gives rise to in-band distortion which may increase the BER at the receiver. The clipped signal may be written as

$$x_c(n) = x(n) + c(n) \quad 0 \leq n < N - 1 \quad (3.6)$$

where $c(n)$ includes the part of the signal whose amplitudes are above the clipping level A. The second term $c(n)$ will clearly be correlated with the input signal $x(n)$.

It is also clear that the clipping process reduces the output power. Because of the central limit theorem, for large values of N, the distribution of the real and imaginary values of the time-domain OFDM signal can be normally assumed to be Gaussian. If the OFDM signal can be modeled as a zero mean complex Gaussian process then the output power of the clipped signal may be calculated as [30]:

$$P_{xc}(n) = (1 - e^{-\gamma^2}) P_x(n) \quad (3.7)$$

The difference between $P_x(n)$ and $P_{xc}(n)$ reduces as γ grows larger and becomes zero when $\gamma = \infty$.

3.1.2 Clipping Oversampled Signals

Applying soft-clipping at the Nyquist sampling rate gives a large increase to the in-band distortion. In addition, extensive simulations indicate that the PAPR reduction capability of Nyquist rate clipping is not so significant due to considerable peak regrowth after upsampling and D/A conversion. As a result, it is recommended that soft clipping should be applied to an oversampled version of the OFDM signal [27].

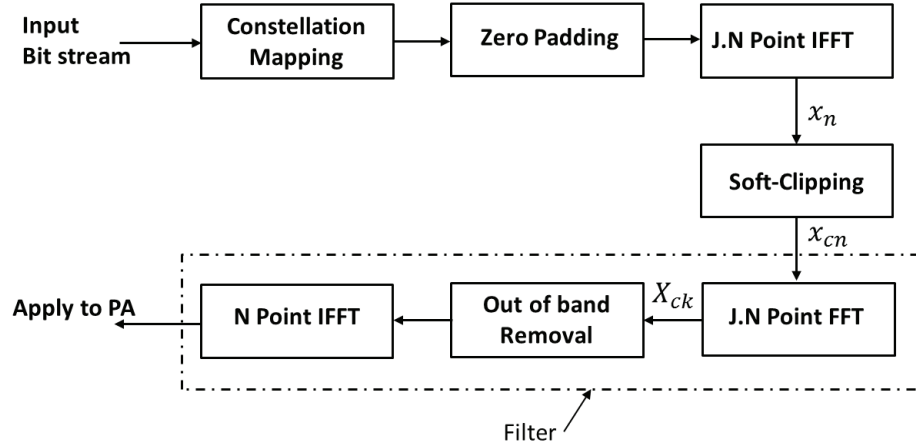


Figure 3.2: Clipping and filtering an oversampled signal

Figure 3.2 shows a block diagram of a PAPR reduction scheme using clipping and filtering at the transmitter. J is the oversampling factor and N is the number of subcarriers. For an oversampling factor J , the input vector is oversampled by inserting $(J - 1) \cdot N$ zero valued frequency-domain samples following the N values of X_k . The oversampled OFDM signal may be written as:

$$x(n) = \frac{1}{\sqrt{N}} \sum_{n=0}^{N-1} X(n) e^{j \frac{2\pi n k}{JN}} \quad 0 \leq n < JN - 1 \quad (3.8)$$

Soft-clipping is applied to the oversampled time-domain samples, and band-pass filtering is then applied to remove the out-of-band components that are generated by the non-linearity.

The signal $x_c(n)$ is converted to the frequency-domain by applying an FFT to produce $X_c(k)$ which may be expressed as

$$X_c(k) = X(k) + C(k) \quad 0 \leq k < JN - 1 \quad (3.9)$$

where $X(k)$ and $C(k)$ are respectively the FFT of $x(n)$ and $c(n)$. Out of band

components are removed before taking the IFFT of $X_c(k)$. After clipping and filtering, the OFDM symbol in the time-domain is

$$x_c(n) = x(n) + \hat{c}(n) \quad 0 \leq n < N - 1 \quad (3.10)$$

3.1.3 Bussgang theorem for memoryless non-linearities

If a Gaussian signal $x(n)$ passes through a memoryless nonlinearity, a coefficient α may be found such that the output $x_c(n)$ may be written as:

$$x_c(n) = \alpha x(n) + d(n) \quad (3.11)$$

where $d(n)$ is a Gaussian signal which is uncorrelated with $x(n)$. α is a scalar value which minimizes the energy of d_n over all possible values of α . To find this optimal value of α , multiply both sides of Equation 3.11 by $x(n)$ and take expectations to obtain:

$$E \{x_c(n)x(n)\} = \alpha E \{x(n)^2\} + E \{x(n)d(n)\} \quad (3.12)$$

If $E \{x(n)d(n)\} = 0$, then $x(n)$ and $d(n)$ are uncorrelated and

$$\alpha = \frac{E \{x_c(n)x(n)\}}{E \{x(n)x(n)\}} \quad (3.13)$$

To show that $E \{d(n)^2\}$ is minimised by this value of α , write:

$$E \{d(n)^2\} = E \{x_c(n)x(n)\} - \alpha E \{x(n)d(n)\} \quad (3.14)$$

Differentiating $E \{d(n)^2\}$ with respect to α and setting the result to zero gives

$$\frac{dE \{d(n)^2\}}{d\alpha} = E \{x(n).d(n)\} = 0 \quad (3.15)$$

The Bussgang theorem may be illustrated for a sinusoidal signal $x(n)$ (even though this is not Gaussian). For $\alpha = 1$, the distortion term $d(n)$ is highly correlated to the input $x(n)$. If we start decreasing the value of α , the correlation between $x(n)$ and $d(n)$ starts decreasing. There is some value of α for which $d(n)$ has minimum energy along with having minimum correlation to $x(n)$. That may be called the best value of α for which the Bussgang theorem is true. The value of α is dependent upon the non-linearity.

For OFDM signals, if the number of subcarriers is adequately large, from the central limit theorem the sequence may be considered approximately Gaussian distributed with zero mean. The clipped signal can be written as sum of an uncorrelated signal and distortion terms. This decomposition can be justified by the Bussgang theorem [53].

In the case of soft-clipping a Gaussian signal such that the clipping ratio is γ , α is called an attenuation factor which may be expressed as the following function of the clipping ratio:

$$\alpha = 1 - e^{-\gamma^2} + \frac{\sqrt{\pi}}{2} \text{erfc}(\gamma)\gamma \quad (3.16)$$

This formula is derived in Appendix A.

3.1.4 Signal to Clipping noise ratio

The in-band distortion produced by clipping is normally measured in terms of signal to clipping noise ratio (SCNR). This term is defined as the ratio of the average received signal power to the average power of the clipping distortion, which can be computed using the Bussgang theorem.

To calculate this, we consider an OFDM system sampled at its Nyquist rate. Calculating the power of the clipped signal in Equation 3.11 gives the following form:

$$\text{Power}(x_c(n)) = E \{x_c(n)^2\} = \alpha E \{x_c(n)x(n)\} + E \{x_c(n)d(n)\} \quad (3.17)$$

$$= \alpha E \{\alpha x(n)^2\} + \alpha E \{d(n)x(n)\} + E \{\alpha x(n)d(n)\} + E \{d(n)^2\} \quad (3.18)$$

Since $E \{x(n)d(n)\} = 0$,

$$E \{x_c(n)^2\} = \alpha^2 E \{x(n)^2\} + E \{d(n)^2\} = \alpha^2 \text{Power}(x(n)) + \text{Power}(d(n)) \quad (3.19)$$

$$\text{Power}(x_c(n)) = \alpha^2 \text{Power}(x(n)) + \text{Power}(d(n)) \quad (3.20)$$

The output power of the clipped signal from calculation, is given by:

$$P_{x_c}(n) = (1 - e^{-\gamma^2})P_x(n) \quad (3.21)$$

The power of the clipping distortion can be calculated by using Equation 3.21 in Equation 3.20 as:

$$P_d(n) = P_{x_c}(n) - \alpha^2 P_x(n) \quad (3.22)$$

$$P_d(n) = (1 - e^{-\gamma^2})P_x(n) - \alpha^2 P_x(n) = (1 - e^{-\gamma^2} - \alpha^2)P_x(n) \quad (3.23)$$

The signal to clipping noise power ratio (SCNR) can be calculated as:

$$SCNR = \frac{\alpha^2 P_x(n)}{P_d(n)} = \frac{\alpha^2}{(1 - e^{-\gamma^2} - \alpha^2)} \quad (3.24)$$

3.2 Clipping noise mitigation techniques

The non-linear distortion produced by clipping can not be corrected efficiently by using a classical linear receiver with equalization. Also, its effect at the receiver is compounded by that of AWGN introduced, largely, by the receiver's front end amplifier.

Several receiver oriented approaches have been proposed to mitigate the non-linear effects of clipping in OFDM systems. Some of them use oversampled signals to retrieve the original amplitude of the clipped samples [54], which tries to reduce the clipping distortion by expanding the bandwidth. There are also iterative receivers for reducing the BER at the receiver. Two widely cited methods are Busgang noise cancellation (BNC) and decision aided reconstruction (DAR) [55], [56], [57]. Both will be explained and discussed here. The BNC method applies an extra pair of IFFT/FFT transforms to try to regenerate the clipping distortion and then subtracts this from the received signal. The DAR method works in the time-domain to try to regain the unclipped amplitudes of the clipped samples. Assuming perfect carrier and timing synchronization, the received signal, after applying the FFT, is as follows:

$$R_k = H_k \cdot (X_k + D_k) + Y_k \quad 0 \leq k < N - 1 \quad (3.25)$$

where H_k is the complex channel gain of the k -th subcarrier assuming it is perfectly known by the receiver and Y_k is the AWGN. For both the receivers, clipping is assumed to be applied to an oversampled signal and the OOB noise is filtered after clipping.

3.2.1 Busgang Noise Cancellation Receiver (BNC)

The statistical properties of OFDM signals that pass through memory-less non-linear distortion, have been widely investigated in the literature [58]. This section describes the use of the Busgang theorem to try to estimate the clipping noise, and subtract it from the received clipped signal. In this scheme, the receiver is assumed to know the clipping level A . There are two key factors involved in this approach. The first one is that the BNC algorithm assumes that most of the bit decisions made at the receiver are correct and hereby can be exploited to estimate the original signal. The second key

factor is the use of the Busgang theorem and the estimation of a value of the scalar α which minimizes the energy of the difference $d(n)$ between the clipped signal $x_c(n)$ and $\alpha x(n)$ where $x(n)$ is the unclipped signal at the transmitter. The received signal for the BNC receiver may be written as:

$$R_k = H_k \cdot (\alpha X_k + D_k) + Y_k \quad 0 \leq k < N-1 \quad (3.26)$$

Figure 3.3 shows the mechanism of the basic BNC feedback loop. The steps of the BNC receiver are as follows:

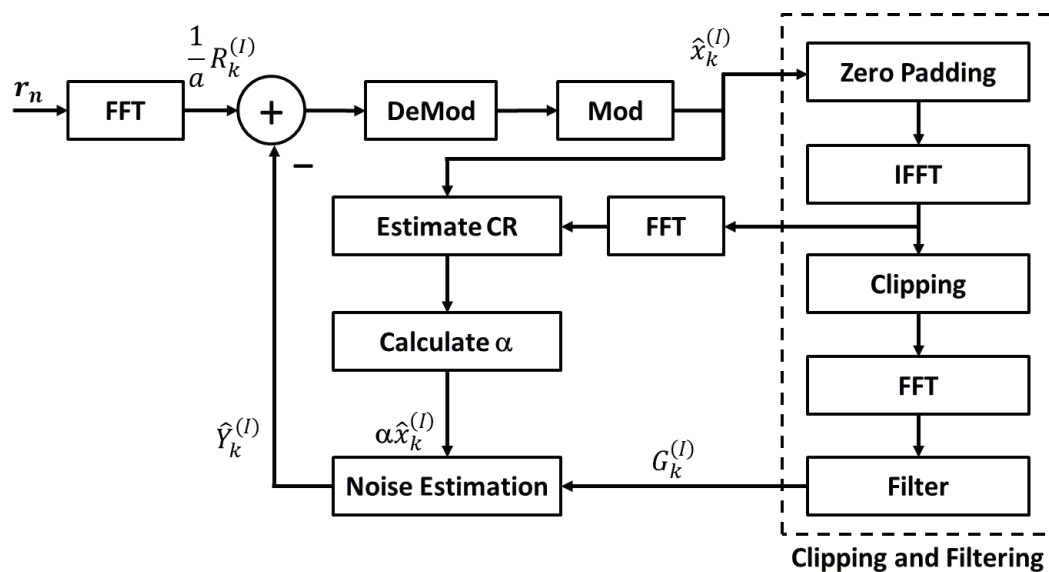


Figure 3.3: BNC Process

1. The received signal after applying the FFT, is as in Equation 3.26. At the receiver, the frequency-domain signal is multiplied by $1/\alpha$ where α is an estimate of the true value at the transmitter. The receiver's initial estimate of α is calculated using Equation 3.16 where the clipping ratio, γ , is estimated from the clipping level A and the RMS value of the received signal used as an initial approximation to the RMS value of the unclipped signal (see Equation 3.4). The scaled frequency-domain vector is de-mapped from the received constellation using hard bit-decisions and checked for any bit-errors using the error-detection facility provided by the packetisation. It may be necessary to process several OFDM symbols at once to be able to access the CRC check appended to the data. If there are possible bit-errors, then the bit sequence is re-mapped or 'snapped'

to the true constellation using the same modulation scheme used at the transmitter, producing $\hat{X}_k^{(I)}$, $k = 0, 1, \dots, N-1$ where I is the current iteration number with initial value set at $I = 1$. We now have a set of ‘snapped’ constellation symbols, though some of them might be wrong. We would like to correct them.

2. The frequency-domain signal $\hat{X}_k^{(I)}$, $k = 0, 1, \dots, N-1$ is processed in two branches. One branch (the central one in the figure) revises the estimate of the clipping ratio from the recently snapped constellation symbols and then recalculates alpha. It can then regenerate the attenuated symbols $\alpha\hat{X}(k)$. The clipping level A is known at the receiver, but the estimated RMS value of the true OFDM signal will be adapted hopefully towards the true value, as the iterative process progresses. In this case, the value of α will approach its true value. So the system calculates the latest RMS value of the signal in the current iteration and uses it to calculate alpha. This step produces $\alpha\hat{X}_k^{(I)}$, $k = 0, 1, \dots, N-1$.
3. The second branch (on the right of Figure 3.3) regenerates the clipped samples by passing the reconstructed frequency-domain signal through the same clipping and filtering process as in Figure 3.2. It produces $G(k)^{(I)}$, $k = 0, 1, \dots, N-1$. By the Bussgang Theorem, the clipped signal $G(k)$ can now be represented as the sum of an attenuated non-clipped signal $\hat{X}_k^{(I)}$, $k = 0, 1, \dots, N-1$ and uncorrelated clipping noise $\hat{Y}_k^{(I)}$, $k = 0, 1, \dots, N-1$.

$$G_k^{(I)} = \alpha\hat{X}_k^{(I)} + \hat{Y}_k^{(I)} \quad (3.27)$$

4. The clipping noise is estimated as:

$$\hat{Y}_k^{(I)} = G_k^{(I)} - \alpha\hat{X}_k^{(I)} \quad (3.28)$$

5. These estimated clipping noise samples are subtracted from the received signal in Step-1 to give new estimated samples for the next iteration.
6. Index I is increased to $I = I + 1$, and the steps 1 – 6 are repeated for more iterations.

3.2.2 Evaluation of BNC algorithm with different levels of AWGN

This section presents and discusses the performance of the BNC receiver as estimated by MATLAB simulations of an OFDM system using 64 subcarriers. Each subcarrier

is modulated with 16-QAM modulation. The clipping threshold is set at $A = 0.6$ with $\gamma = 1.1$ at the transmitter.

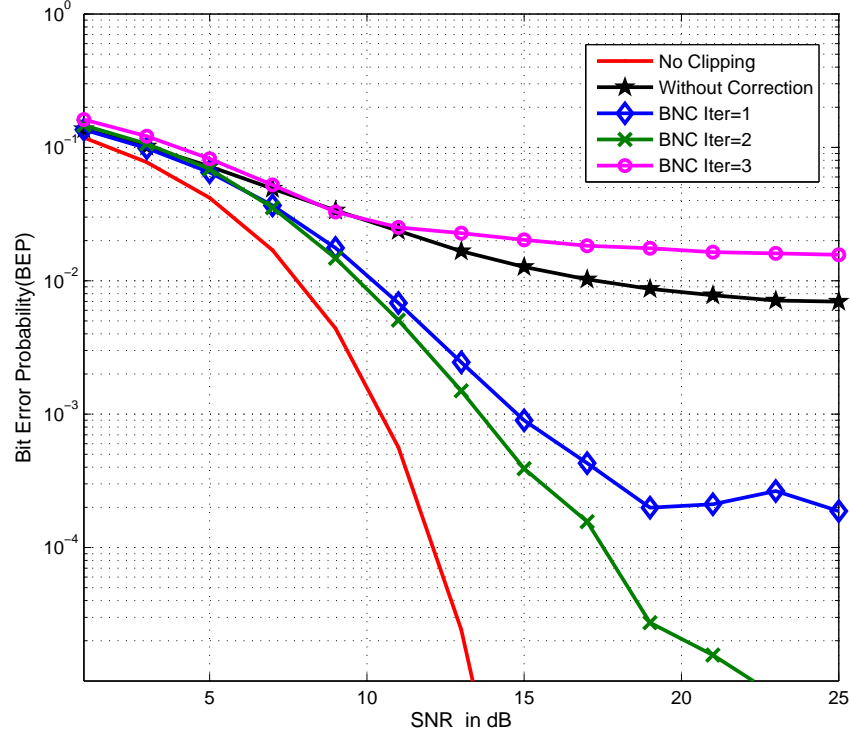


Figure 3.4: Comparison of BNC results

Figure 3.4 shows the BER performance of the BNC mechanism with 1, 2 and 3 iterations in the presence of varying degrees of AWGN. In the first iteration of the BNC algorithm, the estimated signal \hat{X}_k , $k = 0, 1..N - 1$, contains errors. Therefore the estimated noise will not be accurate, initially. It is important that the clipping noise estimated at the receiver is correlated to the noise produced at the transmitter. Since both are assumed to be the zero mean Gaussian noise, subtracting this estimated noise will then make the estimated signal better for the next iteration. The plot shows that the BNC feedback loop does not improve the performance of the receiver after more than 2 iterations. If it is unable to correct all the bit-errors as in this example, it makes matters worse by estimating inaccurate noise.

3.2.3 Finding the best value of α

It is useful to investigate how the performance of a BNC receiver is affected by the calculation of the distortion factor α . We would like to know how critically dependent the algorithm is on achieving an accurate value of α . We would also like to know how good the algorithm would be if the true Bussgang value of α were known at the receiver, and whether this ‘true value’ as known at the transmitter is really the optimum value for the receiver. Is the Bussgang theorem giving us the best possible value of α ?

This will tell us how good this technique can ever be made with the best possible optimisation technique. Three different distortion factors are defined, and the estimates for their optimum values have been produced from 1,000 randomly generated OFDM symbols. The main purpose was to investigate the effectiveness of using the Bussgang theorem to remove the clipping noise in the absence of any other noise like AWGN. Table 3.1 represents the notation to be used for the three different distortion factors.

Table 3.1: Notations of clipping distortion factor used for tests

Distortion factor	Notation
Actual distortion factor at the transmitter	α_t
Distortion factor using BNC algorithm at the receiver	α_{bg}
Distortion factor using trial and error	α_{te}

These three distortion factors are explained below in detail.

1. Actual distortion factor α_t as calculated by the Bussgang theorem at the transmitter.
2. Distortion factor α_{bg} obtained using the Bussgang theorem at the BNC receiver as explained above. Each OFDM symbol is passed through the BNC loop in two iterations to correct bit-errors. In every iteration, a new value of α_{bg} is calculated and the second iteration’s value is recorded to compare with the other two values of α .
3. Distortion factor α_{te} obtained using trial and error at the receiver. This will be the best possible value of distortion factor, even though we do not have a computationally efficient method of generating it. The receiver calculates the value of the α for the received signal and starts iterating the BNC loop but using this new value of α . The loop goes on for 100 iterations and with every iteration, α is

reduced by a factor of .005. For each new value of α , the BNC loop runs for two iterations and resultant bit-errors are calculated. Hence for each one transmitted OFDM symbol, 100 values of α with different numbers of bit-errors are calculated. The value which returns the lowest number of bit-errors, or conversely, which corrects the most bit-errors is chosen as α_{te} and the corresponding number of bit-errors is considered as the best result. There is the possibility that more than one value of α out of 100 gives same best result. In that case, the value of α which is closest to the already known α_t is selected as best.

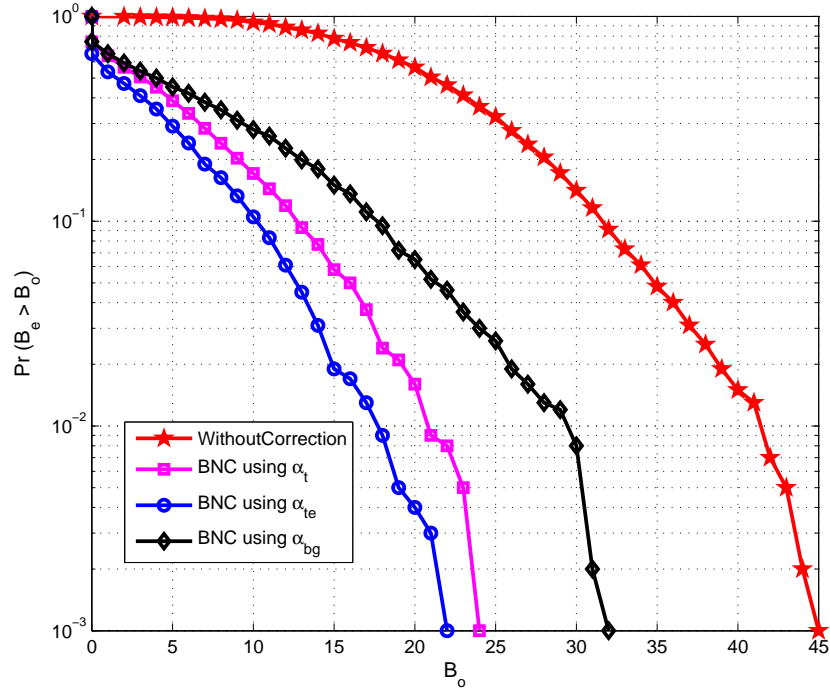


Figure 3.5: Probability of Bits in error using the three distortion factors

Figure 3.5 plots the estimates of the probability that the number of incorrect bits in an OFDM symbol, B_e before and after correction, exceed a given number B_o over a given range of 0 to 256 bits. Each estimate corresponds to three different distortion factors mentioned in Table 3.1. The red curve represents the probability of the incorrect bits received using clipping $CR = 1.0$ at the transmitter. It can be seen that α_t has corrected significantly more bit-errors than α_{bg} . Also, α_{te} is correcting more bit-errors than the other two distortion factors α_t and α_{bg} .

In order to find the relationship between these three distortion factors, we have

plotted the probability distribution functions (PDF) of the differences of the distortion factors. Figure 3.6 shows the PDF of the difference between α and α_{te} .

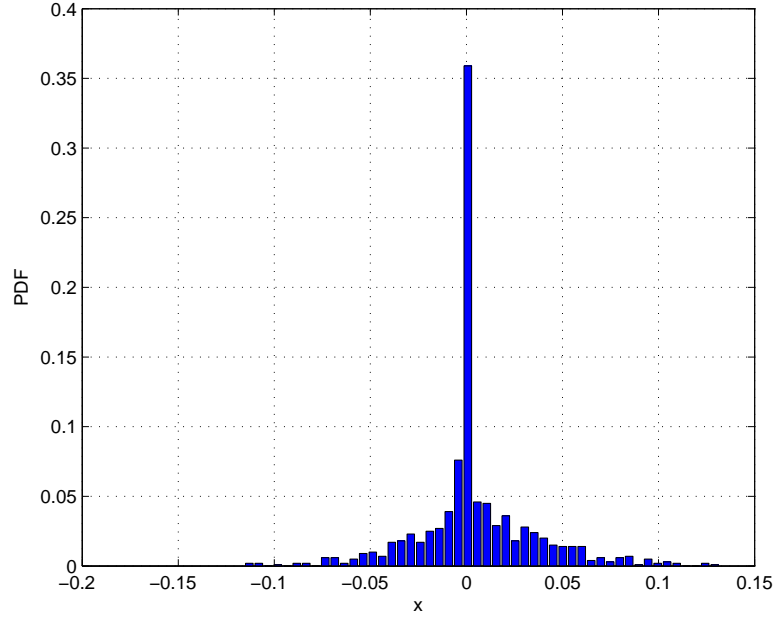


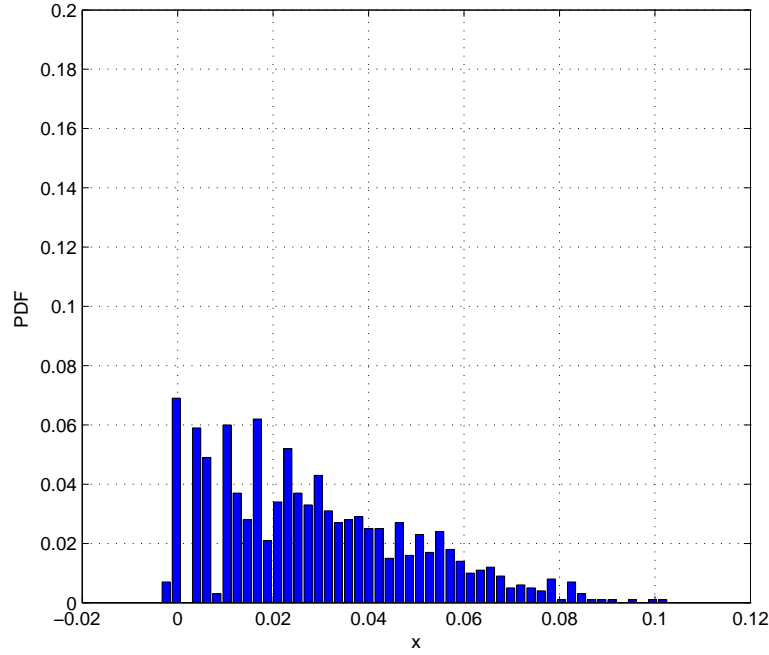
Figure 3.6: The difference of α_t and α_{te}

This plot shows that the probability that α_t and α_{te} being closest in value is approximately 0.35. This may be the reason that we can see more bit-error correction using α_t in Figure 3.5.

Figure 3.7 shows the PDF of the difference between α_t and α_{bg} . There is very low probability that for some of the transmitted OFDM symbols, the BNC receiver is able to get α_{bg} closer to that of α_t .

Figure 3.8 shows the bit-error probability against SNR for OFDM system with the Bussgang algorithm using all three different attenuation factors with BNC, in the presence of AWGN. The clipping ratio is $\gamma = 1.2$. The distortion factor α_{te} shows the least BEP among all the three defined distortion factors. α_t and α_{bg} has nearly same performance at levels of SNR. α_{te} has reduced the BEP approximately 1dB more than the other distortion factors. These differences of the performances is not negligible.

In the literature, some modifications were made to the algorithm to improve its performance, including the use of soft decisions of the received bits and FEC codes [59]. In this study, this algorithm has been simulated without any FEC codes with hard decisions to emphasize the main function of the Bussgang theorem.

Figure 3.7: The difference of α_t and α_{bg}

3.2.4 Decision Aided Reconstruction

This iterative receiver tries to reconstruct the received signal to its non-clipped form using the received equalized signal and the estimated signal in the time-domain. This approach assumes $\alpha = 1$, and therefore Equation 3.25 can be written as

$$R_k = H_k \cdot (X_k + D_k) + Y_k \quad 0 \leq k < N - 1 \quad (3.29)$$

The DAR loop has been presented in the literature with some modifications using a Turbo-DAR loop which takes the advantage of soft input soft output (SISO) nature of Turbo codes and improves the performance [60], [61]. Conventional DAR receivers work at Nyquist sampled signals. Therefore, we have modified the DAR receiver by incorporating a filter in it, to make it work with clipped and filtered signals. Figure 3.9 shows the mechanism of a DAR loop. The clipping amplitude A is assumed to be known at the receiver. The steps of DAR are as follows:

1. The received signal, after applying an FFT to it, is as in Equation 3.29. It is then oversampled in the time-domain by inserting $N \cdot (J - 1)$ zeros symmetrically in the frequency-domain. From here the oversampled signal is processed

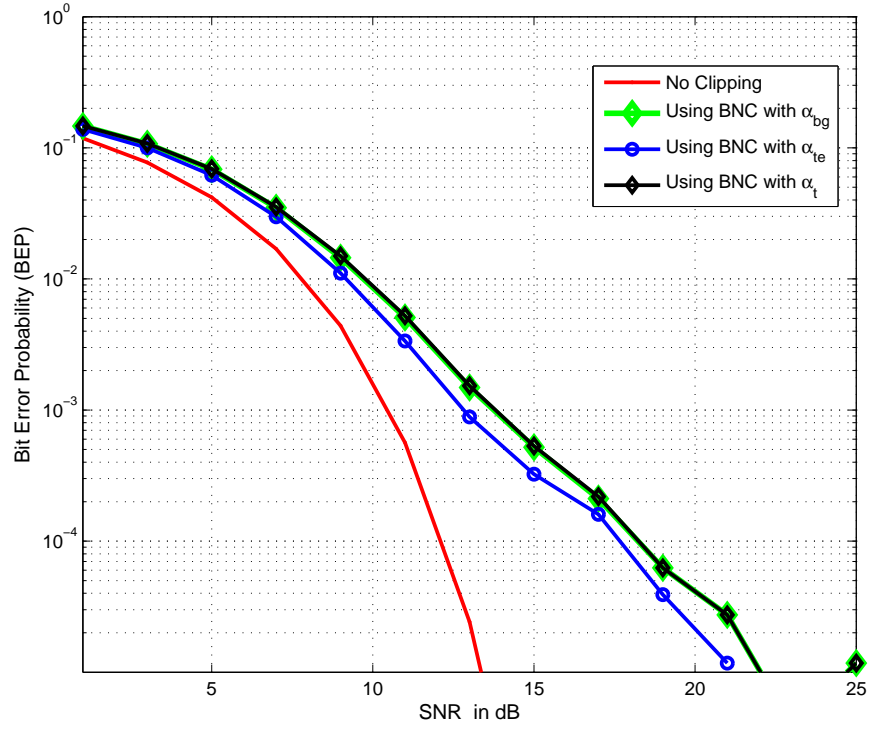


Figure 3.8: BEP against SNR using all three distortion factors with the BNC receiver

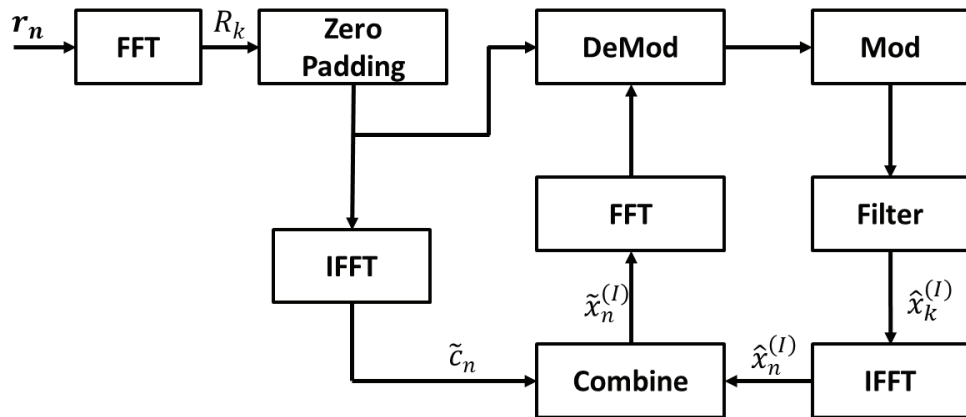


Figure 3.9: DAR Process

through two branches. One branch applies an FFT to obtain the oversampled time-domain clipped signal \tilde{c}_n .

2. The other branch demodulates the oversampled sequence and then remodulates it by snapping (i.e. quantising) to the same modulation scheme as is used at the transmitter. In this way, shrinkage of the constellation caused by clipping is reduced. The modulated sequence is then $\hat{X}_k, k = 0, \dots, JN - 1$ where I represents an iteration number with initial value of $I=1$.
3. An out-of-band frequency-domain filter may be applied on the decisions in step 2 as:

$$\hat{X}_k = \begin{cases} \hat{X}_k, & \text{for } 0 \leq k < \frac{N}{2} \text{ and } JN - \frac{N}{2} < k \\ 0, & \text{elsewhere} \end{cases} \quad (3.30)$$

4. The filtered output in step 3 is converted back to the time-domain using an IFFT producing \hat{x}_n .
5. The samples produced at step 1 and the time-domain samples produced at step 4 are now combined to detect clipped samples and generate a new sequence as

$$\tilde{x}_n = \begin{cases} \tilde{c}_n, & |\hat{x}_n| \leq A \\ \hat{x}_n, & |\hat{x}_n| > A \end{cases} \quad (3.31)$$

6. The sequence \tilde{x}_n is converted back to the frequency-domain by applying an FFT producing \tilde{X}_k .
7. The sequence \tilde{X}_k is demodulated and re-modulated with snapping as in step 2 and the first iteration completes here.
8. The index number I is increased as $I = I + 1$ and the frequency-domain signal in step 3 is replaced with \tilde{X}_k .
9. To continue the iterations, steps 3 – 7 are repeated.

3.2.5 Results and Discussion

The performance of the DAR receiver has been evaluated for an AWGN channel. The BER is calculated by comparing the transmitted and received constellations. Figure 3.10 illustrates the BER performance of DAR with and without band-pass filtering at

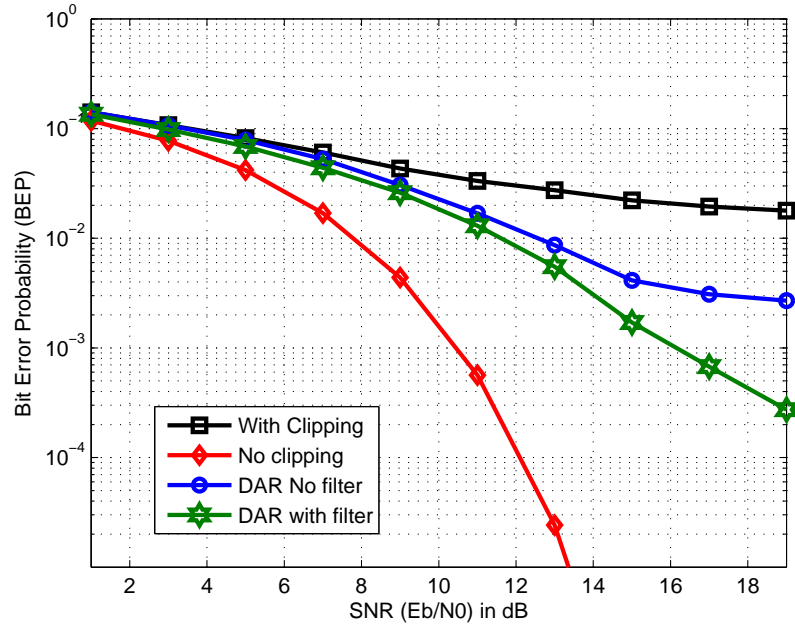


Figure 3.10: Comparison of modified DAR with original DAR

step 3. The 16-QAM modulation has been used for the simulations and the number of OFDM subcarriers N is set to 64, CR is set to 1.2 and number of iterations is 2. There is a lower bound which shows the performance of OFDM in AWGN with no clipping. For the modified DAR, the signal at the transmitter is oversampled and filtered, so all the noise does not fall in-band which makes the performance better at the receiver. The modified DAR loop shows better performance in terms of BER as compared to the original form of DAR. Figure 3.11 shows the BEP obtained using a DAR receiver using different number of iterations. We have observed that the DAR receiver stops improving soon after 2 iterations. For all iterations higher than 2, it shows nearly the same BEP for all levels of SNR.

3.3 Comparison of the BNC and DAR receivers

Figure 3.12 shows a comparison of the performances of the DAR receiver and the BNC receiver plotting the BEP against signal to noise ratio (SNR). The BEP has reduced much in the case of the BNC receiver. The BEP at SNR=14dB for BNC is 0.0005 and for DAR receiver at the same level of SNR it is 0.005. There is a huge difference in the reduction of the BEP at all levels of SNR. The number of iterations for both the

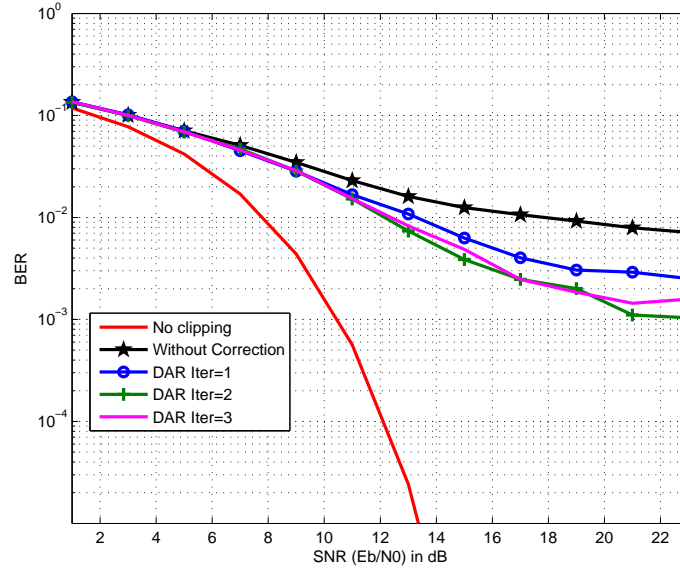


Figure 3.11: DAR with multiple iterations

receivers was kept at 2, as they both stop improving after 2 iterations.

3.4 Inverted Wrap-Around (IWRAP) limiting

In this section, the use of Inverted Wrap (IWRAP) limiting in place of clipping is investigated. The effect of the IWRAP limiting function is illustrated in Figure 3.13. Soft-clipping limits the peaks to a threshold and discards the overshoot, whereas IWRAP wraps-around the peaks inside invertedly. In other words the components of the complex waveform whose magnitude is above the threshold are removed and added back into the signal. The limited samples of the signal are therefore made smaller than the threshold. Equation 3.32 shows the limiting function for IWRAP.

$$c_n = \begin{cases} x_n, & \text{if } |x_n| \leq A \\ e^{j\theta(n)} \cdot (2 \times A - |x_n|), & \text{if } |x_n| > A \end{cases} \quad (3.32)$$

where x_n is the original unclipped time-domain complex signal, c_n is the signal after IWRAP limiting, A is the predefined magnitude threshold, $\theta(n)$ is the argument of the complex sample x_n and $|x_n|$ is the magnitude of x_n . The distortion factor α for IWRAP

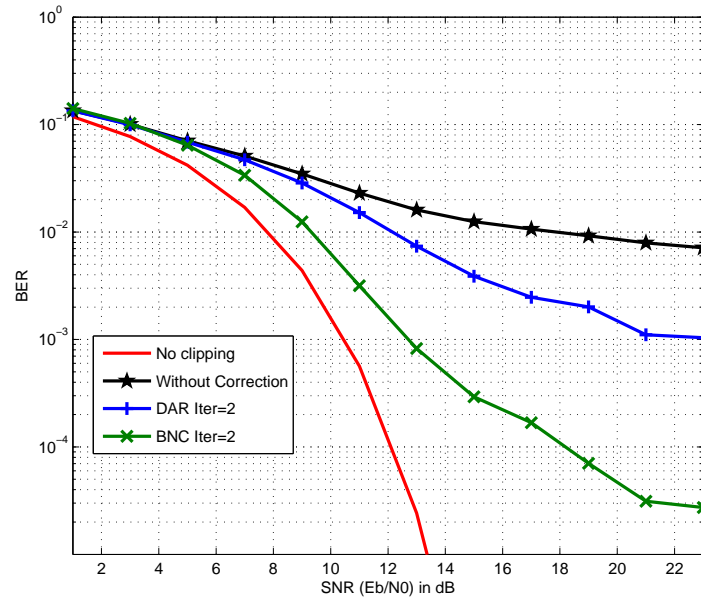


Figure 3.12: Comparison of DAR and BNC

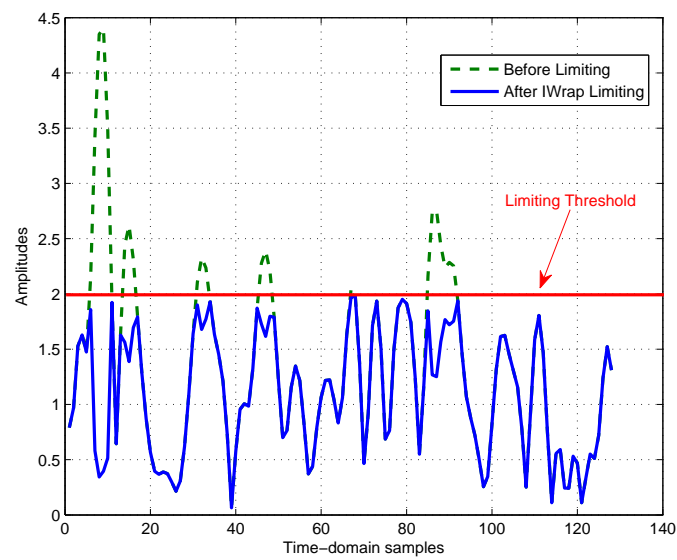


Figure 3.13: Iwrap Limiting

limiting can be calculated using the following equation:

$$\alpha = 1 - 2e^{-\gamma^2} + \sqrt{\pi} \operatorname{erfc}(\gamma) \gamma \quad (3.33)$$

where γ represents the clipping ratio and erfc is the complementary error function defined as:

$$\operatorname{erfc}(x) = \frac{2}{\sqrt{\pi}} \int_x^\infty e^{-t^2} dt \quad (3.34)$$

The derivation of α for this form of limiting is given in Appendix A. The output power of the IWRAP limited signal is given by:

$$P_{xcn} = (1 - 2\gamma\sqrt{\pi}\operatorname{erfc}(\gamma)) P_{xn} \quad (3.35)$$

The derivation for the output power of the IWRAP limited signal is given in Appendix B.

3.5 Evaluating Parameters for limiting

PAPR reduction schemes may be evaluated through the following parameters: PAPR reduction, PSD, BER analysis in coded and uncoded systems.

3.5.1 BER Analysis

Clipping strongly affects the overall performance of the OFDM system when the clipped signals are passed through the AWGN channel.

The Bit-error probability (BEP) for OFDM system with 64 subcarriers, modulated by 16-QAM with uncoded bits is shown in Figure 3.14 with various clipping ratios. It is evident that the system performance is degraded highly even at a moderate clipping ratio, i.e, CR=1.4.

Figure 3.15 shows the OFDM bit-error probability using IWRAP and soft-clipping both with BNC receivers. These probability estimates were produced using MATLAB simulations by transmitting 10,000 OFDM symbols with 16-QAM modulation. The clipping ratio is set to $\gamma = 1.8$. The limiting distortion produced by IWRAP is large than that with soft-clipping. The performance of the BNC algorithm with soft-clipping is much better than the performance of BNC with IWRAP. The use of the BNC receiver with IWRAP still improved the BEP. But clipping without any correction is even better

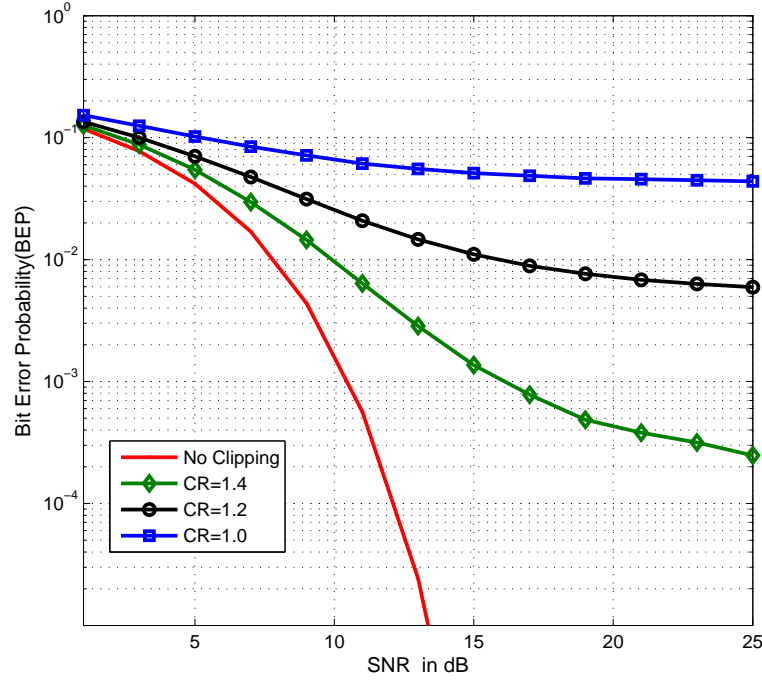


Figure 3.14: BEP of clipped 16-QAM mapped OFDM signal in AWGN channel

than IWRAP with BNC.

3.5.2 Power Spectral Density (PSD)

When limiting is applied to an oversampled signal, energy is generated at frequencies outside of the signal bandwidth. This phenomenon is called spectral regrowth. The PSD plotted in Figure 3.16 shows the effect of the clipping and IWRAP before and after filtering. Both limiting techniques produce out-of-band which is eliminated by applying a filter. The black plot shows the filtered signal after applying a FFT/IFFT filter.

3.5.3 PAPR Reduction and Peaks Re-growth

The main problem of clipping is that we are distorting the signal in-band and out of band. A band-limiting filter is applied to suppress the spectral regrowth but this filtering process increases PAPR.

As mentioned above, repeated clipping and filtering has been proposed by [8] to address the peak regrowth issues. The repeated process significantly reduces peaks

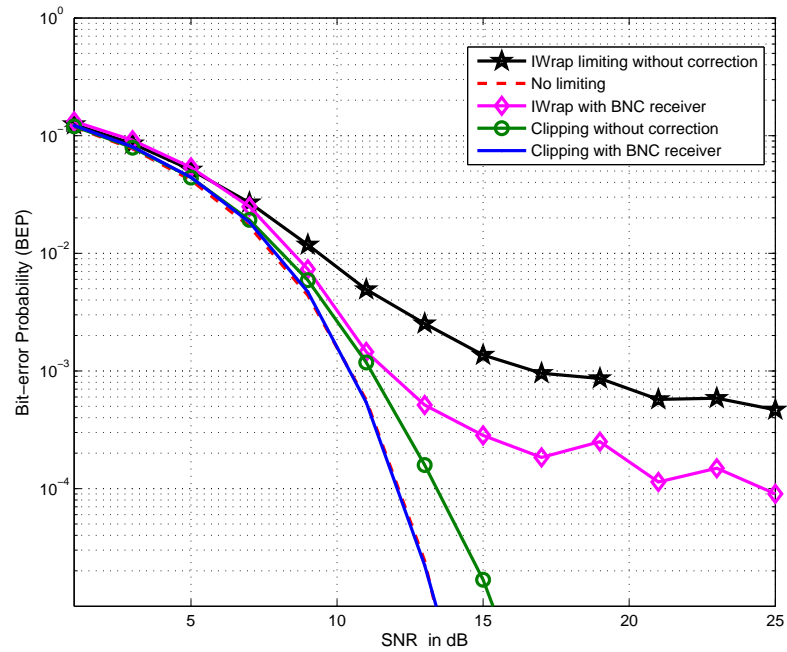


Figure 3.15: IWRAP and soft-clipping with BNC

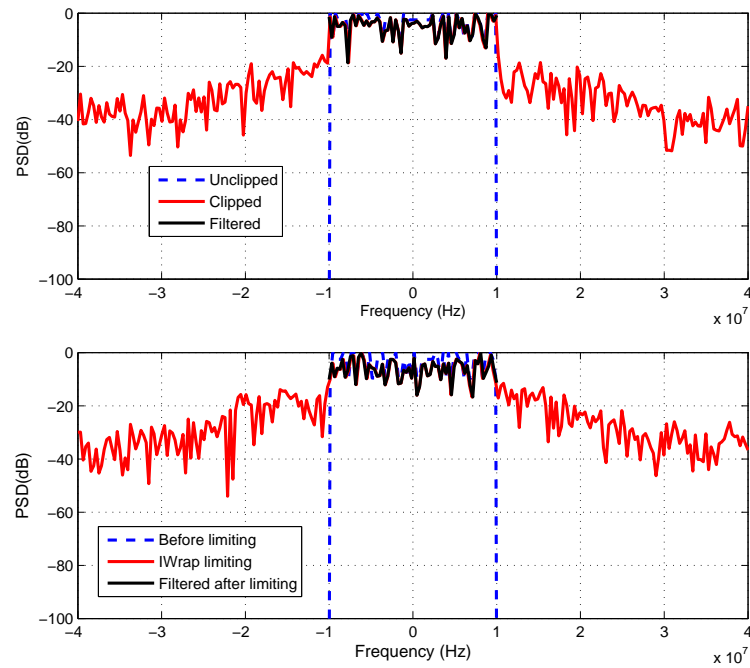


Figure 3.16: PSD for clipping and IWRAP

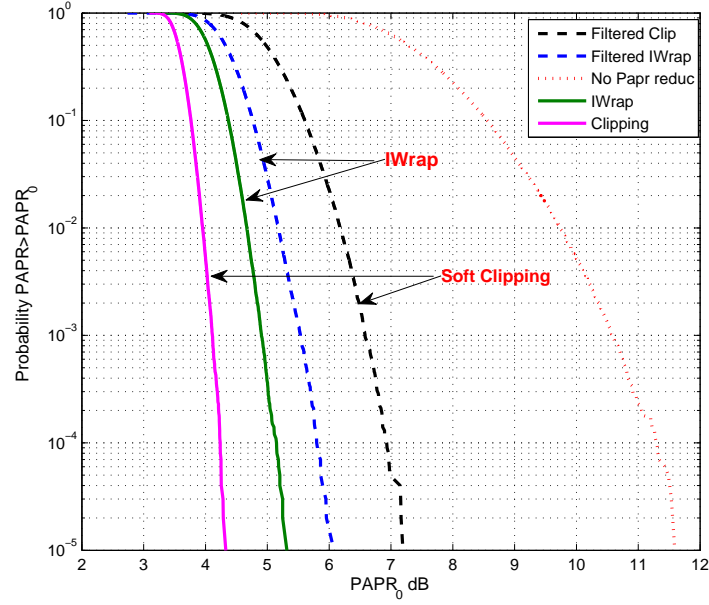


Figure 3.17: Probability of $PAPR > PAPR_0$ for soft-clipping and IWRAP limiting

re-growth at the expense of the number of repeats. However, every iteration costs a lot of computation. The computation involved in repeated clipping and filtering led us to propose IWRAP limiting. Figure 3.17 shows a comparison of PAPR reduction using soft-clipping and IWRAP limiting after limiting and filtering. The peak re-growth using the IWRAP with filtering is clearly smaller than the peaks re-growth obtained using clipping with filtering.

3.6 Conclusions

In this chapter soft-clipping as applied to base-band signals has been described along with its effects and performance. The effect of soft-clipping applied to Nyquist sampled signals and oversampled signals has been explained. Two clipping noise mitigating receivers have been compared in terms of BER. Robust optimisation techniques have not yet been devised and convergence issues have not been fully considered. However, the capabilities of the techniques have been investigated. An investigation of the derivation of the distortion factor α BNC receiver showed that the best value of α , which gives the maximum bit-error correction, is not obtained, also that it is not the value derived at the transmitter. A better value may be obtained by trial and error. Nevertheless, the results show that the BNC algorithm adjusted for attenuation factor

can be made to perform better than a DAR loop with added filter. For the BNC algorithm, if an accurate value of α and CR is estimated in each iteration, the signal can be recovered significantly, for lower levels of clipping. However, the crux in the computation for the BNC receiver is the JN point IFFT and FFT which must be performed in each iteration along with the clipping and filtering block.

Soft-clipping when applied with filtering increases the PAPR after filtering. IWRAP, an alternative limiting technique has been proposed to limit the high peaks of the time-domain OFDM signal. It effectively reduces the re-growth of the high peaks after filtering. The results of CCDF has been presented in comparison to soft-clipping and filtering. A slight BER degradation has been observed as compared to soft-clipping. IWRAP can be effectively used with other techniques in the literature e.g. [32], which are combined to work with soft-clipping and where side information transmitted.

Chapter 4

Equation-Method

This chapter describes a method that has been derived for reducing the non-linear distortion produced by clipping of OFDM signals. It is called the Equation-Method. Most of the ideas presented here were published in contribution [62]. At the transmitter, soft clipping is applied to the time-domain signals before amplification. The clipped signal at the receiver is used to generate equations for calculating the unclipped form of the signal. These equations are based on the fundamental concept of the FFT. Four different enhancements of the basic method are discussed in this chapter.

4.1 Problem Formulation

Soft-clipping is performed in the time-domain as described in Chapter 3 Section 3.1.1. The amplitudes of the time-domain samples are limited to a predefined threshold A , keeping the phases unchanged. The soft-clipping is applied at the Nyquist sampling rate, hence the algorithm has been used so far for mitigating in-band distortion only. The effect of out-of-band distortion will not be addressed.

The receiver applies the received complex clipped time-domain signal to an N th order FFT to convert it into the frequency-domain:

$$Y_k = \sum_{n=0}^{N-1} x_n \cdot e^{\frac{-j2\pi nk}{N}} \quad (4.1)$$

where x_n is the received time-domain signal and Y_k is the frequency-domain version. The algorithm of FFT used for this method is the commonly used Cooley-Tukey formulation. This algorithm computes N discrete frequency components from N discrete

time-domain samples, where $N = 2^r$, r is any integer. Let us denote:

$$P = e^{-\frac{j2\pi}{N}} \quad (4.2)$$

Then we can write the Equation 4.1 as:

$$Y_k = \sum_{n=0}^{N-1} x_n \cdot P^{nk} \quad (4.3)$$

The FFT may be expressed in the matrix form as:

$$\underline{Y} = P \cdot \underline{x} \quad (4.4)$$

where \underline{x} and \underline{Y} are the $N \times 1$ vectors of time-domain and frequency-domain samples respectively, and the elements of the $N \times N$ matrix P are as follows:

$$p(n, k) = \exp(-2 \times \pi \times j \times (n-1) \times (k-1)/N) = P^{nk} \quad (4.5)$$

$$\begin{bmatrix} Y_0 \\ Y_1 \\ \vdots \\ Y_{N-1} \end{bmatrix}_{N \times 1} = \begin{bmatrix} P^0 & P^0 & P^0 & \dots & P^0 \\ P^0 & P^1 & P^2 & \dots & P^{N-1} \\ \vdots & \vdots & \vdots & \dots & \vdots \\ P^0 & P^{N-1} & P^{2(N-1)} & \dots & P^{(N-1)^2} \end{bmatrix}_{N \times N} \times \begin{bmatrix} x_0 \\ x_1 \\ \vdots \\ x_{N-1} \end{bmatrix}_{N \times 1} \quad (4.6)$$

If \underline{x} undergoes a nonlinear function such as clipping, the effect of clipping in the time-domain will be reflected in the frequency-domain constellation symbols, as will be explained in the next section.

4.1.1 Effect of Clipping on Constellation Symbols

Applying an FFT to a received OFDM symbol produces complex constellation symbols which may be mapped onto an Argand diagram with real and imaginary axes. The collection of all possible symbol points forms a constellation. Different modulation schemes have different constellation structures. The constellations for all possible modulation techniques (PSK, QPSK, 16-QAM, etc.) are defined by standardised fixed positions on the complex plane. But when the symbol has been clipped and is also affected by channel noise (AWGN), the received constellation points will be different

from those of the transmitted symbol.

If the clipping distortion and channel noise are small, it is possible that the received constellation symbols are close, in a Euclidean sense, to the fixed constellation points. In this case, ‘snapping’ each received constellation symbol to the nearest fixed constellation point will recreate the original constellation at the transmitter, and no bit-errors at all will then be incurred. The maximum likelihood detection rule is to detect the symbol s_1 if the distance between the received symbol (r_I, r_Q) is closest to the constellation symbol (s_I, s_Q) , where s_1 is the constellation out of fixed 16 points for 16-QAM on the constellation diagram.

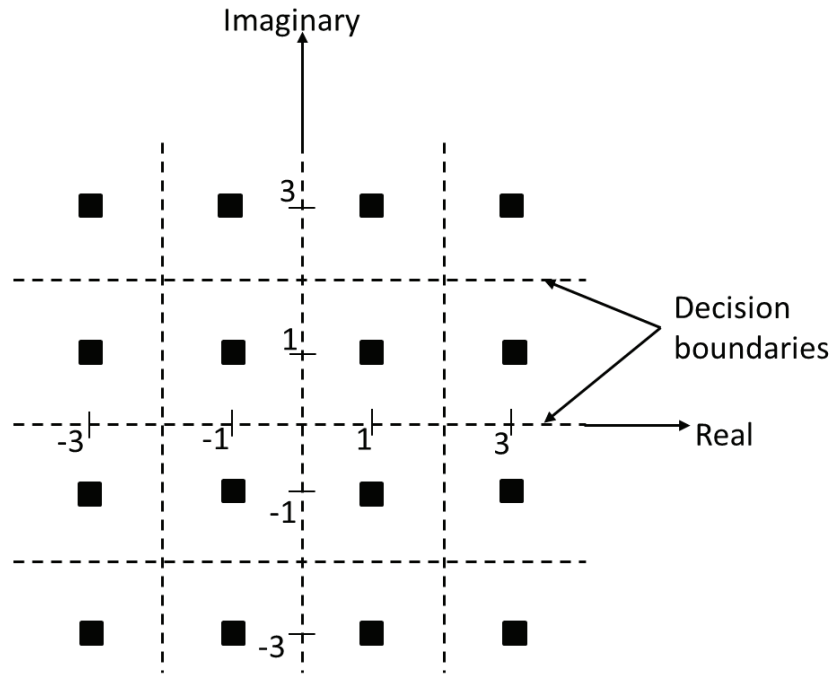


Figure 4.1: Decision boundaries for snapping

The received OFDM symbols after applying an FFT have to be demapped from the constellation. Two steps are involved in this process. On the basis of Euclidean distance all the received constellation symbols are snapped to their nearest constellation points. And then the constellation is demapped to return to the binary output.

Figure 4.2 shows an example with $N = 8$ and 16-QAM modulation. The signal has been clipped at $\gamma = 1.0$. Plot(1,1) in Figure 4.2 shows the fixed constellation points of 16-QAM constellation. The mapped constellation symbols are represented by filled squares in Figure 4.2, Plot(1,2). The effect of clipping on the constellation symbols is demonstrated by displaced blue filled squares in Figure 4.2, Plot (2,1). According

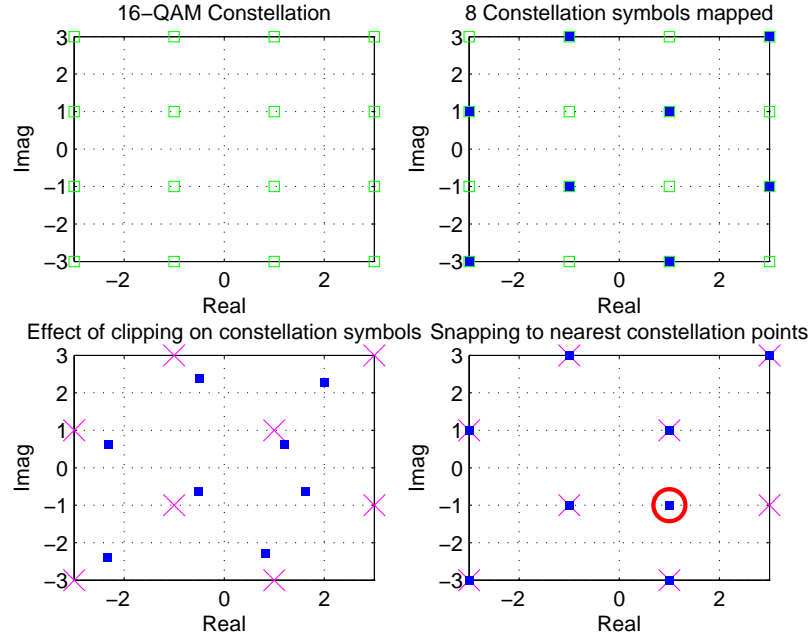


Figure 4.2: An example of constellation snapping

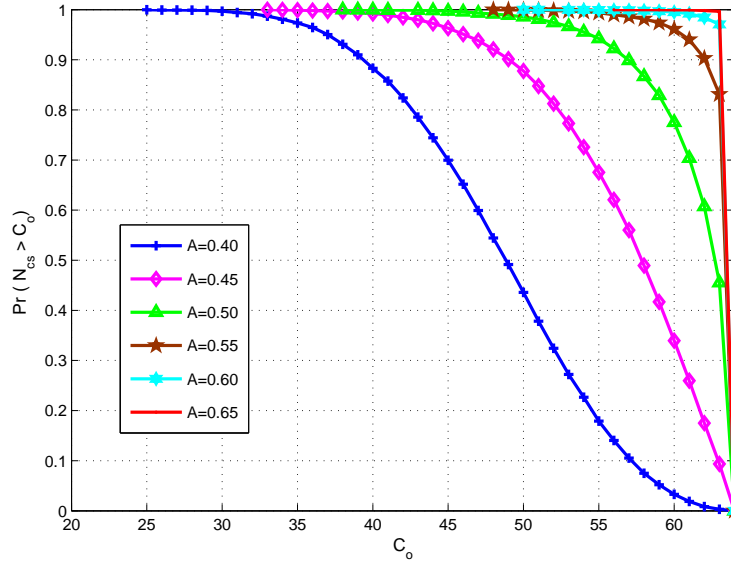
to the snapping process, the distorted constellation symbols will be snapped to their nearest constellation points as illustrated in Figure 4.2, Plot (2,2). Due to the effect of the clipping, one constellation symbol has been snapped to a wrong constellation point which produces bit-errors. The constellation symbol in red circle is representing the wrongly snapped point.

In more interesting cases where clipping distortion and/or channel noise cause some received symbols to move further away from the true constellation points, bit-errors are produced when these received symbols are snapped to incorrect constellation points.

4.1.2 Effect of clipping with no bit-error correction

This section investigates the performance of the proposed algorithm by the MATLAB simulation of an OFDM system with 64 sub-carriers and a 16-QAM constellation on each sub-carrier. The effect of clipping has been assessed when there is no bit-error correction.

Figure 4.3 plots estimates of the probability that the number, N_{cs} , of correctly snapped constellation symbols in an OFDM symbol at the receiver exceeds a given

Figure 4.3: Distribution of N_{cs} with no symbol-error correction

number, C_o , over the range 0 to 63, when there is no attempt at symbol-error correction. Each estimate corresponds to a different value of the clipping threshold A over a range from 0.4 to 0.65. The average power of the OFDM signal, estimated over 10,000 OFDM symbols, is 0.156, therefore the clipping ratio (CR) varies from approximately 1.01, when $A = 0.4$ to 1.64 when $A = 0.65$. The Clipping ratio (CR) is defined as the ratio of the clipping threshold A to the root mean square (RMS) value σ of the OFDM signal. The range therefore encompasses mild to very severe clipping.

The probability estimates were produced from 10,000 randomly generated OFDM symbols for each selection of clipping threshold A . The plots show that even with very severe clipping ($A = 0.4$) and no error correction, there is still a reasonably high probability that more than half of the constellation symbols are correct, though the probability of having all symbols correct is low even for mild clipping.

The curve plotted in Figure 4.4 shows the probability of an OFDM symbol error for different values of A . An OFDM symbol is error-free only when all constellation symbols are correct, and therefore all bits, are received correctly. Without symbol-error correction, the OFDM symbol error rate is seen to increase rapidly as the clipping threshold decreases.

The Equation-Method aims to use the information provided by correctly snapped symbols to correct clipping distortion in the time-domain. Where the majority of the symbols received are correctly snapped, this is likely to be quite straightforward as

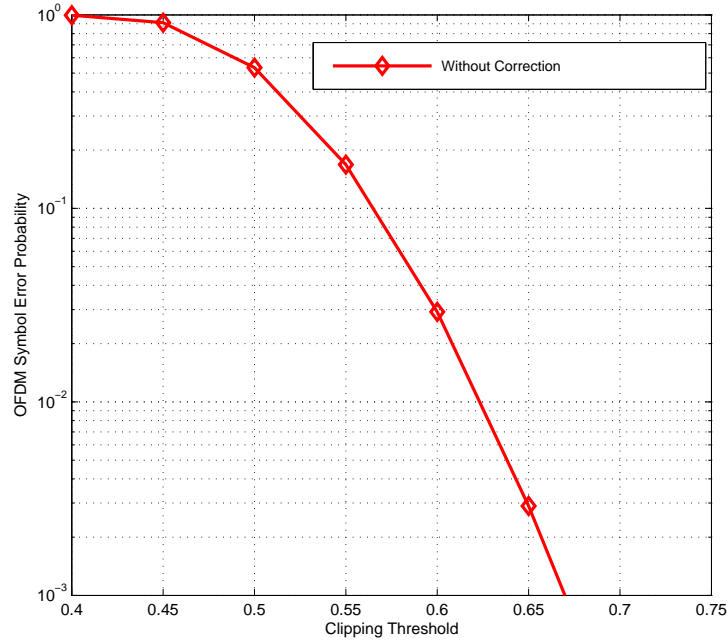


Figure 4.4: OFDM symbol error probability without correction

illustrated by the data in Table 4.1.

Table 4.1 gives details about the maximum and minimum number of clipped samples with different clipping thresholds. This data has been produced by transmitting 10,000 OFDM symbols modulated with 16-QAM for all the clipping thresholds. It is evident from the table that even at severe clipping, there are likely to be enough unclipped correct samples for generating equations to try to correct the clipped ones.

4.2 The Equation-Method

This method relies on the receiver being able to identify which time-domain samples are likely to have been clipped and which constellation symbols are likely to be correctly received. This is reasonably straightforward when the additive white Gaussian channel noise is negligible and the clipping level A is known at the receiver. We consider this case first. At the receiver, the received time-domain samples are converted to frequency-domain complex symbols which are snapped to the fixed constellation points according to the procedure mentioned above in Section 4.1.1. If we can identify which samples are going to be clipped, and which frequency-domain samples will be correct at the receiver after being snapped to the standard constellation, the original

Table 4.1: Estimate of Clipped Samples before Error-Correction

A	Max No. of Clipped Samples	Min No. of Clipped Samples
0.75	7	0
0.70	9	0
0.65	10	0
0.60	14	1
0.55	18	2
0.50	22	4
0.45	26	9
0.40	30	13

FFT Equation 4.6, before clipping or snapping, may be partitioned as:

$$\begin{bmatrix} \underline{Y}_R \\ \underline{Y}_U \end{bmatrix} = \begin{bmatrix} G & F \\ E & D \end{bmatrix} \times \begin{bmatrix} \underline{x}_c \\ \underline{x}_o \end{bmatrix} \quad (4.7)$$

where the vector \underline{Y} is partitioned as \underline{Y}_R representing ‘reliable’ frequency-domain symbols and \underline{Y}_U giving $N - M$ ‘unreliable’ symbols that are considered less likely to be correct at the receiver. Time-domain vector \underline{x} is divided in two sub-vectors: i.e. the set of L samples likely to be clipped \underline{x}_c and the other $N - L$ samples that are not likely to be clipped. Determining L and M is the key to this method, as will be discussed later. The matrix P is partitioned such that G and E are, respectively, $M \times L$ and $(N - M) \times L$ sub-matrices of the sinusoidal coefficients associated with the time-domain samples \underline{x}_c . F and D are, respectively, $M \times (N - L)$ and $(N - M) \times (N - L)$ sub-matrices of the sinusoidal coefficients associated with the ‘other’ time-domain samples held by vector \underline{x}_o . Sub-matrices G and F also correspond to the M ‘reliable’ frequency-domain symbols in vector \underline{Y}_R , whereas E and D correspond to the $(N - M)$ ‘unreliable’ frequency-domain symbols in vector \underline{Y}_U .

Equation 4.7 is the true FFT equation which can be programmed only when we know all the time-domain samples exactly. This will not be the case at the receiver as it will not know the true values of the clipped samples. If the receiver knew the true constellation samples in the \underline{Y} vector it could invert the FFT matrix and thus find the true values of the clipped samples. But this is not possible either because there are likely to be incorrect constellation values in the \underline{Y} vector as constructed at the receiver. In this scenario, after receiving a clipped symbol, the receiver converts it to frequency-domain symbols and snaps them to the standard constellation symbols to

produce vector $\hat{\underline{Y}}$ which is not necessarily equal to \underline{Y} . Dividing the received complex time-domain samples $x(n)$ for $n = 1, 2, \dots, N$, into clipped samples $x_c(n)$ for $n = 1, \dots, L$ and non-clipped samples (the others) $x_o(n)$ for $n = 1, \dots, NL$ allows the FFT Equation 4.4 at the receiver to be written as follows:

$$\begin{bmatrix} \hat{\underline{Y}}_R \\ \hat{\underline{Y}}_U \end{bmatrix} = \begin{bmatrix} G & F \\ E & D \end{bmatrix} \times \begin{bmatrix} \hat{\underline{x}}_c \\ \underline{x}_o \end{bmatrix} \quad (4.8)$$

We have given $\hat{\underline{Y}}_R$ a hat in Equation 4.8 because the identification of ‘reliable’ and ‘unreliable’ will not always be done correctly. In Equation 4.8, the frequency-domain symbols \underline{Y} have been partitioned according to whether they are considered likely to be reliable ($\hat{\underline{Y}}_R$) or unreliable ($\hat{\underline{Y}}_U$), and not according to whether they are correct or incorrect after they have been snapped to the nearest constellation point. The dimensions of $\hat{\underline{Y}}_R$ and $\hat{\underline{Y}}_U$ are $M \times 1$ and $(N - M) \times 1$ respectively. Now, multiplying out the upper part of the partitioned matrix equation, we obtain:

$$\hat{\underline{Y}}_R = G \times \hat{\underline{x}}_c + F \times \underline{x}_o \quad (4.9)$$

If we first consider the case where when $L = M$, provided G is non-singular, the clipped time-domain samples, now treated as unknowns, may be obtained as follows:

$$\hat{\underline{x}}_c = G^{-1}(\hat{\underline{Y}}_R - F \times \underline{x}_o) \quad (4.10)$$

This illustrates that the true values of the clipped time-domain samples may be obtained from a knowledge of the other time-domain samples and the frequency-domain samples considered reliable when the latter are correctly snapped in the constellation. This approach is entirely practical and just requires the identification of L reliable constellation points when there are L clipped samples. There may be more than L reliable constellation points, but just L of them need to be selected in the case.

4.2.1 Equal number of Equations and unknowns

If it is arranged that the number of chosen reliable frequency domain samples is equal to the number of clipped time-domain samples, there are an equal number of equations and unknowns and the matrix G is square. For these equations to be solved for a valid and unique solution, G has to be non-singular. Taking an example for $N = 4$, the matrix

of powers of exponentials for $N = 4$ may be written as:

$$P = \begin{bmatrix} p^0 & p^0 & p^0 & p^0 \\ p^0 & p^1 & p^2 & p^3 \\ p^0 & p^2 & p^4 & p^6 \\ p^0 & p^3 & p^6 & p^9 \end{bmatrix}_{4 \times 4} \quad (4.11)$$

The sinusoidal coefficients from Equation 4.11 are plotted in Figure 4.5. P is a

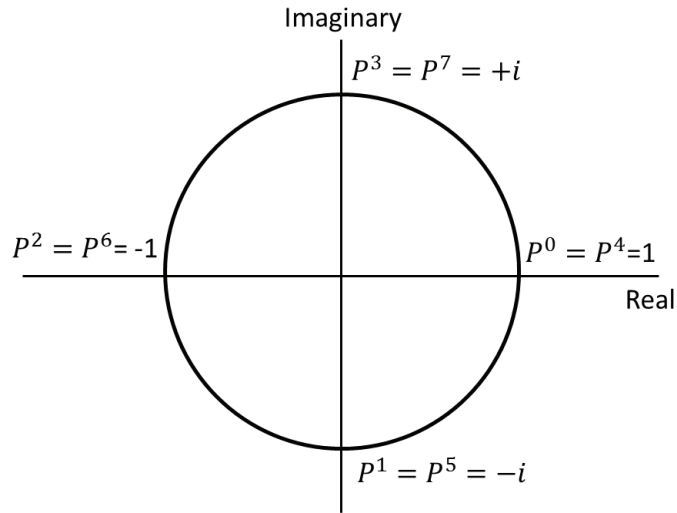


Figure 4.5: Powers of the exponential function P for $N=4$

symmetric and orthogonal matrix and hence invertible. Figure 4.5 shows that the symmetry properties hold where: $P^N = P^0 = 1$, $P^{N/2} = -1 = -P^0$. P is invertible, but we are not sure whether if we extract any sub-matrix from the matrix P , it will also be invertible.

As an example, assume that the 1st and 3rd samples were clipped, which make 2nd and 4th frequency-domain symbols unreliable. So the matrix G for this example will be extracted from Equation 4.11 as:

$$G = \begin{bmatrix} p^0 & p^0 \\ p^0 & p^4 \end{bmatrix}_{2 \times 2} \quad (4.12)$$

Using the values in Figure 4.5 for the matrix G , we can see that it is singular. Similarly there are few more combinations of the exponential which if combined to make the matrix G , will make it singular. Therefore the problem of singularity can occur

when G is square, and it will occur more frequently if the period of the frequency-domain signal is large. The extension of this technique to over-determined sets of equations where G is not square but ‘thin’ rectangular is a good way of avoiding this singularity problem.

4.2.2 Overdetermined number of equations

If we could have total confidence in the selection of L equations for the L unknowns, and guaranteeing a non-singular matrix G , the square matrix approach in the previous section would be optimal. In practice we cannot have such confidence especially when striving to make this method work for ever higher degrees of clipping and ever higher levels of AWGN. In general, the M by L matrix G need not be square. There may be more reliable constellation symbols than clipped samples, in which case G will be rectangular and ‘thin’ meaning that there are more equations than unknowns. This is the over-determined case with $M > L$.

The under-determined case where $M < L$ is also possible under very severe conditions, but as it is unlikely that the method could be made to work for this case, it is disregarded. Where the coefficient matrix G is thin rectangular, rather than just rejecting equations to make it square, it is generally better to use the ‘pseudo-inverse’ approach to calculate a ‘least squares’ solution to the over-determined set of equations. This requires the use of the Moore-Penrose pseudo-inverse [63] which will now be explained. Assume that the possibly over-determined set of equations are expressed as:

$$\underline{W} = G\underline{x} \quad (4.13)$$

where \underline{x} denote $\hat{\underline{x}}_c$, \underline{W} denotes $(\hat{\underline{Y}}_R - F \times \underline{x}_o)$ and G is M by L with $M \geq L$. If G were a non-singular square matrix it would be possible to make $\underline{W} = G\underline{x}$ by taking

$$G\underline{x} = G^{-1}\underline{W} \quad (4.14)$$

Where G is not necessarily square, the ‘least squares’ requirement is that the vector of coefficients, \underline{x} , must be found such that $G\underline{x}$ is made as close as possible to \underline{W} or, in other words, the ‘difference signal’:

$$\underline{D} = G\underline{x} - \underline{W} \quad (4.15)$$

is made close as possible to zero. Multiplying both sides of Equation 4.13 by G^T

(T means ‘transformed’) gives:

$$G^T \cdot \underline{W} = G^T \cdot G \cdot \underline{x} \quad (4.16)$$

and noting that since the dimensions of G and G^T are M by L and L by M respectively, $G^T \cdot G$ will be a square matrix of dimension M by M . When this matrix is non-singular, we can write:

$$\underline{x} = (G^T \cdot G)^{-1} G^T \underline{W} \quad (4.17)$$

or:

$$\underline{x} = G^\# \cdot \underline{W} \quad (4.18)$$

where the L by M matrix $G^\#$ is defined as the ‘pseudo-inverse’ of the M by L matrix G :

$$G^\# = (G^T \cdot G)^{-1} G^T \quad (4.19)$$

Clearly, it cannot be expected that defining vector \underline{x} by Equation 4.18 satisfies Equation 4.13 except when G is square. But let

$$E = \|G\underline{x} - \underline{W}\|_2 \quad (4.20)$$

$$E = (G\underline{x} - \underline{W})^T (G\underline{x} - \underline{W}) \quad (4.21)$$

$$= \sum_{i=1}^M (d_i)^2 = \|D\|_2 \quad (4.22)$$

where d_i are the elements of D and $\|D\|_2$ denotes the ‘norm’ of D . This is the sum of squared differences between elements of \underline{W} and the corresponding elements of $G\underline{x}$ and is a measure of the difference between $G\underline{x}$ and \underline{W} , or in other words the ‘sum of squares’ error. Multiplying out Equation 4.21 gives:

$$E = \underline{x}^T G^T G \underline{x} - \underline{x}^T G^T \underline{W} - \underline{W}^T G \underline{x} + \underline{W}^T \underline{W} \quad (4.23)$$

$$= \underline{x}^T G^T G \underline{x} - 2\underline{x}^T G^T \underline{W} + \underline{W}^T \underline{W} \quad (4.24)$$

To find the vector \underline{x} that gives the minimum value of E , we partially differentiate E with respect to each element of \underline{x} and then set each of the M expressions to zero. In

vector notation, it may be verified that the resulting gradient vector:

$$\nabla E = \partial E / \partial \underline{x} = 2G^T G \underline{x} - 2G^T \underline{W} \quad (4.25)$$

$$= \underline{0} \quad (4.26)$$

to minimise E , where $\underline{0}$ is the M by 1 zero vector. Therefore, to minimize E ,

$$G^T G \underline{x} = G^T \underline{W} \quad (4.27)$$

which means that:

$$\underline{x} = [(G^T G)^{-1} G^T] \underline{W} = G^\# \underline{W} \quad (4.28)$$

To summarise, if $\underline{W} = G \underline{x}$, does not have an exact solution, then Equation 4.28 returns a ‘least square’ solution. The pseudo-inverse can be computed directly from Equation 4.17, but it is also available as the MATLAB function ‘pinv’. MATLAB computes the pseudo-inverse in a robust way using singular value decomposition which is likely to be more accurate for large matrices especially when they are close to being rank-deficient. If the matrix G is rank deficient, i.e. if many of the M equations are identical or linearly dependent on each other, there will be infinitely many solutions. The solution obtained using ‘pinv’ in MATLAB will then be the one that minimises the norm of $(G \underline{x} - \underline{W})$.

4.2.3 The Naive approach

When $M = L$, the resulting square matrix G is not guaranteed to be non-singular. Fortunately, the case where $M = L$ is not the most interesting. When $M > L$, matrix G becomes non-square (thin) and Equation 4.9 becomes over-determined with more linear equations than variables. Now, provided the rank of G is not less than L , the pseudo-inverse solution to Equation 4.9 is:

$$\underline{x}_c = G^\# (\underline{Y}_R - F \times \underline{x}_o) \quad (4.29)$$

Equation 4.29 gives a set of time-domain samples \underline{x}_c that come as close as possible to minimizing the difference between the left-hand and right-hand sides of Equation 4.9 in a least sum of squares sense. Where the time-domain clipping and channel noise are not too severe, and therefore many frequency-domain symbols are correctly

snapped, the pseudo-inverse solution becomes relatively insensitive to the choice of M and the correct identification of reliable symbols at the receiver. If some incorrectly snapped symbols are inadvertently included in the set considered reliable, their effect becomes overwhelmed by the correctly snapped symbols in the pseudo-inverse solution. Without a method of deciding which frequency-domain symbols are reliable, the receiver takes all of them in the Naive Approach. It sets $M = N$, assuming that the large majority of received constellation symbols will be reliable. This naive approach is expected to work reasonably well in conditions of low and moderate distortion and channel noise.

4.2.4 Results and Discussion

The simulations carried out for the zero symbol-error correction case were repeated with the proposed Naive Method implemented with the number of equations M equal to the number of sub-carriers, i.e. 64. The number L of clipped time-domain samples, i.e. the number of unknowns, depends on the value of clipping threshold A . Figure 4.6 shows the results of this implementation of the Equation-Method for different clipping thresholds. Comparing with the no correction case, it can be seen that this naive version of the Equation-Method is effective in reducing the OFDM symbol error rate. At the quite severe clipping level $A = 0.45$, the receiver correctly receives (after correction) about 50% of the transmitted OFDM symbols, where less than 10% would be received correctly without symbol-error correction. Taking $M = N$ means that wrongly snapped constellation symbols are included in the M equations, and it would clearly be beneficial to exclude some or all of these.

4.2.5 Snapping Threshold Strategy

The ‘Naive’ strategy for the receiver can be improved by choosing, as ‘likely to be reliable’ those symbols which are closest (in a Euclidean sense) to the fixed PSK, QPSK or QAM constellation points. This new strategy requires a choice of distance threshold which we call the ‘snapping threshold’ (ST). The constellation symbols which move less than the ST distance when ‘snapped’ to the standard constellation points are considered as reliable constellation symbols and are chosen to generate the equations. This is the mechanism by which the receiver makes its reliability decisions.

The strategy will clearly make mistakes when larger distortion or channel noise drives a symbol well away from the correct constellation point and into the vicinity of

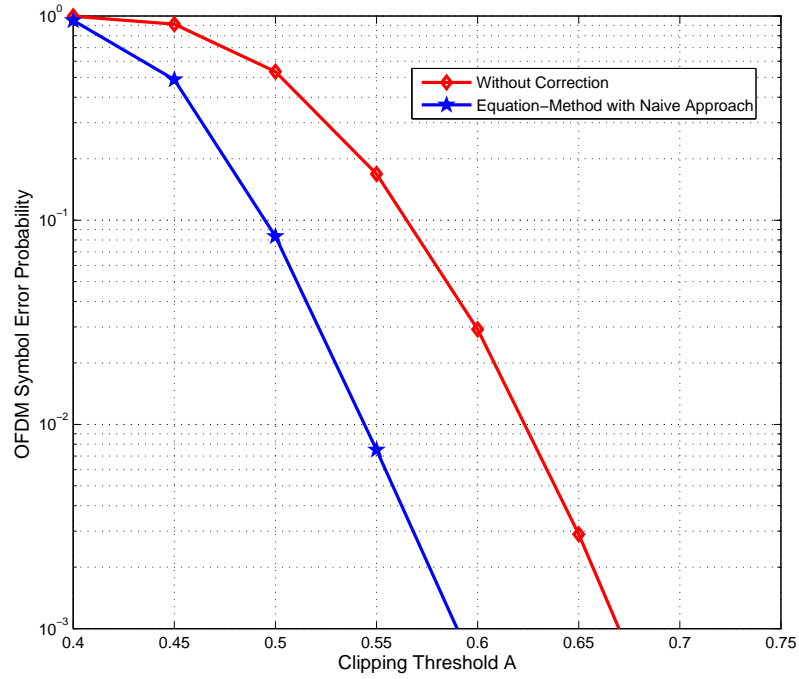


Figure 4.6: OFDM symbol error probability using Naive approach

a different one. To take an example, for 16-QAM, the minimum distance between any two constellation symbols is 2. Figure 4.1 shows the decision boundaries for 16QAM modulation. Clearly, the maximum snapping threshold (ST) must be 1 according to the decision boundaries.

A series of MATLAB simulations was carried out to try to determine the best value of ST for each clipping threshold. The symbol-error correction achieved was calculated over a range of values of ST from 0.5 to 1.0. The value of ST that minimized the OFDM symbol error rate over a number of symbols 10,000, for each clipping threshold is plotted in Figure 4.7.

Therefore, Figure 4.7 shows the best snapping threshold for each clipping threshold when used for 16-QAM modulation with OFDM. For severe clipping, there are more chances of a constellation symbol being closest to the wrong constellation point. Therefore, the optimal ST distance is smaller for severe clipping than for moderate clipping.

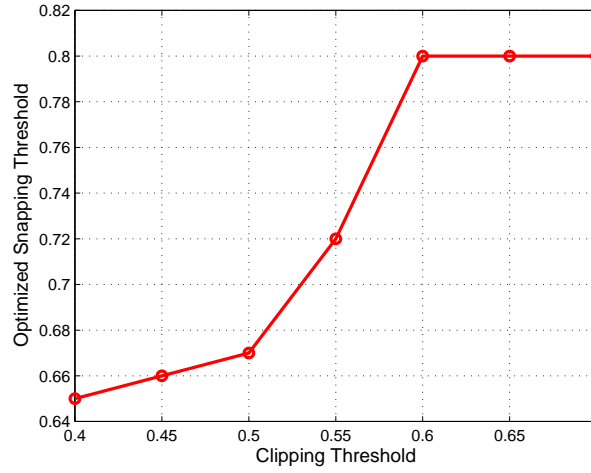


Figure 4.7: Best Snapping thresholds against Clipping thresholds

4.2.6 Results using Optimized Snapping Threshold

The Snapping Threshold strategy aims to exclude unreliable constellation symbols from Equation 4.29 by setting a snapping threshold (ST) distance. Now the receiver only includes those symbols which have moved less than ST on the constellation in the process of snapping from the received symbol to a valid constellation point. The effectiveness of this strategy varies with the choice of ST and the results presented here are for optimized values of ST. Figure 4.8 plots the symbol error probability against clipping threshold using the optimized ST method and may be compared with the previous curves. There is significant improvement over the Naive Method. For the severe clipping threshold, $A = 0.40$, the receiver now correctly receives OFDM symbols with a probability of about 0.4, which means that 40% will be correct as compared with 5% for the earlier Naive strategy ($M = N$) and 0.25% without symbol-error correction.

4.3 Dither and Recursion strategy

This is an enhanced strategy for the Equation-Method which introduces a degree of randomness or ‘Dither’ into the original symbols at the transmitter. It also introduces a form of recursion which allows the transmitter to anticipate the decisions of the receiver. Recursion means that the transmitter has a built-in copy of the receiver and its functions.

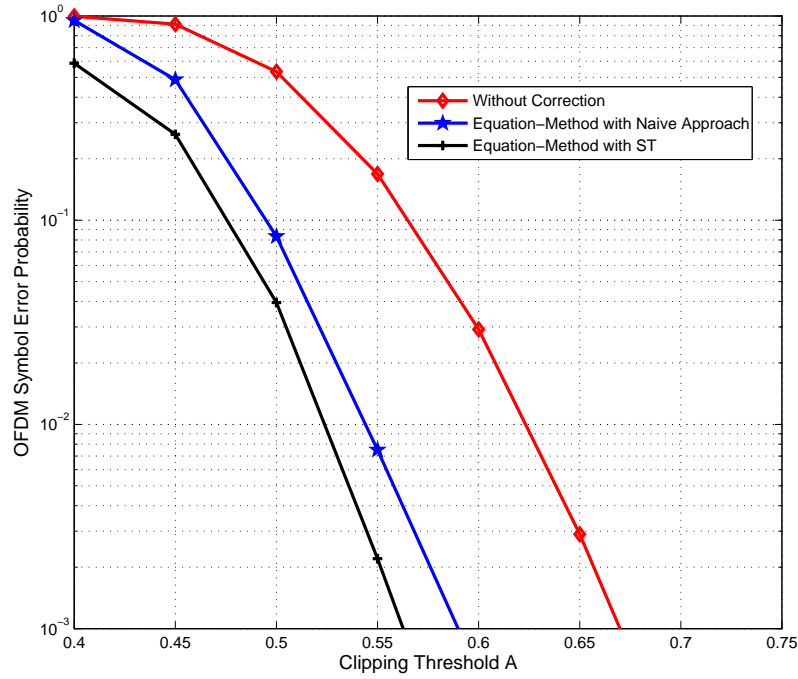


Figure 4.8: OFDM symbol error probability using ST strategy

4.3.1 Dither

At the receiver, each symbol is perturbed by a small random vector but only in such a way that it is not likely to affect the snapping decision at the receiver. It is fundamental to this idea that, because constellation points are effectively quantized there is finite distance between all of them. Therefore, a small amount of dither can be added to what is transmitted without this necessarily affecting the quantized complex numbers that define the constellation. Dither has been used in other work on PAPR mitigation, but for quite different reasons [64].

In the Equation-Method the nature of the dither is chosen to try to ensure that unreliable symbols can be readily identified as such at the receiver. To implement this idea, a copy of the receiver is mirrored at the transmitter to allow the transmitter to monitor, approximately, the effect of a given choice of dither vectors on the likely decisions. The process is approximate because, although the effect of the dither can be anticipated, it is more difficult to anticipate the effect of the channel noise. In the current implementation, a random set of dither vectors of gradually increasing length is tested until one is found that moves the symbols in such a way that a ‘minimum

distance' or ST strategy adopted at the receiver will identify the reliable and unreliable symbols. The 'minimum distance' strategy is simply to take the symbols closest to a constellation point as reliable, therefore the dither must move the unreliable ones away from constellation points. The mirrored receiver aims to anticipate the effect of each choice of dither vectors.

4.3.2 Recursion

The transmitter has a mirror copy of the receiver so that it may predict the behaviour of the receiver. According to this behaviour, the transmitter decides what should be transmitted. This is named as Recursion. It has the following steps:

1. The mirrored receiver converts the soft-clipped base-band signal to the frequency-domain by applying an FFT.
2. The frequency-domain symbols are snapped to the fixed constellation points with a record taken of the distance moved in each case.
3. The snapped constellation points are compared to the true ones to determine which are correct.
4. The Optimised Snapping Threshold strategy is now applied, with some allowance for AWGN, in the mirrored receiver to determine which constellation will be identified as reliable or unreliable by the real receiver.
5. The correctness or otherwise of each identification is determined.
6. Now the transmitter tries to improve the effectiveness of the optimized snapping threshold strategy as mirrored at the transmitter. It does this by introducing dither vectors or random changes to the original constellation symbols and noting the effect on the selection of reliable and unreliable received constellation symbols.
7. The 'Dither' vectors will move some received symbols further away from standard constellation points and others closer.
8. As different dither vectors and degrees of dither are tested, the mirrored receiver decisions will change. A constellation symbol whose distance is less than the snapping threshold (ST) from the wrong standard constellation point can be moved further away and thus be correctly identified as unreliable. Or it may be

moved towards the correct standard constellation point and end up being close enough to be considered reliable. Symbols just beyond the snapping threshold from their correct standard constellation points can be nudged a little closer.

9. Vectors of dither can be tried until there are considered enough correct identifications of reliable and unreliable constellation symbols, and enough correct ones to allow the Equation Method to reliably calculate all the clipped time-domain samples. This is taken as a satisfactory choice of dither, though it is not necessarily the optimum.
10. The transmission is then made with this satisfactory choice of dither.
11. The dither will never be made so great as to affect the decisions that would be made without clipping; i.e. the data being sent must remain correct.
12. Ideally the testing of dither vectors should continue until there are no incorrect decisions. However, if this ideal condition is not reached after a requisite number of trials, the transmission should still be made with the best dither vector obtained so far, since the use of the pseudo-inverse at the receiver can accommodate some wrong decisions as long as there are sufficient equations.

4.3.3 Results

This section investigates the performance of the proposed ‘Dither and Recursion’ strategy algorithm by the MATLAB simulation of an OFDM system with 64 sub-carriers and a 16-QAM constellation on each sub-carrier. We have used the Moore-Penrose pseudo-inverse (pinv) function [63] to solve the possibly over-determined set of equations. Figure 4.9 shows the probability of an ‘OFDM symbol error’ for different values of A . An OFDM symbol is error-free only when all constellation symbols are correct, and therefore all bits are received correctly.

As before optimized ST thresholds are used. Now the probability of a correct OFDM symbol approaches 90% for a clipping threshold of $A = 0.45$ and this is yet another significant improvement. Introducing Dither and Recursion with a mirrored receiver at the transmitter was implemented as described in Section 4.3 where the dither is introduced to try to make the ‘snapping threshold’ strategy described above work better. In our experiments, a maximum of 100 randomized dither vectors was allowed for each OFDM symbol transmission.

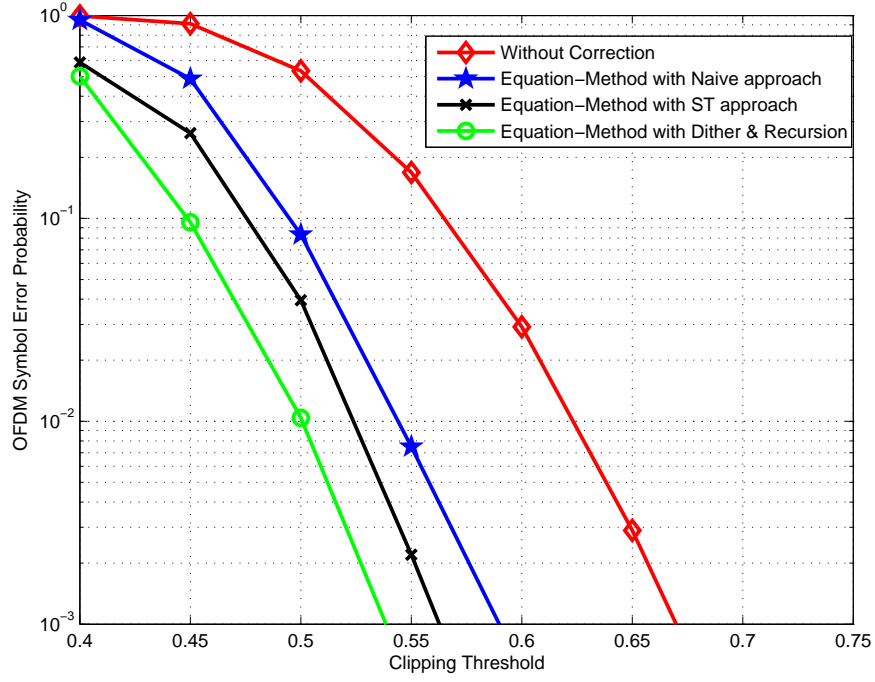


Figure 4.9: Symbol error Probability using Equation-Method with Dither and Recursion

4.4 Selective Dither and recursion

The ‘Dither and Recursion strategy moves constellations symbols which are wrongly going to be selected as reliable further away from the wrong fixed constellation points. Computational savings may be made by applying dither selectively to these symbols only, thus allowing a more efficient search strategy. Dither is applied to selected symbols according to the following ‘Selective Dither and Recursion’ strategy:

1. The complex constellation symbols are converted to the time-domain by applying an IFFT:

$$x(n) = \frac{1}{\sqrt{N}} \sum_{k=0}^{N-1} X_k e^{j2\pi nk/N} \quad 0 \leq n < N-1 \quad (4.30)$$

2. Soft clipping is applied to the time-domain signal.
3. The clipped signal is processed by the mirrored receiver at the transmitter as described in Section 4.3.2.
4. If any of the constellation symbols are wrongly being considered as reliable,

dither is applied, but only to the true versions of these symbols (i.e. before clipping). Dither is not applied to all the true symbols as before, but just to the unreliable ones.

5. The modified constellation symbols are converted to the time-domain and soft-clipped again.
6. Control is again passed to the recursion process as described in Section 4.3.2.
7. The ‘Selective Dither’ and ‘Recursion’ loop continues until no wrong decisions are detected or until a specified number of iterations have elapsed. This process will often be required to apply dither to different symbols as decisions change.
8. Ideally the iterations should continue until there are no incorrect decisions, but transmissions predicting wrong decisions may still be useful when the pseudo-inverse solution method is used at the receiver.

4.4.1 Results and Discussion

The OFDM symbol in the first iteration is passed through the recursion process. If there are wrongly chosen constellation symbols, then the process of Selective Dither starts. After every iteration of Selective Dither and Recursion, the selective dither vector giving the smallest number of incorrect decisions is stored. If the mirrored receiver is unable to find a case when there are no wrong decisions, then it transmits the OFDM symbol using the dither vector which gives the lowest number of wrong decisions.

Figure 4.10 shows the OFDM symbol error probability using the Selective Dither and Recursion method. It is compared to all earlier versions of the Equation-Method. The probability of a correct OFDM symbol approaches 68% for a clipping threshold of $A = 0.4$. This is better than all previously discussed results.

4.4.2 Bit-error Probability for the Equation-Method

We have estimated the likely OFDM symbol error probability for all the four Equation-Method strategies presented in this chapter. In our experiments so far, OFDM symbols which have one or more uncorrected bit-errors after processing by the Equation Method are considered wrong. This would be appropriate for applications without FEC or ARQ error correction. However, it is also useful to consider the effect of the

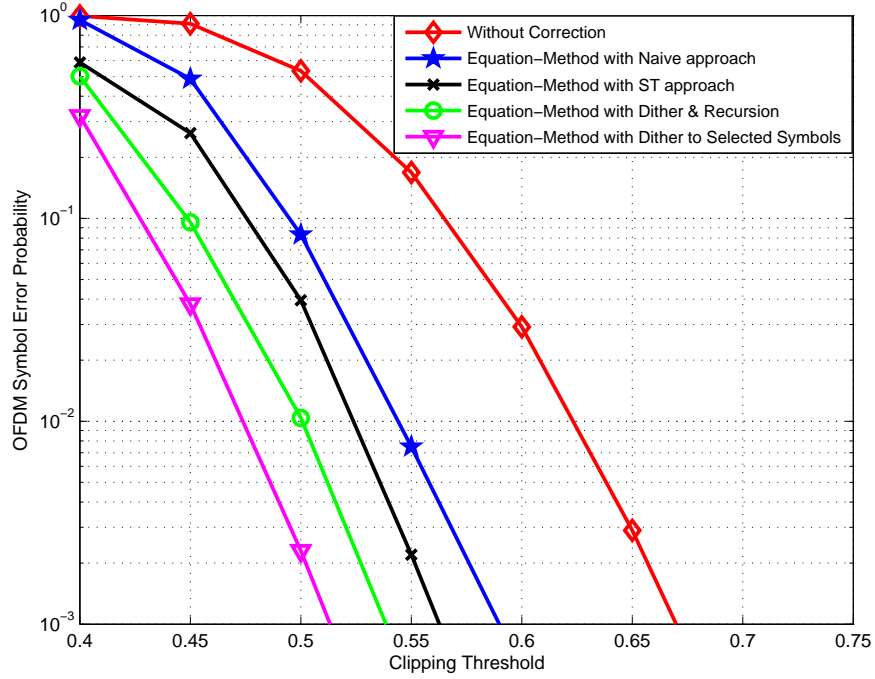


Figure 4.10: Symbol error Probability using the Equation-Method with Selective Dither and Recursion

Equation Method on the ‘bit-error probability’. Figure 4.11 shows the BEP for all the four versions of the Equation-Method. Like the OFDM symbol error probability, we can see that Selective Dither and Recursion gives the best bit-error correction for all the clipping thresholds. It may be observed that the BEP for the ST method has increased for $A = 0.40$. The reason is that the received constellation symbols are affected badly by the high clipping distortion and the decisions based on ST are heavily affected.

4.4.3 Equation-Method in comparison to other approaches

Chapter 3 has explained and evaluated the two most cited iterative receivers that have been proposed in the literature for mitigating the effect of clipping noised at the receiver. With the results, we have observed that the BNC receiver is better than the DAR receiver. We have compared the best results of the Equation-Method with the BNC iterative receiver, at moderate and severe clipping thresholds in the absence of AWGN noise. Figure 4.12 shows the performance of the Equation-Method with Selective Dither and Recursion in comparison to the BNC receiver. The OFDM symbol error probability for the Equation-Method (Selective Dither and Recursion) at clipping

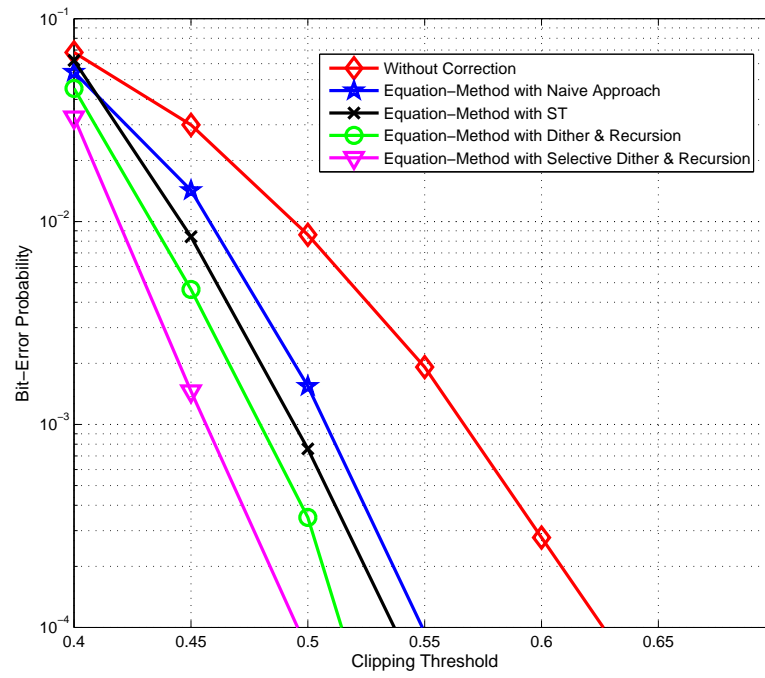


Figure 4.11: Bit error Probability using Equation-Method

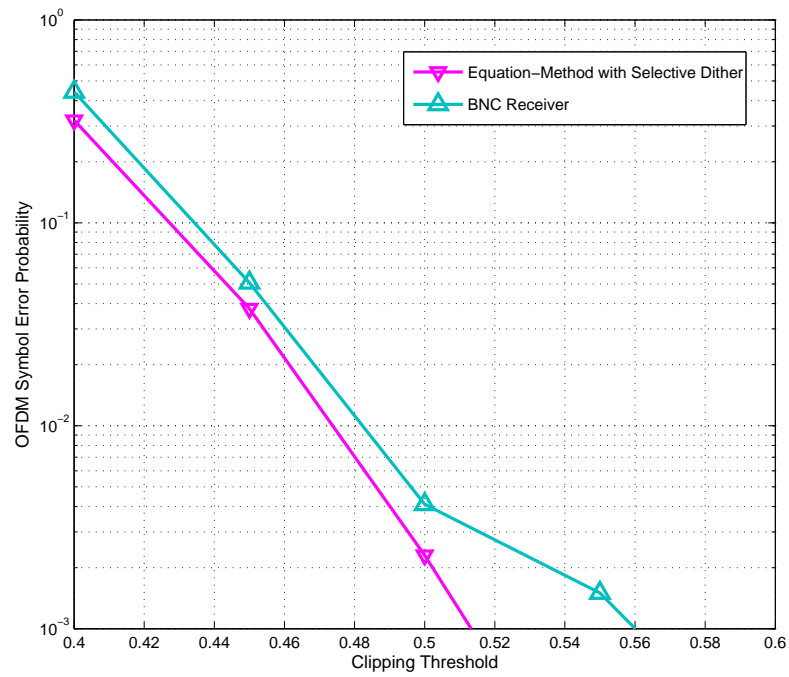


Figure 4.12: Comparison of the Equation-Method with BNC

threshold $A = 0.5$ is 0.02, and using BNC receiver it is 0.04. The Equation-method has low symbol error probability as compared to BNC receiver for all the clipping thresholds.

4.5 Conclusions

A new ‘Equation Method’ has been proposed for correcting bit-errors produced by clipping distortion in OFDM signals. It has been evaluated to determine the percentage of OFDM symbols that can be completely corrected, at moderate to severe clipping thresholds, by different versions of the method. The bit-error rates obtained after applying the various strategies have also been evaluated. This chapter has presented four versions of the Equation-Method. The Selective Dither and Recursion strategy shows the best performance and has been shown to correct the majority of the received OFDM symbols at a severe clipping threshold. The best results are compared with other receiver-oriented approaches, and demonstrate the superiority of the new method for the examples chosen. The performance of the Equation-Method in the presence of AWGN is addressed in the next chapter

Chapter 5

Equation-Method in additive white Gaussian noise (AWGN)

The soft-clipped OFDM signal modulated at the transmitter is transmitted over the channel. A corrupted version of this signal is received at the receiver. The communication channels can suffer from a variety of impairments which include noise, interference and frequency selective fading. The effects of frequency selective fading may be reduced by channel equalization, and OFDM has particular advantages in this respect. Noise and interference cause bit-errors in the signal. Noise is present in all communications channels.

In this chapter we analyze the effect of the additive white Gaussian noise (AWGN) on the performance of the proposed system of the Equation-Method. In particular this chapter deals with the design and implementation of certain strategies to make the Equation-Method work better in the presence of the AWGN.

5.1 Analysis of Equation-Method with Noise

The Equation-Method basically relies on two factors. First is accurate identification of the 'reliable' frequency-domain symbols i.e. symbols that snap correctly and the second important factor is to recognize the time-domain samples which were clipped at the transmitter. In the absence of channel noise it is possible for the receiver to identify all the clipped samples correctly. If AGWN is present, it becomes more difficult to identify the clipped samples, also the constellation symbols become less reliable. In this section the previously described four methods, without modification, will be analyzed when there is AWGN and without any other channel impairment.

The effect of the addition of noise to a time-domain signal may increase/decrease the amplitudes of the time-domain samples. The receiver transforms the time-domain signal to the frequency-domain by applying an FFT. In the matrix notation of Chapter 4, the receiver partitions the clipped signal into two matrices as follows:

$$\underline{x} = \begin{bmatrix} \hat{\underline{x}}_c \\ \underline{x}_o \end{bmatrix} \quad (5.1)$$

According to our partition, the time-domain signal has two sub-matrices, $\hat{\underline{x}}_c$ and \underline{x}_o with dimensions $L \times 1$ and $(N - L) \times 1$ for all $n = 0, 1, \dots, N - 1$ respectively. $\hat{\underline{x}}_c$ are those time-domain samples which are believed to have been clipped and \underline{x}_o consists of all others which are assumed as non-clipped. The receiver has to partition the received signal into these two sub-matrices. The effect of increasing amplitudes by the addition of the noise is not going to effect the set of truly clipped samples $\hat{\underline{x}}_c$ because they will still be identified as clipped at the receiver. Similarly, the increase in the amplitudes of elements of \underline{x}_o may not be too serious a problem as long as there are not too many and there are sufficient equations available. Such samples will be considered as clipped even though they were not clipped. Ultimately they will be replaced with unknowns, increasing number of unknowns in the equations. Eventually a large increase in the amplitudes may increase the size of the matrix $\hat{\underline{x}}_c$ which may result in an under-determined set of the equations.

If the AWGN causes a decrease in amplitude for any of the truly clipped samples from the matrix \underline{x}_c will make it fall below the clipping threshold and the receiver will then not recognize it as clipped. This is going to increase the size of the sub-matrix \underline{x}_o the results at the receiver. A decrease in the amplitudes of the \underline{x}_o samples is not going to effect the performance because they were not clipped so will still be a part of the sub-matrix \underline{x}_o not be identified as clipped.

Addition of noise in the time-domain signal will be reflected in the frequency-domain constellation symbols. The noise may move the constellation symbols farther on the constellation making the snapping process less reliable.

On the basis of the above theoretical analysis, two experiments have been defined to analyze the effect of noise on clipping decisions and constellation symbols.

1. Experiment 1: This experiment makes the assumption that the receiver has knowledge of the number of the samples clipped and their indexes. The purpose of this experiment is to see the effect of the noise on the constellation symbols, when there is no noise effecting the clipping decisions.

Table 5.1: Simulation parameters for the experiments

FFT Size	64
Modulation on subcarriers	16-QAM
Total OFDM symbols transmitted	10000
Clipping Threshold	$A = 0.6, 0.4, \gamma = 1.5, 1.0$

2. Experiment 2: This experiment investigates the situation where the constellation symbols and clipping decisions are both effected by the AWGN noise. Now the receiver does not have any prior information of which time-domain samples are clipped, and this information must be deduced from the noise effected received signal. This is the real scenario. The only known information is the clipping threshold at which the samples were clipped.

Table 5.1 shows the simulation parameters for the experiments conducted in MATLAB. All the experiments follow these parameters. To investigate the methods, 10000 randomly generated OFDM symbols were clipped at $A = 0.40$ and $A = 0.60$, and transmitted through an AWGN channel with Signal-to-Noise ratio ratio (SNR) varying from 0 to 25dB.

5.1.1 Effect of noise on Naive Method

This section explains the results produced simulating both the defined experiments using the Naive method and discusses the results.

Experiment 1: Effect of AWGN on constellation symbols

The Naive approach to the Equation-Method is used in this simulation experiment. Figure 5.1 shows the Bit-error Probability (BEP) against SNR using the Naive method at the receiver. The top most two plots represent the OFDM BEP using the clipping levels set at $A = 0.40$. The top first (in brown) plot is the BEP with clipping at the transmitter with no bit-error correction at the receiver, whereas, the top second (green) plot represents the BEP using the Equation-Method with the Naive approach, when the noise is assumed not to affect the clipping decisions. For severe clipping threshold, there is very little improvement even at the higher SNR values. Comparing with the results in Chapter 4, we conclude that the Naive method does not work very well with severe clipping when there will be many clipped time-domain samples. The problem

is that there are many clipped samples up to 30 and therefore not enough reliable equations to correct them.

The third curve from the top (in black) shows the OFDM BEP against SNR at $A = 0.60$ without any correction, and the fourth curve (blue) is the result produced by the Naive method when the clipping decisions are not effected by the noise. If we compare the third and fourth curve, at SNR= 15dB, the BEP has been reduced from nearly 0.001 to 0.00003. The bottom most curve is the OFDM BEP for an ideal transmitter without clipping. The difference between the fourth curve and the ideal plot is at most approximately 2dB. Therefore the Naive method is working quite well for moderate clipping.

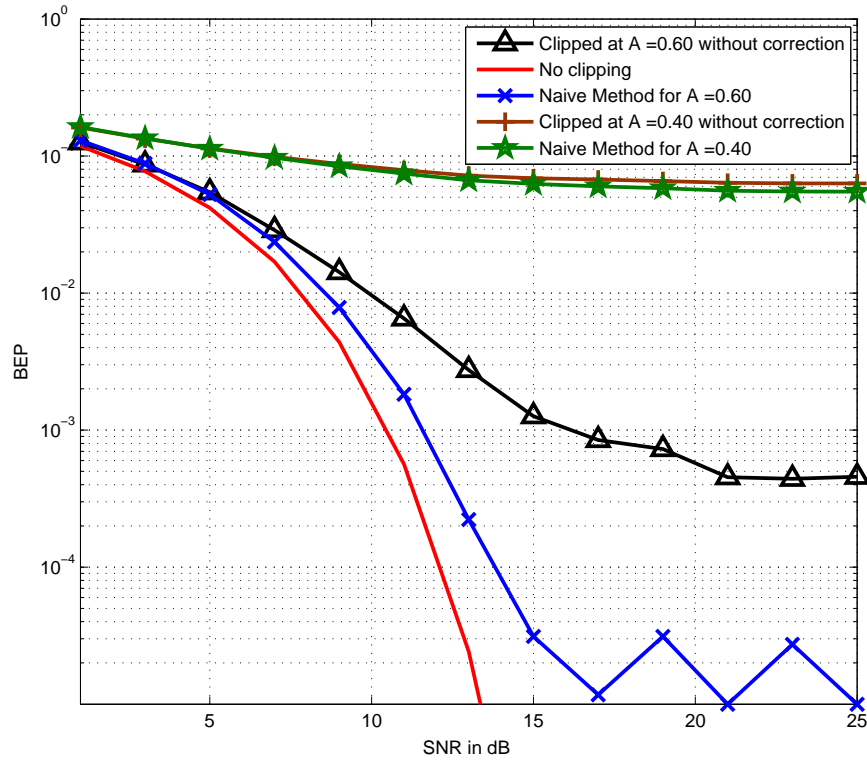


Figure 5.1: Bit-error Probability against SNR using Naive method Experiment 1

Experiment 2: Effect of AWGN on clipping decisions and constellation symbols

The Figure 5.2 shows the BEP against SNR using the Naive method at clipping thresholds $A = 0.60$ and $A = 0.40$ respectively. This experiment was carried out under the

assumption that the receiver does not have any information of the clipped samples except the clipping threshold. The first (brown) and the third (in black) curve remains

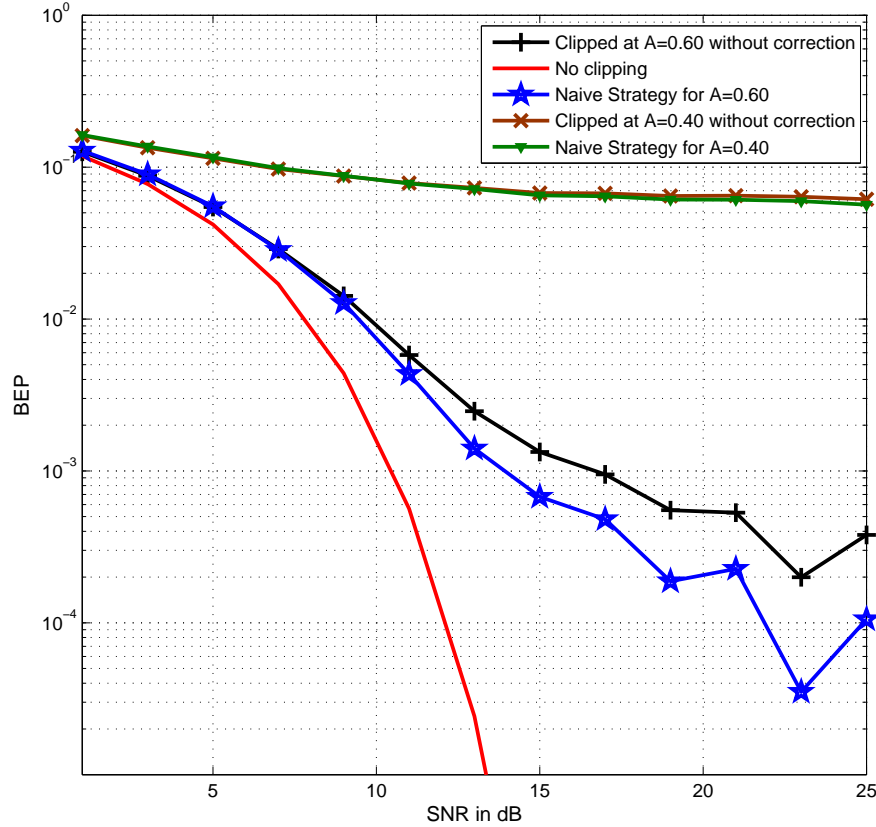


Figure 5.2: OFDM Bit-error Probability against SNR using Naive method Experiment 2

the same as these are BEPs with clipping without any correction. The second curve (in green) from the top shows the BEP using the Naive method with noise on clipping decisions now. There is almost no difference for this severe clipping case as the receiver is hardly able to make any difference with effected decisions by noise. The fourth curve (blue) for the Naive method with a moderate clipping level $A = 0.60$ shows the BEP using the Naive approach affected with noise.

Discussion

In order to compare the results in Figure 5.1 to the results produced in the absence of AWGN noise from Chapter 4, Section 4.4.2, BEP at $A = 0.60$ without AWGN, is

0.00001. Whereas, the BEP using the Naive method with AWGN and no noise on the clipping decisions, at SNR=15dB is 0.00003. Therefore, we can conclude that if the receiver is able to make accurate decisions for clipped samples, it may be able to get the closest BEP using the Naive method to that which is using the Naive method without AWGN.

By comparing Figure 5.1 and Figure 5.2, taking SNR=15dB and fourth plot for $A = 0.60$, the BEP has increased from 0.00003 to 0.007, which is a large increase in terms of bit-error correction. It is easy to conclude now, that the effect of noise on the clipping decisions is more critical than the effect of noise on the constellation symbols. The difference of BEP becomes more and more as SNR increases.

Comparing the curves of BEP clipped at $A = 0.4$, from Figure 5.1 and Figure 5.2, there is not a prominent difference for bit-error correction at this severe clipping. We have seen from Chapter 4, the results using the Naive method in the absence of noise are not impressive at severe clipping. Hence we may conclude that the Naive method is not working at severe clipping in the presence of the noise, whereas it works effectively, if the receiver is able to make correct clipping decisions at moderate clipping.

5.1.2 Effect of noise on Snapping Threshold Method

The Snapping threshold method improves the selection of the reliable frequency-domain symbols. It uses the snapping distances the constellation symbols move on the constellation during the snapping process. The optimized Snapping threshold for these two experiments is $ST = 0.8$ for 16QAM modulation.

Experiment 1: Effect of AWGN on constellation symbols

Figure 5.3 shows the BEP against SNR using the ST method for two different clipping thresholds, i.e, $A = 0.60$ and 0.40 . From the top, first (brown) and third (black) plots are the BEP using ST method without correction clipped at $A = 0.40$ and $A = 0.60$, respectively. The second (green) and fourth (blue) plots show the BEP after using ST method with no noise on clipping decisions clipped at $A = 0.40$ and $A = 0.60$. The discussion of the first and second plots is not necessary as there is not prominent improvement in the BEP at $A = 0.40$. For the third and fourth curves, taking SNR=15dB, the BEP has reduced from 0.001 (without correction) to BEP below 0.00001 (using ST with no noise on clipping decisions).

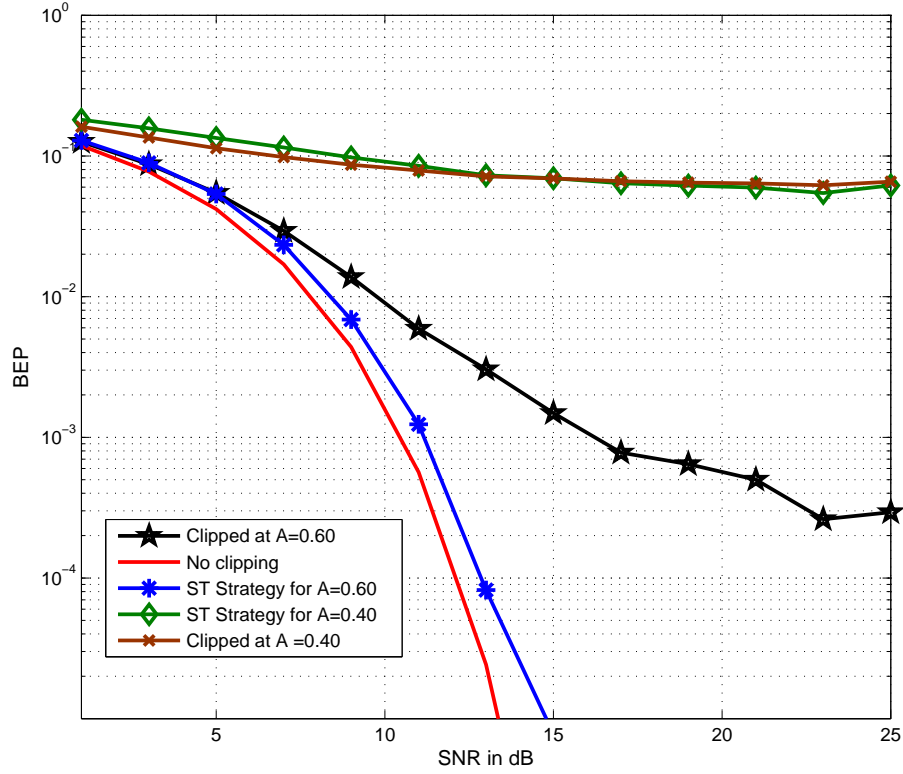


Figure 5.3: OFDM Bit-error Probability against SNR using ST method Experiment 1

Experiment 2: Effect of AWGN on clipping decisions and constellation symbols

The Figure 5.4 is the BEP obtained using the Snapping threshold method to investigate the effect of noise on constellation symbols and clipping decisions both. The top two plots show the BEP at $A = 0.40$ without correction and with ST (noise on constellation symbols and clipping decisions). There is no improvement in BEP at $A = 0.40$ because the constellation symbols and clipping decisions both are heavily affected by the noise. Therefore the Snapping threshold is unable to make any improvements for severe clipping.

Discussion

The results with AWGN and without AWGN need to be compared to get the idea of the effect of noise and performance of the method. Chapter 4, Section 4.4.2 the BEP using ST at $A = 0.60$ in the absence of AWGN is below 0.00001, the same figure has been achieved in Figure 5.3 at SNR=15dB and higher. Comparing Figure 5.3 and

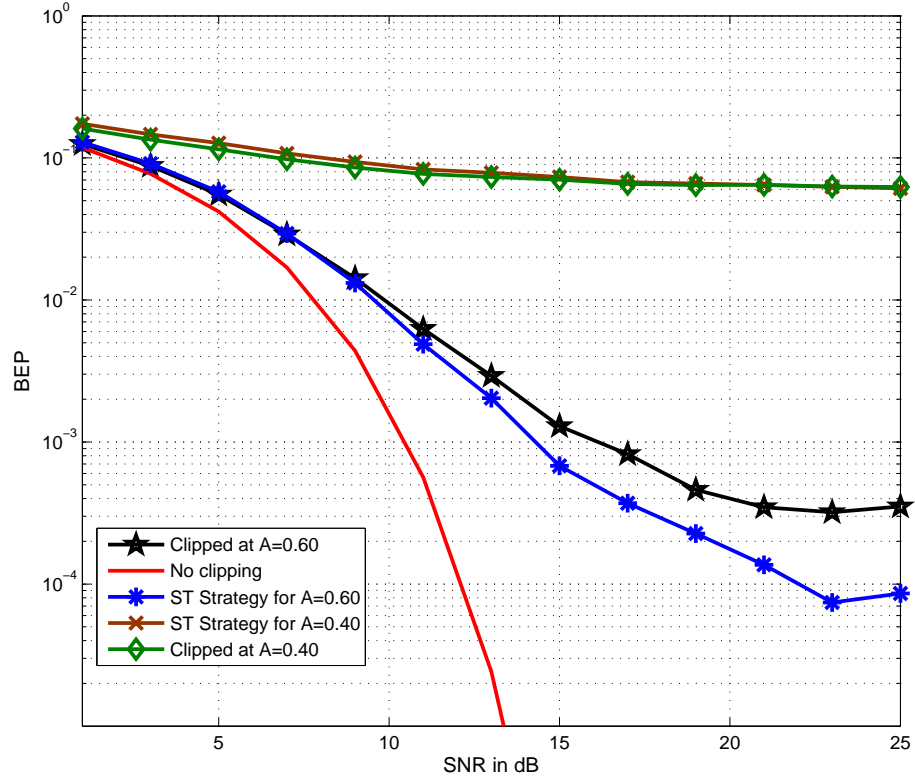


Figure 5.4: OFDM Bit-error Probability against SNR using ST method Experiment 2

Figure 5.4, taking SNR=15dB, BEP has increased from 0.00001 to 0.0007. The results support the fact that the effect of noise on clipping decisions is more critical than the effect of noise on constellation symbols.

5.1.3 Effect of noise on Dither and Recursion Method

In this method, the transmitter applies dither to all the constellation symbols and uses recursion to observe the behavior of the real receiver. The maximum number of iterations for Dither and Recursion is fixed to 100 with a snapping threshold of $ST = 0.8$.

Experiment 1: Effect of AWGN on constellation symbols

Figure 5.5 shows the results of the experiment 1 performed on the receiver applying Dither and recursion method. The method has been analyzed in the presence of AWGN at two different levels of clipping $A = 0.60$ and $A = 0.40$.

The top two curves show the BEP at $CT = 0.40$ without correction and with Dither method. There is a small reduction in BEP for $SNR=20\text{dB}$ and higher. The third (in black) and fourth (blue) plot show the BEP at $A = 0.60$ without correction and with Dither method (no noise on clipping decisions). Taking $SNR=10\text{dB}$, BEP has reduced from 0.01 to 0.003.

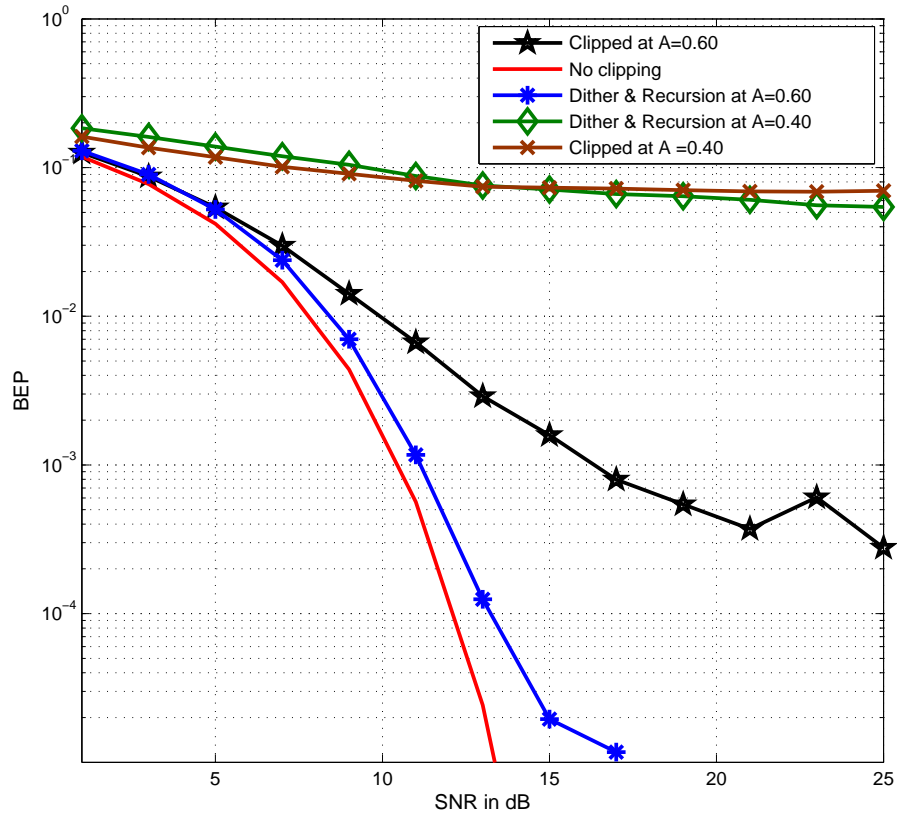


Figure 5.5: OFDM Bit-error Probability against SNR using Dither and Recursion method Experiment 1

Experiment 2: Effect of AWGN on clipping decisions and constellation symbols

Figure 5.6 shows the BEP against SNR under the assumption that the receiver does not know which of the samples were clipped. The clipping levels are the same as that of experiment 1, i.e. $A = 0.40, 0.60$

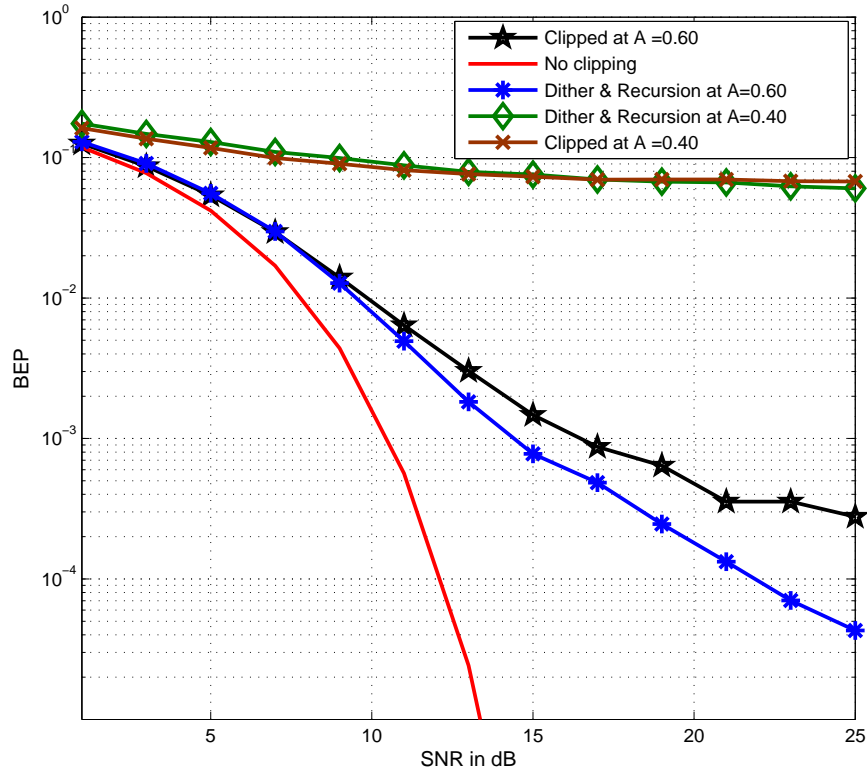


Figure 5.6: OFDM Bit-error Probability against SNR using Dither and Recursion method Experiment 2

Discussion

It is important to compare the performance of the method in the presence of the noise and in the absence of the noise. From Chapter 4, Section 4.4.2, BEP at $A = 0.60$ in the absence of AWGN is below 0.00001. BEP in the presence of noise (clipping decisions are not effected) from Figure 5.5 is 0.00002 at SNR=15dB and is below than this for higher values of SNR.

Comparing Figure 5.5 and Figure 5.6, taking SNR=15dB, the BEP of the method is decreased from 0.00002 to 0.0008. there is much reduction in BEP as SNR increases. It may be concluded that the effect of the noise on the clipping decisions is effecting the performance of the method more critically than the effect of noise on the constellations for higher clipping thresholds. Therefore, it is a good idea to concentrate on improving the way the clipping decisions are made at the receiver.

5.1.4 Effect of noise on Selective Dither and Recursion Method

This method applies Dither to only selected symbols which have been identified as wrongly chosen reliable in the very first recursion step. The maximum number of iterations is fixed to 100. The performance of this method in the presence of the AWGN using two defined experiments is explained below.

Experiment 1: Effect of AWGN on constellation symbols

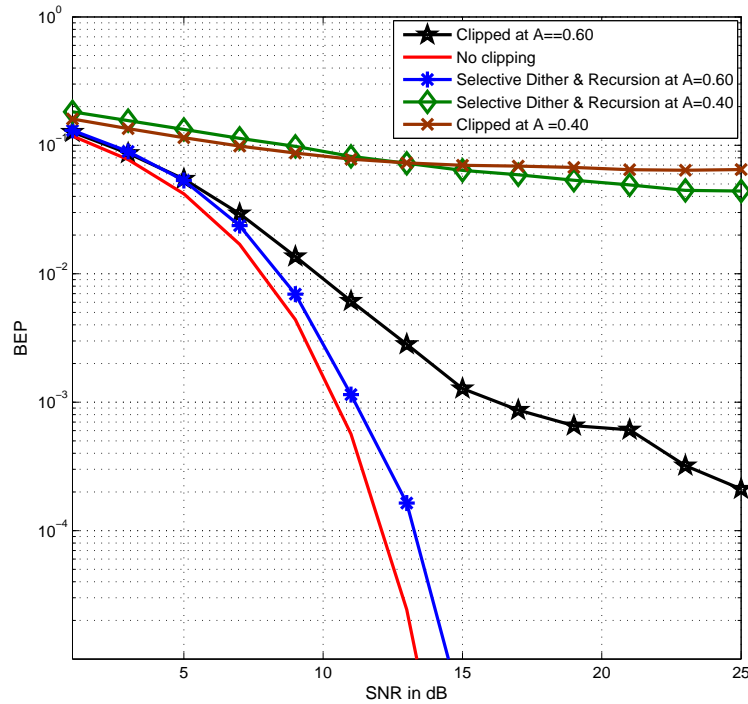


Figure 5.7: OFDM Bit-error Probability against SNR using Selective Dither and recursion method Experiment 1

The results in Figure 5.7 have been obtained using the Selective Dither and Recursion method using the experiment 1. The first (brown) and third (black) curve in the figure show the BEP without correction at $A = 0.40$ and $A = 0.60$ respectively. The second (green) and fourth (blue) curves from the top show the BEP after using the method with no noise on clipping decisions. There is a little reduction in BEP at $A = 0.40$ which is the signal has been severely effected by the noise. At $A = 0.60$, the receiver is able to produce good results of BEP with a difference of only 1dB to the ideal case.

Experiment 2: Effect of AWGN on clipping decisions and constellation symbols

Figure 5.8 shows the results for performing Experiment 2 for the Selective Dither and Recursion method. Comparing curves clipped at $A = 0.60$, at $\text{SNR}=15\text{dB}$ the BEP using the Selective dither and recursion method is 0.0006, whereas, the BEP without correction at the same level of SNR is .001. We may conclude that the Selective Dither and Recursion still corrects the bit-errors at moderate clipping.

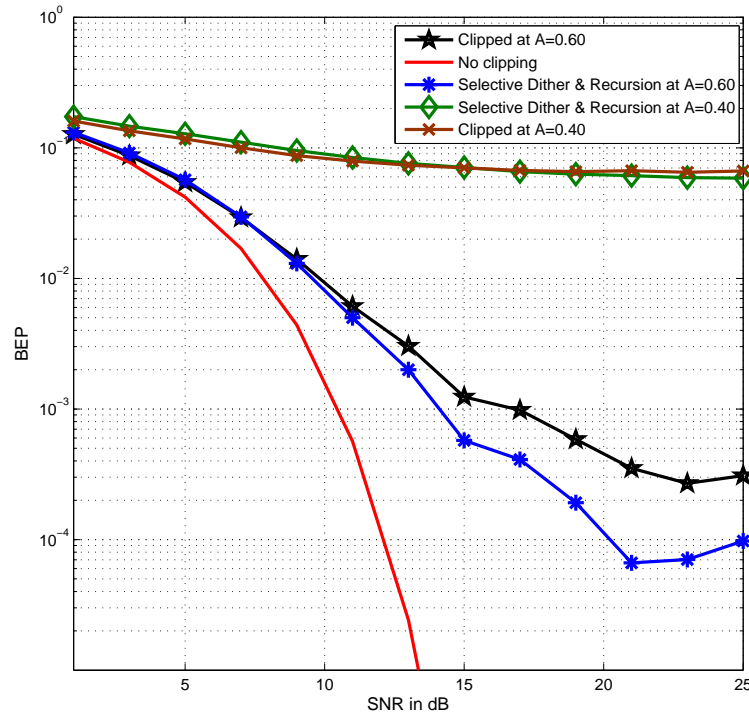


Figure 5.8: OFDM Bit-error Probability against SNR using Selective Dither and recursion method Experiment 2

Discussion

OFDM BEP using the Selective Dither and recursion at $A = 0.60$ in the absence of AWGN from Chapter 4, Section 4.4.2 is below 0.00001, as it has been achieved in the presence of noise on constellations symbols in Experiment 1 Figure 5.7. Comparing both Figures 5.7 and 5.8 at $A = 0.60$, taking $\text{SNR} = 10\text{dB}$, BEP has increased from 0.003 to 0.009 respectively, and this increase becomes larger with the higher values of SNR .

5.1.5 Conclusions for analysis of the methods with noise

This section investigated the effect of noise on the performance of the four approaches for the Equation-method. All the methods have been analysed for severe and moderate clipping in the presence of noise for both the experiments. The results have been compared to the results from Chapter 4, which were produced without AWGN.

First, the case of Experiment 1 will be discussed for all the methods. The BEP for severe clipping levels make a minor difference and there is not a lot of improvement for severe clipping such as $A = 0.40$. For all the four strategies of the Equation-Method, as in presented in Figures 5.1, 5.3, 5.5, 5.7, there is not a prominent decrease in the BEP at the $A = 0.40$. We proposed these methods to increase the selection of the reliable frequency-domain symbols. Even if, the clipping decisions are not effected, but with low level of clipping, the constellation symbols are more distorted with the addition of the noise.

Taking the case of moderate clipping, when $A = 0.60$, from Figures 5.1, 5.3, 5.5, 5.7, the best results are using the ST method and the Selective Dither method, where the BEP is closest to the ideal case and has only 1dB difference.

Regarding Experiment 2 at $A = 0.60$, we may conclude from Figures 5.2, 5.4, 5.6, 5.8, the BEP using the Naive, ST and the Dither method is nearly the same comparing at SNR=20dB, the BEP for these three methods is 0.0002, as compare to the Selective Dither, which has the BEP 0.0001 at SNR=20dB. The performance of all the methods at moderate clipping for experiment 2 seems the same, as the clipping decisions are affected along with the noise on the constellation symbols. All four strategies of the Equation-method try to improve the selection of the reliable constellation symbols better in every next strategy. The noise is affecting the reliability decisions of the constellation symbols, therefore, we do not see a large difference of the BEP among these methods.

5.2 Strategies for reducing the effect of AWGN on the Equation-Method

After looking at the results above, the question is what can be done at the receiver to reduce the effect of the AWGN on the effectiveness of the Equation-Method. In the absence of noise, the receiver is able to identify the clipped time-domain samples by knowing the exact clipping threshold. For the simulations carried out so far, we

have set a margin factor MF which is multiplied by the clipping threshold to allow for a small margin of error in the values of the clipped signal. They do not have to be exactly equal to the clipping threshold A to be considered clipped. Any amplitude that is slightly less than CT, but greater than $A \times MF$ is also considered to have been clipped. This is done to try to take care of any minor differences in the amplitudes of the time-domain signal. One approach to try to reduce the effect of noise in the received signal is to increase the margin factor of the clipping threshold. This approach is explored in the next section.

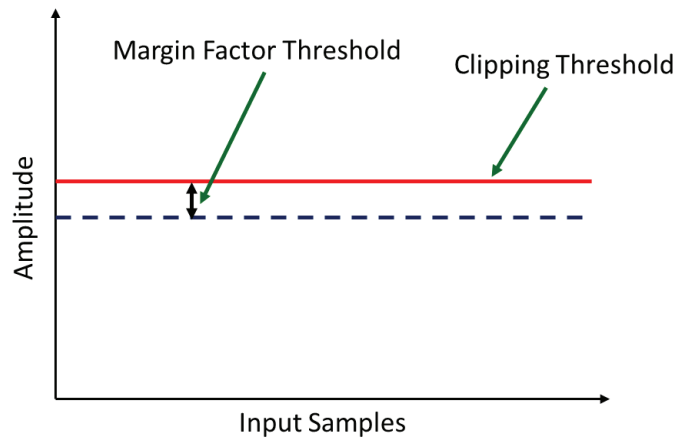


Figure 5.9: Margin Factor Threshold

5.2.1 Margin Factor Threshold

To accommodate the effect of the AWGN, we have designed a strategy for increasing the 'margin factor' for the clipping threshold at the receiver. The margin factor is a very small number which is multiplied with the clipping threshold to increase the range of the margin factor threshold (MFT). A small increase in the margin factor will increase the MFT to accommodate more time-domain samples which may have been clipped but due to the effect of noise, have had their amplitudes reduced. Figure 5.9 illustrates the margin factor threshold. It was found reasonable to allow MFT vary between the limits $0.999 \times A$ and $0.9 \times A$.

Figure 5.10 shows the block diagram of an algorithm for dynamically adjusting MFT. It is an iterative process and in each iteration there may be a change in the MFT. MFT is then used as the threshold to identify the possibly clipped samples in the time-domain signal. Each decrease in MF will increase the size of the \hat{x}_c matrix which

will take more time-domain samples as unknowns in the equations. An increase in the number of unknowns is not a serious problem as long as we have enough equations to solve. The algorithm is designed in such a way that it keeps on decreasing the MFT until the number of unknowns is less than the number of equations and MFT reaches to its maximum. The value of MF is reduced in every iteration with a small number which is kept at 0.004.

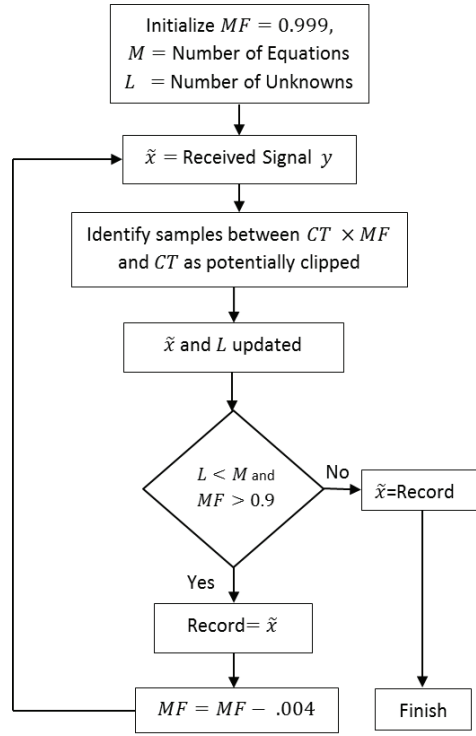


Figure 5.10: MFT algorithm block diagram

The received time-domain signal y is saved as \tilde{x} which is then passed on to the next step. All the time-domain samples in \tilde{x} exceeding MFT are made unknowns in the signal \tilde{x} . The number of unknowns L may vary in each iteration. So L is checked at each step to see if it is still less than the number of the equations and MF is within its defined range. In case of $L < M$, the algorithm keeps a copy of the updated time-domain signal \tilde{x} as *Record* which may be retrieved in the next iteration if L exceeds M .

The experiments using the proposed algorithm of MFT have been carried out in MATLAB for all the four approaches of the Equation-Method mentioned in Chapter 4. A total of 10,000 OFDM symbols with 16-QAM modulation on each subcarrier, were transmitted with clipping at $A = 0.60$. The plots of BEP against SNR were produced

for each one of the approaches as explained in the next sections.

5.2.2 MFT with naive method

Figure 5.11 shows the BEP against SNR using the Naive method with MFT. Curve 1 shows the BEP of the clipped signal without correction. Curve 2 and 4 have already been explained in the Section 5.1.1, where curve 2 shows the BEP using the Naive approach without modification in AWGN, where the clipping decisions and constellation symbols both are affected with noise. Curve 4 shows the BEP using the Naive method when the clipping decisions are not affected by noise. Curve 3 shows the BEP using the Naive method with MFT. Comparing curves 3 and 2, taking $\text{SNR} = 16\text{dB}$, the BEP has reduced from 0.0006 to 0.00004 for MFT algorithm, and the difference increases for the higher values of SNR.

Comparing curves 3 and 4, there is a difference of only approximately 1dB for all SNR values. The BEP for the Naive method with no noise from Section 4.2.4, is .00001 at $A = 0.60$. Whereas, curve 3 shows the BEP below 0.00001 at $\text{SNR}=18\text{dB}$. Hereby we can conclude that for $\text{SNR}=18$ and above, the Naive approach in AWGN with MFT achieves the same performance as it has achieved in the absence of noise.

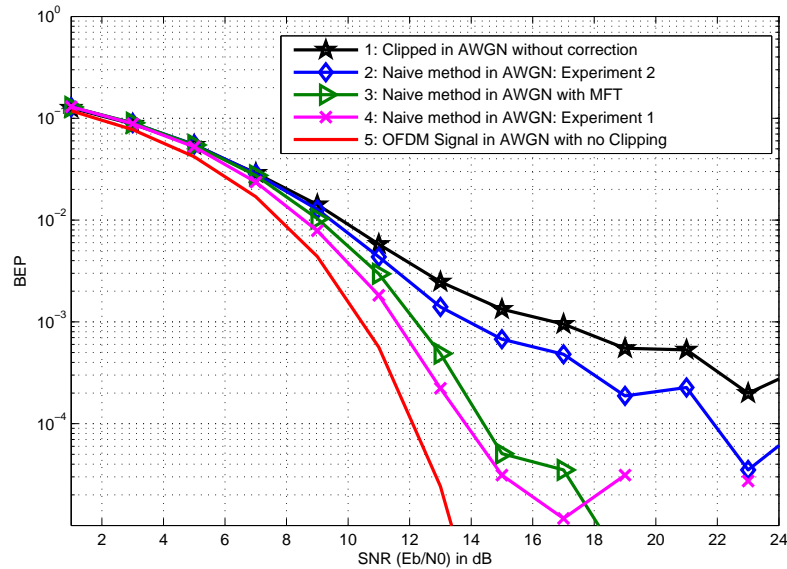


Figure 5.11: OFDM Bit-error Probability against SNR using Naive method with MFT

5.2.3 Margin factor with ST method

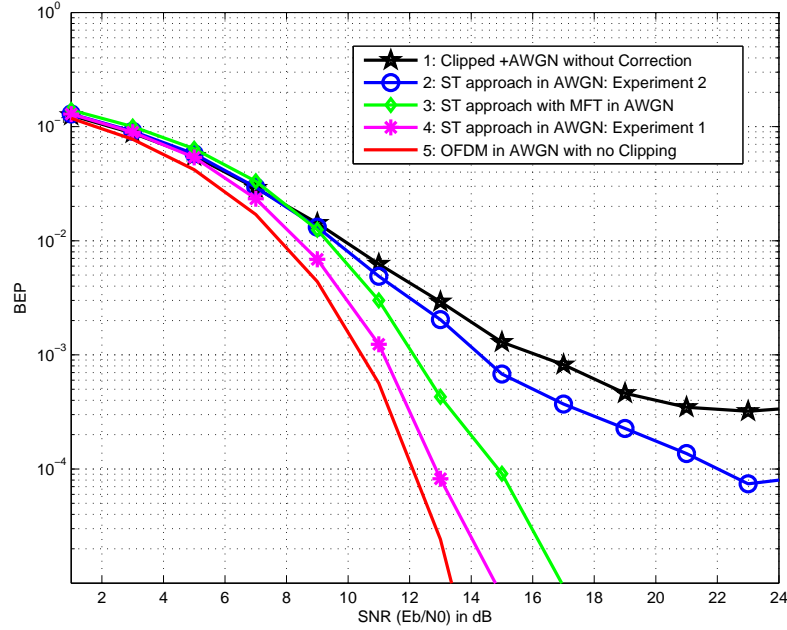


Figure 5.12: OFDM Bit-error Probability against SNR using ST with MFT

Figure 5.12 shows the plot of BEP against the SNR using the Snapping Threshold strategy with MFT. Curve 1 represents the BEP with clipped OFDM signal at $A = 0.60$ in AWGN without correction. Curve 2 is representing the performance of the Snapping Threshold method in the presence of the AWGN when the clipping decisions and constellation symbols both were affected by noise. Curve 2 and 4 have been explained in the above Section 5.1.2. Curve 3 shows the BEP using the Snapping threshold method with the proposed algorithm MFT in the presence of the AWGN. Curve 5 is the BEP for an undistorted transmitter or a perfectly linear transmitter.

Comparing curves 2 and 3, taking $\text{SNR}=16\text{dB}$, the BEP has reduced from .0005 to .00003 for the curve 3. Whereas, for $\text{SNR}=17\text{dB}$ and above, the BEP for curve 3 is below 0.00001. Comparing curves 3 and 4, taking $\text{SNR}=14\text{dB}$, the BEP has increased from 0.00003 to 0.0002. The BEP using the Snapping Threshold method with MFT lies in between the two curves from the Section 5.1.2.

If we look back in Chapter 4, Section 4.2.6, the BEP in the absence of noise at $A = 0.60$ is below 0.00001. Comparing the case of the Snapping threshold with no noise, and curve 3 in Figure 5.12, at $\text{SNR}=17\text{dB}$ and above, the BEP using the Snapping threshold with MFT is the same as that of the case with no noise.

It may be concluded from the results explained above, that designing a strategy for clipping decisions has improved the results.

5.2.4 Margin factor with Dither and Recursion Method

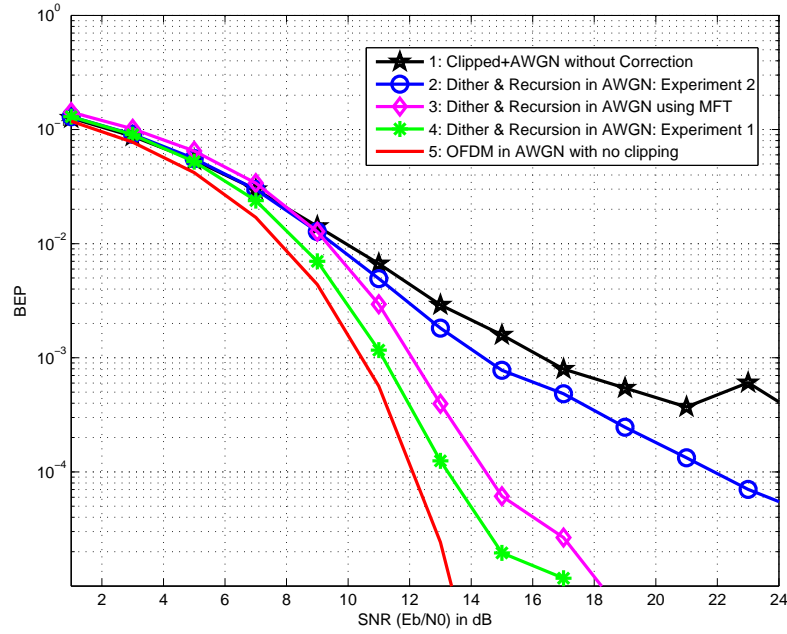


Figure 5.13: OFDM Bit-error Probability against SNR using Dither & Recursion with MFT

Figure 5.13 shows the BEP for the Dither and Recursion method using MFT. Curve 1 is the BEP without correction. Curves 2 and 4 have been explained above Section 5.1.3. Curve 3 shows the BEP using the Dither and recursion method with the MFT. Curve 4 represents the OFDM BEP without clipping.

Comparing curves 2 and 3, taking SNR=16dB, the BEP has reduced from 0.0006 to 0.00004 for the Dither and recursion with MFT. Comparing curves 3 and 4, the difference of BEP for the two plots is nearly 1dB. Curve 4 may be considered as the ideal case when the receiver has accurate knowledge of the clipped samples, whereas, curve 3 may be considered as the real case scenario. If we compare curves 1 and 3, at SNR=16dB, BEP has been reduced from .001 to 0.00004 using the Dither and recursion method with MFT in AWGN.

The BEP using the Dither and Recursion method in the absence of the noise from Section 4.4.2 at $A = 0.60$ is below 0.00001. If we compare this value to the BEP

achieved using the Dither and recursion method with MFT in AWGN, at SNR=18dB and onwards, the proposed method of MFT achieves a BEP of 0.00001. It may be concluded from the presented results that the BEP may be improved and reduced by using the MFT algorithm with the Dither and recursion method in AWGN.

5.2.5 Margin factor with Selective Dither and Recursion

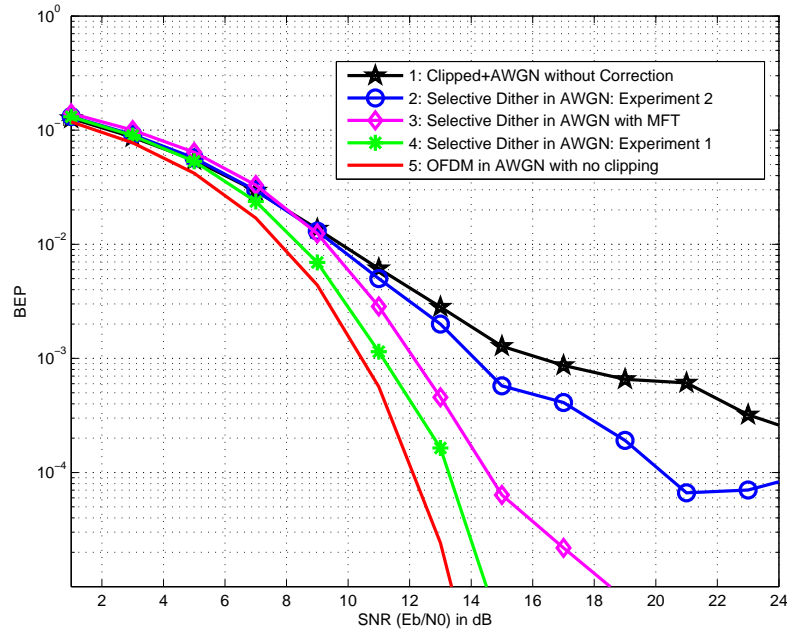


Figure 5.14: OFDM Bit-error Probability against SNR using Selective Dither & Recursion with MFT

Figure 5.14 presents the results using the Selective Dither and Recursion method. Curve 1 is the BEP of OFDM clipped signal without correction. Curves 2 and 4 are the results produced in Section 5.1.4. Curve 3 presents the OFDM BEP using the Selective Dither and Recursion method in AWGN with MFT. Curve 5 is the BEP in AWGN with no clipping.

Comparing curves 2 and 3, at SNR=16dB, the BEP using the Selective Dither and Recursion method with MFT has been reduced to .00004 from .0005. Comparing curves 3 and 4, at SNR=14dB, the BEP using Selective Dither with MFT is approximately 0.0002 whereas, for curve 4 at the same SNR it is 0.00002.

5.3 Conclusions

The effect of the channel noise (AWGN) on the performance of the Equation-Method has been investigated at two clipping levels $A = 0.40$ and $A = 0.60$. The analysis has been accomplished using two experiments for all the four approaches of the Equation-Method. From the analysis we concluded that all four versions of the Equation-Method, as developed for the noise-free case, do not work well at severe clipping levels ($A = 0.40$) in the presence of the noise. It was concluded from two experiments carried out for each of the four approaches that although the reliability of the constellation symbols is a significant issue, especially for severe clipping, the major problem is the identification of clipping at the receiver. Based on this conclusion, a new strategy based on the margin factor threshold is designed to tackle the noise on the clipping decisions and improve the Equation-method. All the four variations of the Equation-Method have been simulated with AWGN and results are presented. The performance of the Equation-Method at moderate clipping is effectively improved and BEP reduced prominently.

Chapter 6

Hybrid ARQ for Clipping

This chapter is concerned with the use of Automatic Repeat Request (ARQ) for correcting bit-errors in situations when these have occurred because of clipping as well as AWGN. ARQ is a data link layer protocol where error detection codes (ED) such as cyclic redundancy checks (CRC) are used to identify any bit-errors in the transmissions and if necessary, retransmissions are requested. The term ‘Hybrid ARQ’(Type I) is generally applied to a combination of ARQ and the use of FEC codes where uncorrectably damaged packets are discarded. Some forms of HARQ, often referred to HARQ Type II or Type III, allow damaged packets to be combined with retransmitted packets in an attempt to produce a corrected packet at the receiver. Chase combining (CC) is a form of HARQ (Type II) when the same set of coded bits is transmitted for the retransmission. Incremental Redundancy (IR) is another form of HARQ (Type III) which combines multiple transmissions by sending a different set of coded bits in every retransmission. HARQ (Type II) with Chase Combining works efficiently for bit-errors that have been caused by AWGN. It can not be expected to work for bit-errors caused by clipping, because the clipping error will remain the same in every retransmission. IR and CC were not designed primarily to work with bit-errors caused by clipping. Therefore, combining multiple transmissions of clipped signals may not be effective in correcting bit-errors. The focus of this chapter is to design a strategy which makes changes at the transmitter for the second transmission to allow an efficient combining algorithm to be used at the receiver in combination with the Equation-Method. This strategy will be referred to as ‘HARQ for Clipping’. ‘HARQ for Clipping’ is independent of FEC coding. It will work without and with FEC codes, in both cases. This method is specifically designed to deal with clipping errors. IR works at data link layer with FEC codes, but our method works at the physical layer. ‘HARQ for Clipping’ is

independent of which FEC technique, if any, is being employed. Its use in transmissions badly affected by clipping will allow the functionality of data link layer FEC to be successful where otherwise, it might fail, specially as clipping error tends to be bursty. The use of Turbo Codes with IR is still possible at the data link layer with the new ‘HARQ for Clipping’ working underneath it.

6.1 HARQ

Hybrid ARQ is categorized in two types. In type I the received erroneous packet is discarded and replaced by a re-transmitted packet. Type II HARQ has two classes:

1. Chase Combining
2. Incremental Redundancy

David Chase [52] has proposed to combine more than one received damaged packets when retransmissions have been necessary. For this purpose, maximum likelihood decoding is done at the receiver and soft decisions are made on the bits. After each failed retransmission the erroneous packet is saved in a buffer. Retransmissions repeat the same set of coded bits which was transmitted originally. The receiver uses Maximal Ratio Combining (MRC) [65] to combine all these packets and then the combined packet is fed to the decoder to decode. Chase combining does not increase the coding gain. It only effectively increases the signal to noise ratio E_b/N_o for each retransmission by increasing E_b . Figure 6.1 shows the block diagram for Chase combining.

In Incremental redundancy (IR), each retransmission is not identical to the original transmission. IR is normally combined with the use of punctured FEC coding, for example using Turbo Codes [19]. A low ratio FEC code (e.g. 1/3 rate) may be generated and punctured (e.g. to 1/2 rate) for the first transmission. If a retransmission becomes necessary, a different punctured set of coded bits are selected. The code rate of the combined transmissions is lowered with each retransmission.

6.2 Performance of HARQ- Chase Combining

This section investigates the performance of the HARQ-Chase combining on the OFDM signals in the presence of AWGN with and without clipping. A simple combining algorithm has been designed and explained in the next section. The effect of the AWGN and the clipping is investigated and discussed.

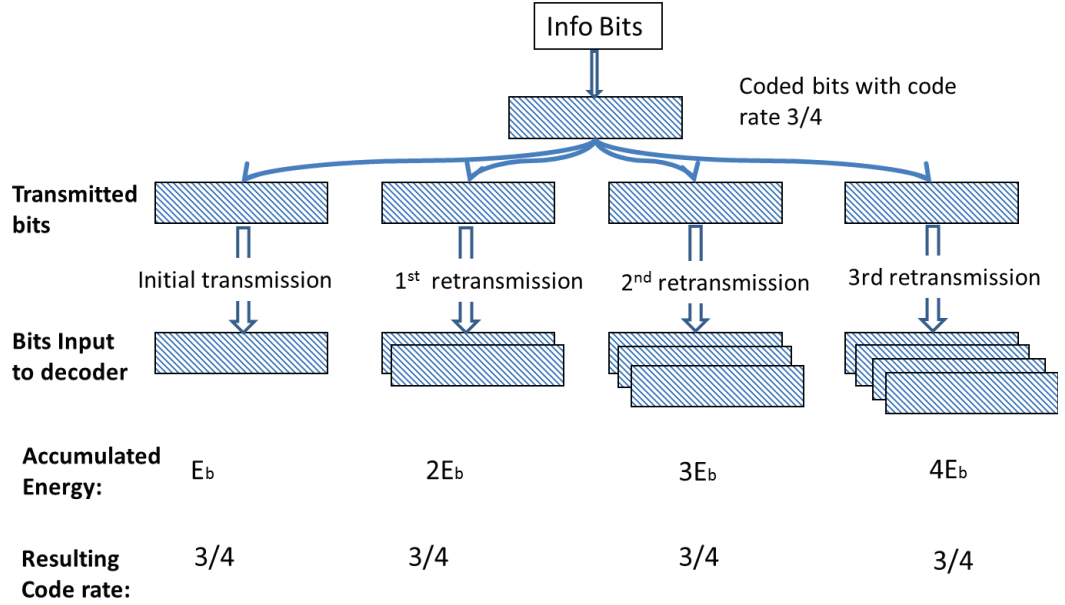


Figure 6.1: Chase Combining

6.2.1 Chase Combining Algorithm

Chase combining is investigated here without the use of FEC coding. The receiver uses normal hard-bit decisions for de-mapping the received constellation symbols to bits. Equation 6.1 represents the received signal, where x_n is the OFDM signal and a_n is the AWGN. The signal is converted to the frequency-domain by the FFT, and, for the first transmission, the transformed signal is labelled Y_{1k} for $k = 0, 1, \dots, N-1$

$$y_n = x_n + a_n, n = 0, 1, \dots, N-1 \quad (6.1)$$

1. The received frequency-domain signal Y_{1k} is de-mapped to bits using hard-bit decisions. With the help of the EC codes, it is determined if there are any bit-errors. In the case of bit-error occurrence, a retransmission is requested. The receiver keeps a copy of the first transmission Y_{1k} .
2. The transmitter re-transmits the same signal which is received as y_{2n} at the receiver. The frequency-domain equivalent of this signal is obtained and labeled as Y_{2k} .
3. Y_{1k} and Y_{2k} are two copies of the same signal where the difference is only the addition of AWGN. These two copies are combined at constellation symbol level, as follows:

$$C_k = (Y_{1k} + Y_{2k})/2, k = 0, 1, \dots, N - 1 \quad (6.2)$$

4. The combined signal C_k gives a new set of constellation symbols which are then de-mapped from the constellation to bits.

6.2.2 Errors due to AWGN

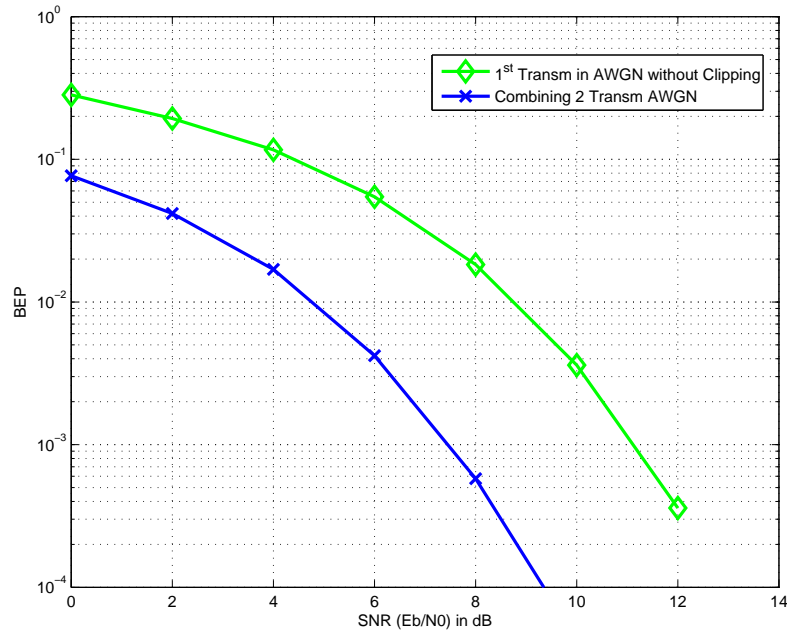


Figure 6.2: OFDM Bit-error Probability against SNR using Combining without clipping

The receiver combines the two copies of the transmissions at the constellation symbol level by using the above combining method. Figure 6.2 shows the OFDM BEP against SNR using combining in the presence of AWGN without clipping. The plots are produced after transmitting 1000 randomly generated OFDM symbols without clipping.

The BEP clearly reduced at all values of SNR. At SNR = 8dB, the first transmission $BEP = 0.02$ and after combining the two transmissions, the BEP at the same level of SNR is 0.0006. The next section repeats the same experiment with clipped OFDM signals.

6.2.3 Errors due to Clipping

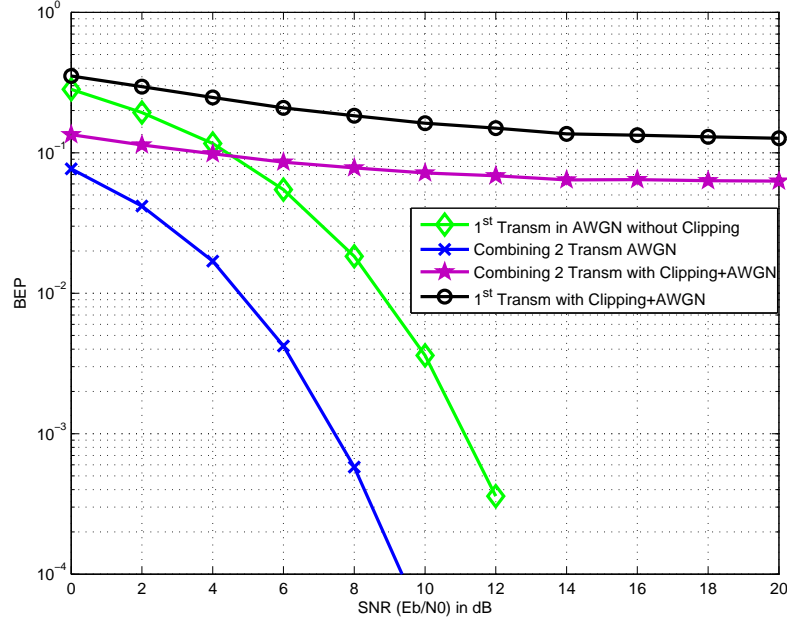


Figure 6.3: OFDM Bit-error Probability against SNR using Combining at $A = 0.40$

The same Chase Combining algorithm has been used for clipped OFDM signals with clipping levels at $A = 0.40$ and $A = 0.60$. Figure 6.3 shows the OFDM BEP, when clipping levels were at $A = 0.40$. The BEP has drastically increased in the first transmission because of the clipping noise. The BEP using Chase Combining for two clipped OFDM transmissions has reduced after the second transmission but not impressively. The difference between the first and combined BEP remains almost the same for all the values of Signal-to-Noise ratio (SNR).

Figure 6.4 shows the OFDM BEP using the same Chase combining method when the signal was clipped at $A = 0.60$. For the curve showing the results with clipping after the first transmission, the BEP has increased as expected. After combining two transmissions, the BEP has reduced more at lower values of E_b/N_0 than at higher values of the E_b/N_0 . The reason is that, for the higher values of E_b/N_0 , the clipping distortion is dominant.

This experiment confirms that Chase Combining is not effective for clipping distortion that remains the same in retransmissions. The second transmission has to be different from the first one so that the clipping distortion may be different from the first transmission. The next section explains how this may be achieved.

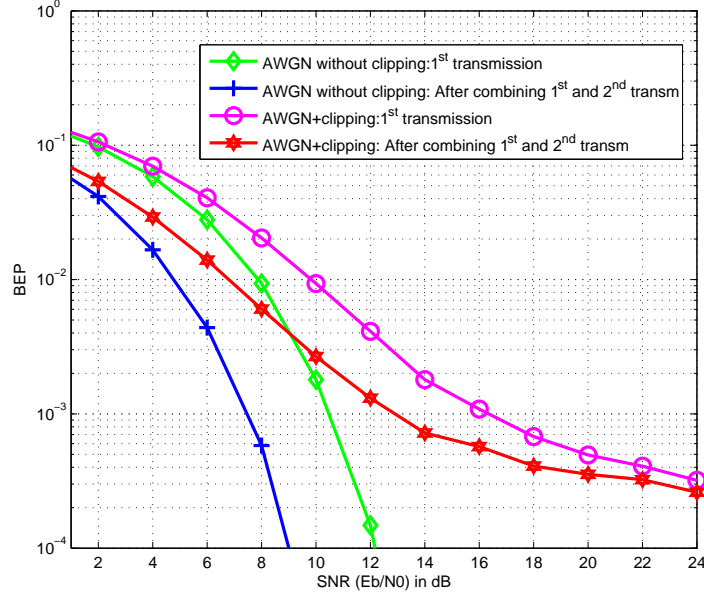


Figure 6.4: OFDM Bit-error Probability against SNR using Combining at $A = 0.60$

6.3 HARQ for Clipping

This section explains a new method for combining multiple transmissions of the same signal at the receiver. This method uses soft bit decisions for the received bits at the receiver.

6.3.1 Soft Decisions

The method we have proposed for ‘HARQ for Clipping’ uses soft decisions for the bit-stream derived from the received constellation. These soft decisions take into account the a priori probabilities of the received constellation symbols. It produces the soft output indicating the reliability of the decision. The received signal is corrupted by AWGN.

For uncoded communication systems, conditional probabilities may be used to extract maximum a priori probability (MAP) from the received channel observations. Table 6.1 shows the bit mapping for 16-QAM constellation. b_0b_1 are mapped on real and called I, b_2b_3 correspond to imaginary part of the signal and called Q. The signal at the transmitter is mapped according to this table to 16-QAM constellation.

The received signal in frequency-domain is Y_k which has to be de-mapped. According to [66], [67] the Log-likelihood ratios (LLR) values for a bit $b \in 0, 1$ conditioned

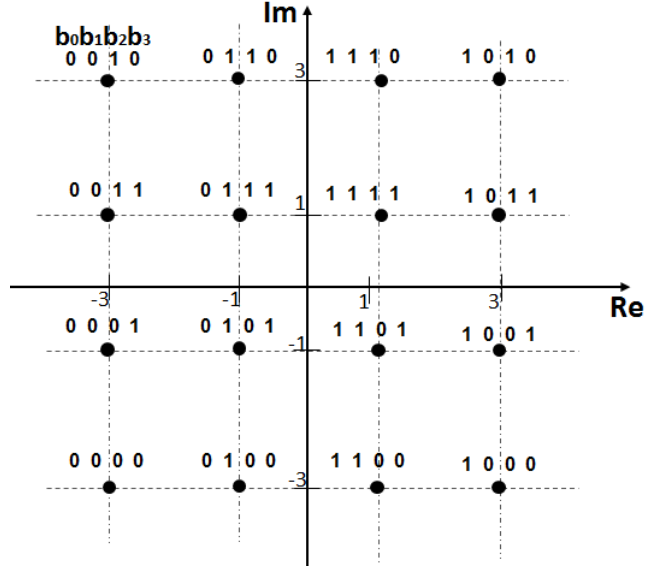


Figure 6.5: A Grey-coded 16-QAM Constellation

Table 6.1: Constellation mapping for 16-QAM

b_0b_1	Real	b_2b_3	Imaginary
00	-3	00	-3
01	-1	01	-1
10	3	10	3
11	1	11	1

on the received constellation symbol Y is given by:

$$L(b|Y) = \log \frac{p(b=1|Y)}{p(b=0|Y)} \quad (6.3)$$

The mathematical expression for computing the channel LLR's for each bit $b_m \in b_0, b_1, b_2, b_3$ of the received signal $Y_k = Y_I + jY_Q$

$$L(b_m) = \log \frac{\sum_{s_{1,b_m} \in \{s(b_m=1)\}} e^{-\frac{(Y-s_{1,b_m})^2}{2\sigma^2}}}{\sum_{s_{0,b_m} \in \{s(b_m=0)\}} e^{-\frac{(Y-s_{0,b_m})^2}{2\sigma^2}}} \quad (6.4)$$

Equation 6.4 involves computing LLR for each bit of the transmitted signal, which is actually ratio of the sum of 8 probabilities where that bit is 1 to the sum of the 8

probabilities where that bit is 0. For AWGN the conditional probability function may be written as:

$$p(Y|b_m) = \frac{1}{\sqrt{2\pi\sigma}} \exp -\frac{1}{2\sigma^2} (Y - b_m)^2 \quad (6.5)$$

To simplify the calculation of the probabilities, the values which return the smallest Euclidean distances may be considered only. We need to find the value which has the smallest Euclidean distance. That is given the received constellation symbols Y , we have to find the closest neighbor where $b_m = 1$ and the closest neighbor where $b_m = 0$. Assuming that the transmitted symbols are equally distributed, using the Bayes rule and the a priori LLR, from the Equation 6.4, the likelihood ratio for the bit b_m of the symbol Y , may be written as

$$\tilde{L}(b_m) = \log \frac{e^{-\frac{(Y - S_{1,b_m})^2}{2\sigma^2}}}{e^{-\frac{(Y - S_{0,b_m})^2}{2\sigma^2}}} \quad (6.6)$$

Taking log on both sides

$$LLR(b_m) = \frac{1}{2\sigma^2} \left[(Y - S_{0,b_m})^2 - (Y - S_{1,b_m})^2 \right] \quad (6.7)$$

This equation can be further simplified as

$$LLR(b_m) = \frac{Y_I}{\sigma^2} (S_{1I,b_m} - S_{0I,b_m}) + \frac{Y_Q}{\sigma^2} (S_{1Q,b_m} - S_{0Q,b_m}) + \frac{1}{2\sigma^2} (S_{0I,b_m}^2 - S_{1I,b_m}^2) + \frac{1}{2\sigma^2} (S_{0Q,b_m}^2 - S_{1Q,b_m}^2) \quad (6.8)$$

where \tilde{S}_{1,b_m} and \tilde{S}_{0,b_m} are the closest 16-QAM symbols in the sense of Euclidean distance to Y_k , where bit b_m is equal to 1 and 0, respectively. Equation 6.8 can be further simplified for all the four bits in one symbol $b_m \in b_0, b_1, b_2, b_3$. Bits b_0 and b_1 make the real part of the constellation symbol. The imaginary symbols remain the same and any change for bits b_0 and b_1 does not affect the imaginary part of the Equation 6.8. Therefore, if we take the expressions for real part only from the Equation 6.8, the expressions for b_0 and b_1 may be written as

$$L(b_0) = \frac{Y_I}{\sigma^2} (S_{1I,b_0} - S_{0I,b_0}) + \frac{1}{2\sigma^2} (S_{0I,b_0}^2 - S_{1I,b_0}^2) \quad (6.9)$$

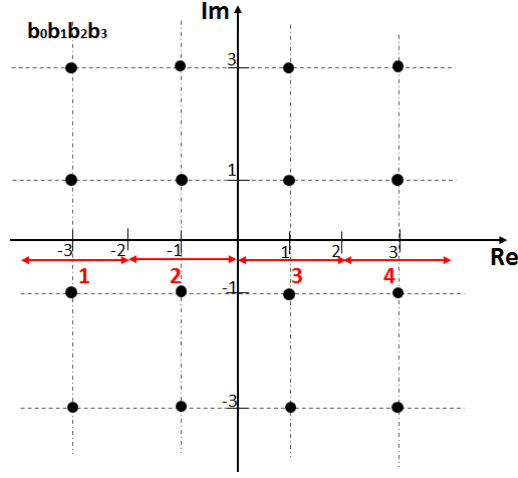


Figure 6.6: Decision regions for soft bits

$$L(b_1) = \frac{Y_I}{\sigma^2} (S_{1I,b_1} - S_{0I,b_1}) + \frac{1}{2\sigma^2} (S_{0I,b_1}^2 - S_{1I,b_1}^2) \quad (6.10)$$

In Equation 6.9, when bit b_0 is 0, $S_{0I,b_0} = -3$ or $S_{0I,b_0} = -1$, and when b_0 is 1, $S_{1I,b_0} = 3$ or $S_{1I,b_0} = 1$. We can define four regions on the constellation for which we have to calculate the log-likelihood ratios as presented in Figure 6.6.

1. when $Y_{re} < -2$
2. when $-2 \leq Y_{re} < 0$
3. when $0 \leq Y_{re} < 2$
4. when $Y_{re} \geq 2$

When $Y_{re} < -2$ then $S_{1I,b_0} = 1$ and $S_{0I,b_0} = -3$. For $-2 \leq Y_{re} < 0$, $S_{1I,b_0} = 1$ and $S_{0I,b_0} = -1$. For $0 \leq Y_{re} < 2$, $S_{1I,b_0} = 1$ and $S_{0I,b_0} = -1$. For $Y_{re} \geq 2$, $S_{1I,b_0} = 3$ and $S_{0I,b_0} = -1$. Therefore, Equation 6.9 may be re-written as:

$$b_0 = \begin{cases} \frac{4}{\sigma^2}(Y_{re} + 1), & \text{if } Y_{re} < -2 \\ \frac{2}{\sigma^2}Y_{re}, & \text{if } -2 \leq Y_{re} \leq 2 \\ \frac{4}{\sigma^2}(Y_{re} - 1), & \text{if } Y_{re} > 2 \end{cases} \quad (6.11)$$

For bit b_1 , when $Y_{re} < -2$ then $S_{1I,b_1} = -1$ and $S_{0I,b_1} = -3$. For $-2 \leq Y_{re} < 0$, $S_{1I,b_1} = -1$ and $S_{0I,b_1} = -3$. For $0 \leq Y_{re} < 2$, $S_{1I,b_1} = 1$ and $S_{0I,b_1} = 3$. For $Y_{re} \geq 2$,

$S_{1I,b_1} = 1$ and $S_{0I,b_1} = 3$. Therefore, Equation 6.10 may be re-written as:

$$b_0 = \begin{cases} \frac{2}{\sigma^2}(Y_{re} + 2), & \text{if } Y_{re} < -2 \\ \frac{2}{\sigma^2}(Y_{re} + 2), & \text{if } -2 \leq Y_{re} < 0 \\ \frac{2}{\sigma^2}(-Y_{re} + 2), & \text{if } 0 < Y_{re} \leq 2 \\ \frac{2}{\sigma^2}(-Y_{re} + 2), & \text{if } Y_{re} > 2 \end{cases} \quad (6.12)$$

The factor $\frac{2}{\sigma^2}$ is common in all terms, so it may be removed. The soft bit for b_1 may be further simplified and can be written as in Equation 6.14.

$$b_0 = \begin{cases} 2(Y_{re} + 1), & \text{if } Y_{re} < -2 \\ Y_{re}, & \text{if } -2 \leq Y_{re} \leq 2 \\ 2(Y_{re} - 1), & \text{if } Y_{re} > 2 \end{cases} \quad (6.13)$$

$$b_1 = \left\{ (-|Y_{re}| + 2), \quad \text{for all } Y_{re} \right. \quad (6.14)$$

As we can see from the Figure 6.5, the mapping of the Imaginary part is the same as the real part, so using similar analysis the approximate expressions for bits b_2 and b_3 may be extracted from the Equations 6.15 and 6.16 as:

Bits b_2 and b_3 make the imaginary part of the constellation symbol, so taking the imaginary part of the Equation 6.8, may be written as:

$$L(b_2) = \frac{Y_Q}{\sigma^2} (S_{1Q,b_2} - S_{0Q,b_2}) + \frac{1}{2\sigma^2} (S_{0Q,b_2}^2 - S_{1Q,b_2}^2) \quad (6.15)$$

$$L(b_3) = \frac{Y_Q}{\sigma^2} (S_{1Q,b_3} - S_{0Q,b_3}) + \frac{1}{2\sigma^2} (S_{0Q,b_3}^2 - S_{1Q,b_3}^2) \quad (6.16)$$

$$b_2 = \begin{cases} 2(Y_{im} + 1), & \text{if } Y_{im} < -2 \\ Y_{im}, & \text{if } |Y_{im}| \leq 2 \\ 2Y_{im} - 1), & \text{if } Y_{im} > 2 \end{cases} \quad (6.17)$$

$$b_3 = -|Y_{im}| + 2 \quad (6.18)$$

6.3.2 Combining to correct bit-errors caused by clipping

Chase combining of two transmissions will not reduce the number of bit-errors due to clipping. The basic idea of ‘HARQ for Clipping’ is to change the original bit-sequence by *XOR*ing with a pseudo-random sequence at the transmitter to generate the second transmission. The purpose is to make the pattern of clipping different for the second transmission so that the same time-domain samples will not always be clipped. Because of the change in the bit-stream, multiple packets cannot be directly combined at the receiver at symbol level. The soft combining will be accomplished using the log-likelihood ratios (LLR) as described in Section 6.3.1. Soft bits for each received bit are calculated. The receiver uses soft-bit decisions to combine the multiple transmissions of the same signal. The HARQ transmission scheme for the proposed work has R_h transmissions, where h is the transmission index.

Both the transmitter and receiver agree on a random sequence. We have used a Barker sequence [68]. The Barker sequence is a finite random binary sequences whose auto-correlation function has minimum correlation at all delays apart from zero. They are widely used for direct sequence spread spectrum communications [69]. A different Barker sequence must be used for each re-transmission where more than one is required. The proposed method uses re-transmissions to be combined at the receiver in order to correct the bit-errors. The following sections provide a more detailed description of the transmissions and soft combining.

6.3.3 First Transmission:

1. The base-band signal x_n is clipped using the defined clipping threshold and transmitted to the receiver. The first transmission is called R_1
2. The receiver gets the frequency-domain signal Y_k by applying an FFT.
3. With the help of EC codes, the receiver determines if there are any bit-errors in the signal received. In the case of bit-errors, a re-transmission of the same signal is requested.

6.3.4 Re-transmission

To make the re-transmissions, the transmitter has to change the modulated signal so that the time-domain signal will be different from the first transmission in Section

6.3.3. For this purpose, the transmitter uses Barker sequences which the receiver already know. The logical operation Exclusive-OR is used at the transmitter. Generally it is denoted by the symbol \oplus . The original bit-sequence of the signal is bit-wise *XOR*ed with the Barker sequence B as follows:

$$\tilde{D}_l = B_l \oplus D_l, l = 0, 1, \dots, N \times 4 - 1 \quad (6.19)$$

The output \tilde{D}_l of the *XOR* operation is taken as the new bit-sequence and mapped on 16-QAM constellation producing \hat{X}_k , for $k = 0, 1, \dots, N - 1$. The complex constellation symbols are converted to time-domain and applied to clipping. The second transmission of the signal is transmitted as R_2 .

6.3.5 ‘HARQ for Clipping’ Soft Combining

The received signal has to be decoded in the form of soft bits. The received signal after converting to the frequency-domain is Y_{1k} and Y_{2k} . To allow efficient combining of the constellation symbols, it is a good idea to derive a soft representation of each received bit for each re-transmission. Our soft representation will be quantized to 8 levels, ‘000’ (strongly 0) to ‘111’ (strongly 1). Both the transmissions Y_{1k} and Y_{2k} will undergo the same procedure of estimating soft bits as explained below.

1. Soft bits b_0 and b_1 are calculated from the real part of the constellation symbols, and soft bits for b_2 and b_3 are calculated from the imaginary part as explained in Section 6.3.1. The soft bit representation is determined by calculating Euclidean distances to the snapping points and determining the soft bits according to the probability (based on distance) of the original bit being 1 or 0.
2. The calculated soft bits for both the transmissions are stored in $LLR(Y_1)$ and $LLR(Y_2)$ respectively.
3. Since the re-transmissions are *XOR*ed with a Barker bit sequence B at the transmitter, so now at the receiver its effect needs to be undone. $LLR(Y_2)$ is in the form of decimal digits in the range of 0 – 7, whereas the sequence B is in the form of binary digits. They both need to be in the same format to apply the *XOR* operation. The B sequence is first converted to another sequence \hat{B} which has

the format as of $LLR(Y_2)$ as follows:

$$\hat{B}_l = \begin{cases} 7, & \text{if } B_l == 1 \\ 0, & \text{if } B_l == 0 \end{cases} \quad (6.20)$$

4. The next step is to apply bit-wise XOR operation on the sequences \hat{B}_l and $LLR(Y_2)$ as follows:

$$U_l = LLR(Y_{2l}) \oplus \hat{B}_l, \text{ for } l = 0, 1, \dots, (N \times 4) - 1 \quad (6.21)$$

5. $LLR(Y_1)$ from the first transmission and U_l from the second transmission both are added and average is calculated as follows:

$$\hat{C} = (LLR(Y_{1l}) + U_l) / 2, \quad l = 0, 1, \dots, (N \times 4) - 1 \quad (6.22)$$

6. \hat{C} is the resultant bit-sequence after soft combining. The decisions for the transmitted bits has to be made according to the following equation:

$$\hat{D}_l = \begin{cases} 1, & \text{if } \hat{C}_l \geq 4 \\ 0, & \text{if } \hat{C}_l < 4 \end{cases} \quad (6.23)$$

6.4 Simulation Results

This section presents the simulation results for the bit-error probability of the proposed ‘HARQ for Clipping’ Soft Combining method with clipping. A total of 10,000 OFDM symbols are transmitted with 16-QAM modulation on each subcarrier.

Figure 6.7 shows the results of OFDM BEP after applying ‘HARQ for Clipping’ algorithm at clipping level $A = 0.60$ and $A = 0.40$. The BEP of the clipped signal ($A = 0.60$) after combining two transmissions has reduced largely for higher values of SNR.

Taking SNR=12dB, the BEP for clipped signals has reduced from 0.004 to 0.00009 after Soft-combining has applied. From SNR=15dB and onwards, the BEP for combined signals has fallen below than 0.00001. Comparing Figure 6.7 and Figure 6.4, at SNR=12dB, the BEP for Chase Combining algorithm was nearly 0.001, which has reduced to 0.00009 after using the new Soft-combining algorithm.

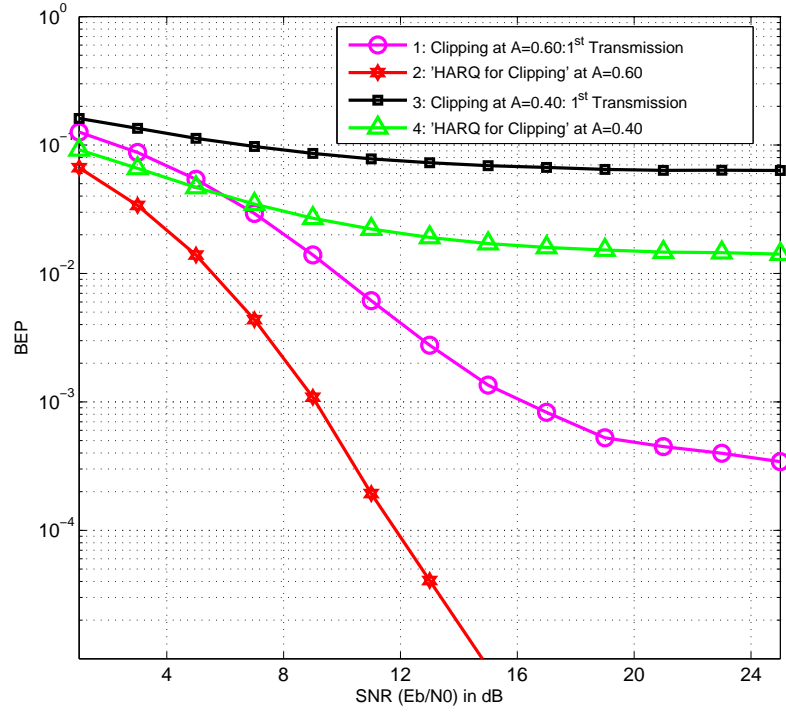


Figure 6.7: OFDM Bit-error Probability against SNR using ‘HARQ for Clipping’ at $A=0.6$ and $A=0.40$

Curves 3 and 4 represent the BEP, when the signal is clipped at 0.40, after first transmission and combining two transmissions, respectively. The BEP has reduced significantly after using the Soft-combining algorithm. Taking $\text{SNR}=12\text{dB}$, the BEP is 0.02 for Curve 4 and 0.08 for Curve 3. There is a further decrease in the BEP for the Curve 4 as SNR increases.

6.5 ‘HARQ for Clipping’ with the Equation-Method

The best strategy of the Equation-Method, i.e. Selective Dither and Recursion, has been combined with the ‘HARQ for Clipping’ method. The maximum number of transmissions are kept at two. The clipping level is at $A = 0.60$. The Figure 6.8 shows the OFDM BEP using the ‘HARQ for Clipping’ with the Selective Dither and Recursion strategy of the Equation-Method. The results have been produced in the presence of AWGN, so the Margin Factor Threshold strategy has been used at the receiver to reduce the effect of noise, before determining soft bit decisions. The BEP has reduced

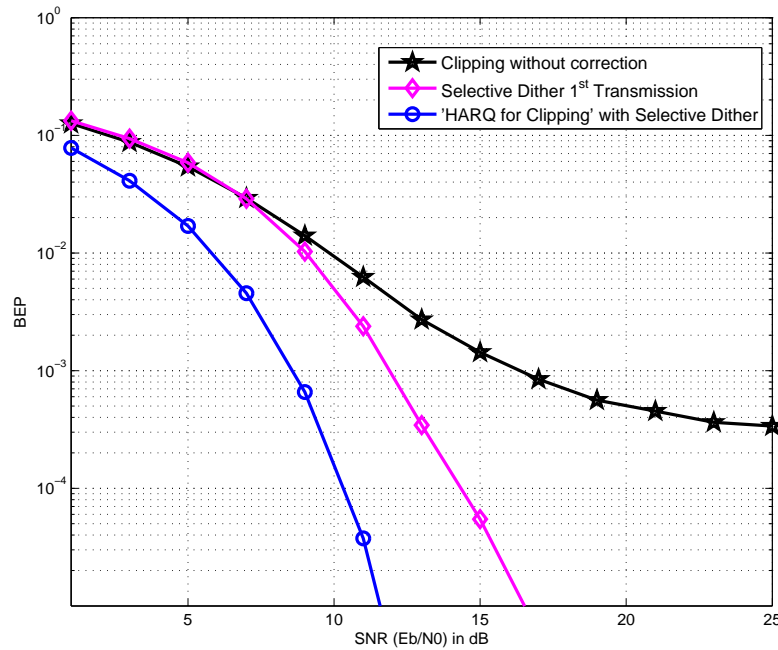


Figure 6.8: OFDM Bit-error Probability against SNR using ‘HARQ for Clipping’ with EM-Selective Dither at $A = 0.6$

from .01 at $\text{SNR} = 10\text{dB}$, when there is no correction, to the BEP of 0.0002 after using the ‘HARQ for Clipping’ using Selective Dither.

For the first transmission, when the Selective Dither and Recursion is applied to the transmission, the BEP is at $\text{SNR} = 10\text{dB}$ is 0.005. Comparing the first transmission, and the Soft combining ‘HARQ for Clipping’, there is a prominent reduction in the BEP.

Figure 6.9 shows a comparison of the BEP for ‘HARQ for Clipping’ without the Equation Method and ‘HARQ for Clipping’ with the Equation Method using Selective Dither and Recursion. There is a slight increase in the BEP at lower values of SNR for the curve plotted using ‘HARQ for Clipping’ using Selective Dither as compared to the one which has been produced with ‘HARQ for Clipping’ without the Equation-Method. For higher values of SNR, there is a prominent decrease in the BEP starting off from $\text{SNR} = 8\text{dB}$ and onwards. Taking $\text{SNR} = 10\text{dB}$, the BEP has reduced to nearly .0002 using the ‘HARQ for Clipping’ with the Equation-Method, from the BEP of 0.0005.

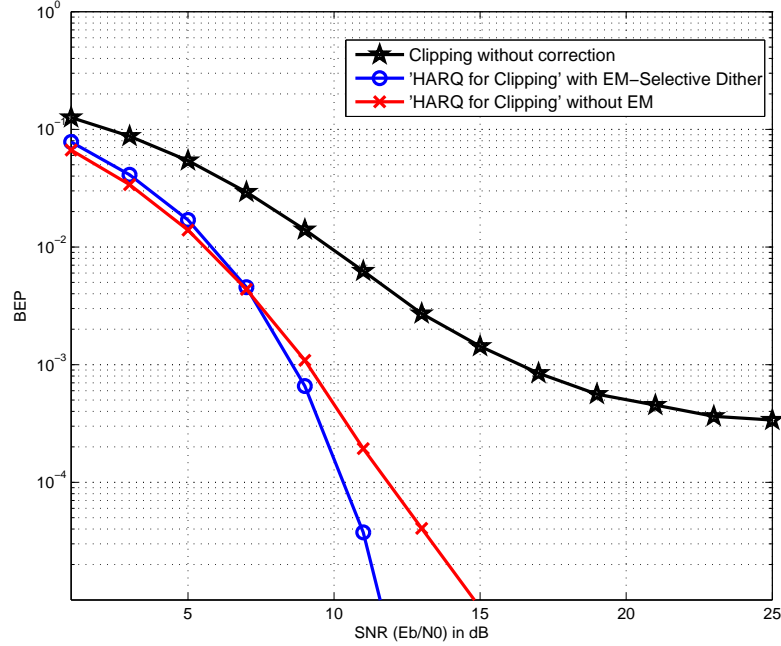


Figure 6.9: Comparison of BEP for 'HARQ for Clipping' with/without Equation-Method (EM) with clipping at $A = 0.6$

6.6 Comparison to other approaches

The performance of this method is compared to other approaches from the literature which aim to reduce the non-linear distortion produced by limiting. Two of the most cited approaches have been presented in Chapter 3. Comparing the BEP obtained using Selective Dither and Recursion without HARQ from Figure 6.9 with BNC receiver in Figure 6.10, at levels of SNR above about 17dB, the Selective Dither and Recursion method has reduced the BEP significantly as compared to the BNC receiver. There is less difference for lower levels of SNR.

Further reduction in BEP for the Equation-Method (Selective Dither and Recursion) has been achieved by combining with the 'HARQ for Clipping' method. Figure 6.10 shows the comparison of the bit-error probability of the combined method of the 'HARQ for Clipping' & Equation-Method with the BNC iterative receiver at clipping threshold $A = 0.60$. There is a significant reduction in the bit-error probability for our technique as compared to BNC at all levels of SNR, though the BNC method used does not have the advantage of retransmission and combining. Accepting this, 'HARQ for Clipping' with the best version of the Equation-Method outperforms the BNC iterative

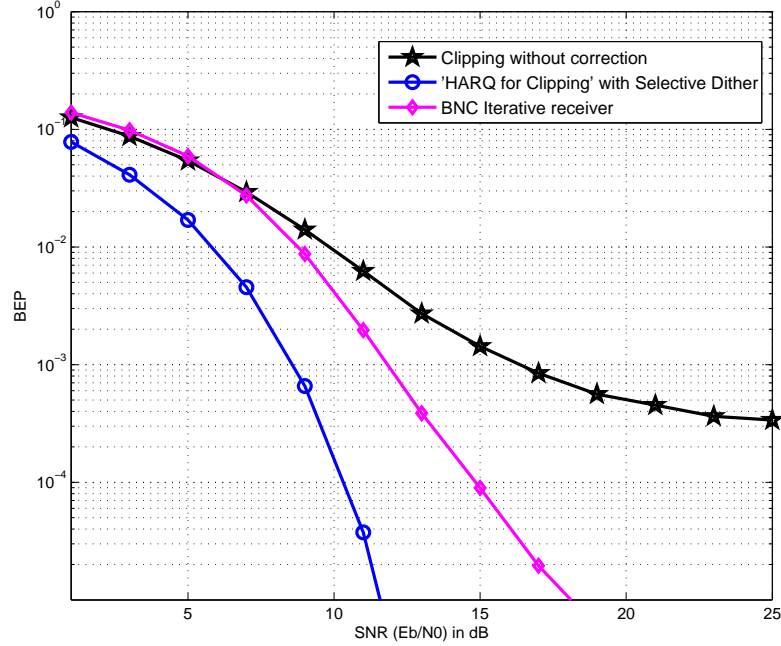


Figure 6.10: Comparison of BEP for 'HARQ for Clipping' with the Equation-Method to BNC receiver, clipping at $A = 0.6$

receiver (without HARQ) by 3dB. It is concluded that 'HARQ for Clipping' with the best version of the Equation-Method has outperformed BNC iterative receiver by 3dB.

6.7 Conclusions

Chase combining will not work effectively for the bit-errors due to clipping in clipped OFDM signals. There is a need to make changes to the second transmission so that clipping noise may differ in both transmissions. A new form of Soft-combining (HARQ for Clipping) has been proposed in this chapter which uses a highly uncorrelated random sequence to make changes to the second transmission of the same signal. The results are presented to support the algorithm and the BEP at moderate clipping threshold has reduced largely after using the new combining technique. It may be concluded that making changes to the re-transmissions such as different time-domain samples are affected by clipping from the first transmission, helps to reduce the BEP. The proposed method has been extended to a combination of the Equation- Method with the HARQ for Clipping combining. The Selective Dither and Recursion strategy has been used

along with the HARQ for Clipping method. Comparing the results shows a significant reduction at lower levels of SNR. The advantage of the proposed method is that it works for clipping and AWGN noise both, while it has been designed specially to correct bit-error occurred by clipping.

Chapter 7

Conclusions

OFDM is multicarrier modulation technique which is now widely used for both wireless and wired communication systems. It has been proven to be effective at dealing with multipath effects and inter-symbol interference. However, the need for highly linear amplification and the high peak to average power ratio of the signals produced is a impediment to the use of OFDM in battery powered mobile systems. Highly linear amplifiers tend to require a high power consumption. In order to solve this problem, many PAPR reduction or mitigation techniques have been proposed. Since the occurrence of high peaks in OFDM signals are an event with non-negligible probability, therefore effective PAPR mitigation techniques are essential to enable the efficient use of power amplifiers. Soft-limiting to avoid the possibility of amplifier non-linearities is a starting point for many solutions published in the literature. It produces non-linear distortion in the signal which without further processing would increase the BER at the receiver. This thesis has investigated the time-domain and frequency-domain effects of soft-clipping on OFDM signals. Two novel methods the ‘Equation-Method’ and ‘HARQ for Clipping’, to mitigate the effects of the clipping have been presented in this thesis.

Soft-limiting techniques are described along with their effects and performances. Two clipping noise mitigating iterative receivers have been compared in terms of the BER. These are decision aided reconstruction (DAR) and Busgang noise cancellation (BNC). The BNC receiver, based on the Busgang theorem has been investigated for reducing the effect of limiting distortion by eliminating any correlation with the original signal and thus reducing its power. This receiver tries to estimate the limiting distortion so that it may be subtracted from the received signal. The technique works reasonably well for low degrees of limiting. It has been concluded that if accurate

value of the distortion factor is estimated in each iteration, the signal can be recovered for lower levels of clipping.

A novel limiting technique has been presented which uses ‘wrap-around’ rather than clipping. It effectively reduces the PAPR as measured after limiting and filtering as compared to clipping. However, BER degradation as compared to clipping has been observed.

The Equation-Method has been proposed for correcting the bit-errors produced by clipping distortion in OFDM signals. This method uses the unclipped time-domain samples and the received frequency-domain symbols to generate a set of linear equations which may be solved for the clipped samples. The method has been further improved by presenting four strategies. It has been evaluated to determine the percentage of OFDM symbols that can be completely corrected, at moderate to severe clipping thresholds, by different versions of the method. The best results are compared with other receiver-oriented approaches (presented in this thesis and in the literature), and demonstrate the superiority of the new method. The method has also been evaluated by calculating the BEP for the four approaches.

All four versions of the Equation-Method were developed initially for the noise-free case. Experiments were carried out for each of the four approaches in the presence of channel noise (AWGN). It was concluded, that although the reliability of the constellation symbols is a significant issue, especially for severe clipping, the major problem when AWGN is present, is the identification of clipping at the receiver. A new strategy based on a margin factor threshold (MFT) has been designed to tackle the noise on the clipping decisions and improve the Equation-method. All the four variations of the Equation-Method have been simulated using MFT with AWGN and results are presented. The performance of the Equation-Method at moderate clipping is effectively improved and the BEP has been reduced significantly. The BEP at severe clipping is not reduced significantly for all the four approaches of the Equation-Method.

The conventional HARQ schemes known as Chase Combining and Incremental Redundancy are designed to work for bit-errors caused by AWGN. Chase combining cannot be expected to work for clipped OFDM signals because the clipping distortion will remain the same in every re-transmission. We have proposed a new method ‘HARQ for Clipping’ which changes every re-transmission by XORing it with a finite Barker sequence. The effect of this XOR operation is removed at the receiver, as the receiver knows the Barker sequences. Soft-bit values are calculated for the transmissions and combined at the receiver efficiently at the bit-level. The Selective Dither

and Recursion strategy of the Equation-Method has been combined with the ‘HARQ for Clipping’ method. Comparing the results show a significant reduction at lower SNR values. This seems to be the best result of all previously published PAPR mitigation techniques at an expense of the re-transmissions. The advantage of the proposed method is that it works for soft-clipping and AWGN noise both, while it has been designed specially to correct bit-errors caused by soft-clipping.

7.1 Future Work

The following topics have been identified as worthy of future research:

1. The combination of the Equation-method with FEC codes such that if the Equation-Method is able to correct some of the wrong constellation symbols, FEC codes may be used to correct rest of the others.
2. The probability of the Equation-Method introducing any bit-errors to a correctly received OFDM symbol.
3. The evaluation of the Equation-Method in terms of the complexity and computational time and then comparison with the existing approaches has to be done yet.
4. The improvement in the performance of the Equation-Method in the presence of AWGN for severe clipping threshold may be the focus for further work. Recursion as applied in the Equation-Method may be used to handle the effects of the AWGN.
5. The effect of RF systems on the performance of the Equation-Method has to be investigated. We are not sure if the low pass filtering is going to cause any problems for the Equation-Method.
6. There are many ways of using HARQ for correcting bit-errors caused by soft-clipping. We have explained and used only one way. IWRAP and soft-clipping may be used as an alternative for re-transmissions and then soft combining may be used at the receiver to combine the clipped and limited transmissions. By knowing the clipping threshold, the receiver may identify the clipped samples and can just combine the clipped and limited transmissions to make one corrected copy.

7. We have used HARQ without any FEC codes. If it is used with FEC codes, this will improve the performance of the technique. It would be useful to evaluate the improvement.
8. For the HARQ second transmission, the amplitudes of the time-domain signal may be halved and transmitted. This is a very simple way of eliminating clipping in the second transmission. The receiver, knowing the effect on the amplitudes of the re-transmission, may double the amplitudes of the re-transmission and then use soft-combining. The effectiveness of this idea has already been explored. It works quite well, and appear worthy of future research.

Bibliography

- [1] S.-K. Deng and M.-C. Lin, “Ofdm papr reduction using clipping with distortion control,” in *IEEE International Conference on Communications, ICC 2005*, vol. 4, pp. 2563–2567 Vol. 4, May 2005.
- [2] Y. Wu and W. Zou, “Orthogonal frequency division multiplexing: a multi-carrier modulation scheme,” *IEEE Transactions on Consumer Electronics*,, vol. 41, pp. 392–399, Aug 1995.
- [3] M. Ergen, *Mobile Broadband Including Wimax and LTE*. Springer Science+Business Media, 2009.
- [4] D. J. G. Hyung G.Myung, Junsung Lim, “Peak-To-Average Power Ratio of Single Carrier FDMA Signals with Pulse Shaping,” in *IEEE 17th International Symposium on Personal, Indoor and Mobile Radio Communications*,, pp. 1–5, 2006.
- [5] C. A. A.-M. . K. L. . K. Lee, “PAPR Reduction in Single Carrier FDMA Uplink by Pulse Shaping Using a β - α Filter,” *Wireless Personal Communications*, vol. 71, pp. 23–44, 2013.
- [6] M. Rumney, “3GPP LTE: Introducing Single-Carrier FDMA,” tech. rep., Agilent Technologies, 2008.
- [7] H.-G. Ryu, B.-I. Jin, and I.-B. Kim, “PAPR reduction using soft clipping and ACI rejection in OFDM system,” *IEEE Transactions on Consumer Electronics*,, vol. 48, pp. 17–22, Feb 2002.
- [8] J. Armstrong, “Peak-to-average power reduction for ofdm by repeated clipping and frequency domain filtering,” *Electronics Letters*, vol. 38, no. 5, pp. 246–247, 2002.

- [9] X. Li and L. Cimini, "Effects of clipping and filtering on the performance of OFDM," in *IEEE 47th Vehicular Technology Conference*, vol. 3, pp. 1634–1638 vol.3, May 1997.
- [10] H. Ochiai and H. Imai, "Performance analysis of deliberately clipped OFDM signals," *IEEE Transactions on Communications*, vol. 50, pp. 89–101, Jan. 2002.
- [11] D. Wulich, "Reduction of peak to mean ratio of multicarrier modulation using cyclic coding," *Electronics Letters*, vol. 32, no. 5, 1996.
- [12] S. Fragiaco, C. Matrakidis, and J. J. O'Reilly, "Multicarrier transmission peak-to-average power reduction using simple block code," *Electronics Letters*, vol. 34, no. 10, pp. 953–954, 1998.
- [13] J. Cimini, L. J. and N. R. Sollenberger, "Peak-to-average power ratio reduction of an ofdm signal using partial transmit sequences," in *Proc. IEEE Int. Conf. Communications ICC '99*, vol. 1, pp. 511–515, 1999.
- [14] S. H. Muller and J. B. Huber, "Ofdm with reduced peak-to-average power ratio by optimum combination of partial transmit sequences," *Electronics Letters*, vol. 33, no. 5, pp. 368–369, 1997.
- [15] R. Baxley and G. Zhou, "Comparing selected mapping and partial transmit sequence for par reduction," *IEEE Transactions on Broadcasting*, vol. 53, pp. 797–803, Dec 2007.
- [16] S.-J. Heo, H.-S. Noh, J. seon No, and D.-J. Shin, "A modified slm scheme with low complexity for papr reduction of ofdm systems," *IEEE 18th International Symposium on Personal, Indoor and Mobile Radio Communications, PIMRC 2007*, pp. 1–5, Sept 2007.
- [17] B. S. Krongold and D. L. Jones, "Par reduction in ofdm via active constellation extension," in *Proc. IEEE Int. Conf. Acoustics, Speech, and Signal Processing (ICASSP '03)*, vol. 4, 2003.
- [18] H. Yang, "A road to future broadband wireless access: Mimo-ofdm-based air interface," *IEEE Communications Magazine*, vol. 43, no. 1, pp. 53–60, 2005.
- [19] E. Dahlman, S. Parkvall, and J. Skld, *4G LTE/LTE-Advanced for Mobile Broadband*. Elsevier Ltd, 2011.

- [20] S. Shukla, S. Shukla, and N. Purohit, "PAPR reduction in SC-FDMA using NCT technique," *Procedia Technology*, vol. 10, no. 0, pp. 927 – 934, 2013. First International Conference on Computational Intelligence: Modeling Techniques and Applications (CIMTA) 2013.
- [21] A. Mohammad, F. Newagy, and A. E. haleem Zekry, "Influence of Utilizing the Selective Mapping Technique for PAPR Reduction in SC-FDMA Systems," *International Journal of Computer Applications*, vol. 48, pp. 11–14, June 2012. Published by Foundation of Computer Science, New York, USA.
- [22] C. Azurdia-Meza, K. Lee, and K. Lee, "PAPR reduction in SC-FDMA by pulse shaping using parametric linear combination pulses," *IEEE Communications Letters*, vol. 16, pp. 2008–2011, December 2012.
- [23] "IEEE standard for information technology–telecommunications and information exchange between systems local and metropolitan area networks–specific requirements part 11: Wireless LAN medium access control (MAC) and physical layer (PHY) specifications," 2012.
- [24] T. Jiang and Y. Wu, "An overview: Peak-to-average power ratio reduction techniques for ofdm signals," *IEEE Transactions on Broadcasting*, vol. 54, no. 2, pp. 257–268, 2008.
- [25] R. Van Nee and A. de Wild, "Reducing the peak-to-average power ratio of OFDM," in *48th IEEE Vehicular Technology Conference, 1998. VTC 98.*, vol. 3, pp. 2072–2076 vol.3, May 1998.
- [26] R. O'Neill and L. B. Lopes, "Envelope variations and spectral splatter in clipped multicarrier signals," in *'Wireless: Merging onto the Information Superhighway', Sixth IEEE International Symposium on Personal, Indoor and Mobile Radio Communications*, vol. 1, pp. 71 –75, Sept. 1995.
- [27] H. Ochiai and H. Imai, "On clipping for peak power reduction of ofdm signals," in *IEEE Global Telecommunications Conference*, vol. 2, pp. 731 –735, 2000.
- [28] J. Armstrong, "New ofdm peak-to-average power reduction scheme," in *IEEE 53rd Vehicular Technology Conference*, vol. 1, pp. 756 –760, 2001.
- [29] J. Urban and R. Marsalek, "OFDM PAPR reduction by combination of Interleaving with Repeated clipping and filtering," in *Proc.14th Int. Workshop Multimedia*

Communications and Services Systems, Signals and Image Processing and 6th EURASIP Conf. focused Speech and Image Processing, pp. 249–252, 2007.

- [30] H. Ochiai and H. Imai, “Performance of the deliberate clipping with adaptive symbol selection for strictly band-limited ofdm systems,” *IEEE Journal on Selected Areas in Communications*, vol. 18, pp. 2270–2277, Nov 2000.
- [31] J. Urban and R. Marsalek, “Ofdm papr reduction by partial transmit sequences and simplified clipping with bounded distortion,” in *Proc. 18th Int Radioelektronika Conf*, pp. 1–4, 2008.
- [32] M. A. Taher, J. Mandeep, M. Ismail, S. A. Samad, and M. Islam, “Reducing the power envelope fluctuation of ofdm systems using side information supported amplitude clipping approach,” *International Journal of Circuit Theory and Applications*, 2013.
- [33] X. Wang, T. T. Tjhung, and C. S. Ng, “Reduction of peak-to-average power ratio of OFDM system using a companding technique,” *IEEE Transactions on Broadcasting*, vol. 45, no. 3, pp. 303–307, 1999.
- [34] T. Jiang, Y. Yang, and Y. hua Song, “Exponential companding technique for papr reduction in ofdm systems,” *Broadcasting, IEEE Transactions on*, vol. 51, pp. 244–248, June 2005.
- [35] Y. Wang, J. Ge, L. Wang, and J. Li, “Reduction of papr of ofdm signals using nonlinear companding transform,” *Wireless Personal Communications*, vol. 71, no. 1, pp. 383–397, 2013.
- [36] A. E. Jones, T. A. Wilkinson, and S. K. Barton, “Block coding scheme for reduction of peak to mean envelope power ratio of multicarrier transmission schemes,” *Electronics Letters*, vol. 30, no. 25, pp. 2098–2099, 1994.
- [37] C. Tellambura, “Multicarrier transmission peak-to-average power reduction using simple block code,” *Electronics Letters*, vol. 34, no. 17, 1998.
- [38] Y. Zhang, A. Yongacoglu, J.-Y. Chouinard, and L. Zhang, “Ofdm peak power reduction by sub-block-coding and its extended versions,” in *Proc. IEEE 49th Vehicular Technology Conf*, vol. 1, pp. 695–699, 1999.

- [39] M. Tan, J. Cheng, and Y. Bar-Ness, "OFDM peak power reduction by a novel coding scheme with threshold control," in *IEEE VTS 54th Vehicular Technology Conference, VTC 2001 Fall.*, vol. 2, pp. 669–672 vol.2, 2001.
- [40] S. H. Han and J. H. Lee, "An overview of peak-to-average power ratio reduction techniques for multicarrier transmission," *IEEE Wireless Communications*, vol. 12, pp. 56–65, April 2005.
- [41] S. H. Muller and J. B. Huber, "A novel peak power reduction scheme for ofdm," in *Proc. 8th IEEE Int Personal, Indoor and Mobile Radio Communications 'Waves of the Year 2000'. PIMRC '97. Symp*, vol. 3, pp. 1090–1094, 1997.
- [42] A. Ghassemi and T. Gulliver, "A Low-Complexity PTS-Based Radix FFT Method for PAPR Reduction in OFDM Systems," *IEEE Transactions on Signal Processing*, vol. 56, pp. 1161–1166, March 2008.
- [43] D. Kumar, P. Singh, and J. Singh, "Article: Complexity reduction in pts based ofdm system: A survey," *International Journal of Computer Applications*, vol. 69, pp. 10–14, May 2013. Published by Foundation of Computer Science, New York, USA.
- [44] R. W. Bauml, R. F. H. Fischer, and J. B. Huber, "Reducing the peak-to-average power ratio of multicarrier modulation by selected mapping," *Electronics Letters*, vol. 32, no. 22, pp. 2056–2057, 1996.
- [45] S. H. Muller and J. B. Huber, "A comparison of peak power reduction schemes for ofdm," in *Proc. IEEE Global Telecommunications Conf. GLOBECOM '97*, vol. 1, pp. 1–5, 1997.
- [46] M. Breiling, S. Muller-Weinfurtner, and J. Huber, "Slm peak-power reduction without explicit side information," *IEEE Communications Letters*, vol. 5, pp. 239–241, June 2001.
- [47] C.-L. Wang and Y. Ouyang, "Low-complexity selected mapping schemes for peak-to-average power ratio reduction in ofdm systems," *IEEE Transactions on Signal Processing*, vol. 53, pp. 4652–4660, Dec 2005.
- [48] L. Yang, K. Soo, Y. Siu, and S. Li, "A low complexity selected mapping scheme by use of time domain sequence superposition technique for PAPR reduction in

- OFDM system,” *IEEE Transactions on Broadcasting*, vol. 54, pp. 821–824, Dec 2008.
- [49] K.-H. Kim, H.-B. Jeon, J.-S. No, and D.-J. Shin, “A new selected mapping scheme for papr reduction in ofdm systems,” in *Proc. Int Information Theory and its Applications (ISITA) Symp*, pp. 1054–1057, 2010.
- [50] D. L. Jones, “Peak power reduction in ofdm and dmt via active channel modification,” in *Proc. Conf Signals, Systems, and Computers Record of the Thirty-Third Asilomar Conf*, vol. 2, pp. 1076–1079, 1999.
- [51] A. D. S. Jayalath and C. Tellambura, “The use of interleaving to reduce the peak-to-average power ratio of an OFDM signal,” in *IEEE Global Telecommunications Conference, 2000. GLOBECOM '00.*, vol. 1, pp. 82–86 vol.1, 2000.
- [52] D. Chase, “Code combining—a maximum-likelihood decoding approach for combining an arbitrary number of noisy packets,” *IEEE Transactions on Communications*, vol. 33, pp. 385–393, May 1985.
- [53] H. E. Rowe, “Memoryless nonlinearities with gaussian inputs: Elementary results,” *The Bell System technical Journal*, vol. 61, Sept. 1982.
- [54] H. Saeedi, M. Sharif, and F. Marvasti, “Clipping noise cancellation in OFDM systems using oversampled signal reconstruction,” *IEEE Communications Letters*, vol. 6, pp. 73–75, Feb 2002.
- [55] H. Chen and A. Haimovich, “An iterative method to restore the performance of clipped and filtered OFDM signals,” in *IEEE International Conference on Communications*, vol. 5, pp. 3438 – 3442, May 2003.
- [56] D. Kim and G. L. Stuber, “Clipping noise mitigation for ofdm by decision aided reconstruction,” *IEEE Communications Letters*, vol. 3, pp. 4–6, 1999.
- [57] N. Bibi and B. Cheetham, “Clipping noise mitigating iterative receivers for OFDM,” in *IEEE International Conference on Networked Embedded Systems for Every Application (NESEA)*, pp. 1–5, 2012.
- [58] D. Dardari, V. Tralli, and A. Vaccari, “A theoretical characterization of nonlinear distortion effects in ofdm systems,” *IEEE Transactions on Communications*, vol. 48, pp. 1755–1764, Oct 2000.

- [59] M. C. Romain D'ejardin and G. Gell'e, "Comparison of iterative receivers mitigating the clipping noise of OFDM based systems," *European Wireless Conference*, 2007.
- [60] M. C. Guillaume Gelle and D. Declercq, "Turbo decision aided reconstruction of clipping noise in coded ofdm," in *IEEE 5th Workshop on Signal Processing Advances in Wireless Communications*, pp. 591–595, July 2004.
- [61] G. G. Maxime Colas and D. Declercq, "Turbo decision aided receivers for clipping noise mitigation in coded ofdm," *EURASIP Journal on Wireless Communications and Networking*, vol. volume 2008, p. 10, 2008.
- [62] N. Bibi, A. Kleerekoper, B. Cheetham, and N. Filer, "Equation-Method for Reducing the Bit-Errors Caused by Clipping Distortion in OFDM Signals," in *2013 European Modelling Symposium (EMS)*, pp. 652–656, Nov 2013.
- [63] R. Penrose, "On best approximate solutions of linear matrix equations," in *Proceedings of the Cambridge Philosophical Society*, vol. 52, pp. 17–19, Cambridge Univ Press, 1956.
- [64] K. Bae, J. G. Andrews, and E. J. Powers, "Adaptive active constellation extension algorithm for peak-to-average ratio reduction in OFDM," *IEEE Communications Letters*, vol. 14, no. 1, pp. 39–41, 2010.
- [65] M. Hossain and M. Mondal, "Effectiveness of selection and maximal ratio combining diversity techniques on a ds-cdma wireless communication system impaired by fading," in *12th International Conference on Computers and Information Technology, 2009. ICCIT '09.*, pp. 115–120, Dec 2009.
- [66] F. Tosato and P. Bisaglia, "Simplified soft-output demapper for binary interleaved cofdm with application to hiperlan/2," in *IEEE International Conference on Communications, ICC 2002.*, vol. 2, pp. 664–668 vol.2, 2002.
- [67] S. Allpress, C. Luschi, and S. Felix, "Exact and approximated expressions of the log-likelihood ratio for 16-qam signals," in *Conference Record of the Thirty-Eighth Asilomar Conference on Signals, Systems and Computers, 2004.*, vol. 1, pp. 794–798 Vol.1, Nov 2004.
- [68] R. H. Barker, "Group synchronizing of binary digital sequences," *Communication Theory*, pp. 273–287, 1953.

- [69] R. Ullah and S. Latif, “Improving the security level in direct sequence spread spectrum using dual codes (DC-DSSS),” *International Journal of Security and Its Applications*, vol. 6, no. 2, pp. 133–136, 2012.
- [70] J. Minkoff, “The role of AM-to-PM conversion in memoryless nonlinear systems,” *IEEE Transactions on Communications*, vol. 33, pp. 139–144, Feb 1985.

Appendix A

Deriving non-linear distortion factor Alpha for limiting

A.1 Introduction

This appendix explains the derivation of non-linear distortion factor α for soft clipping and IWRAP limiting, using Bussgang theorem.

A.1.1 Alpha for Clipping

Taking Equation 3.13 for α from Chapter 3, Section 3.1.3:

$$\alpha = \frac{E \{x_c(n)x(n)\}}{E \{x(n)x(n)\}} \quad (\text{A.1})$$

Auto-correlation of a signal at zero gives average power of the signal. Equation A.1 may be written as:

$$\alpha = \frac{E \{x_c(n)x(n)\}}{\sigma^2} \quad (\text{A.2})$$

The non-linearity is applied to the envelope characteristics of the signal, therefore, as shown in [70], the distortion factor α can also be calculated using the envelope characteristics as:

$$\alpha = \frac{E \{z(n)f(z(n))\}}{\sigma^2} \quad (\text{A.3})$$

where $z(n)$ is the amplitude of the complex OFDM signal $x(n)$, $f(z(n))$ is the non-linearity applied to the $z(n)$. $f(z(n))$ could be written as follows:

$$f(z(n)) = \begin{cases} z(n), & \text{if } 0 \leq z(n) < A \\ A, & A \leq z(n) < \infty \end{cases} \quad (\text{A.4})$$

According to central limit theorem, the OFDM signal may be considered Gaussian for large number of subcarriers. Hence the amplitude values of the signal follow a Rayleigh distribution. The probability density function (Pdf) of an OFDM symbol is:

$$P(z) = \frac{2z}{\sigma^2} e^{-\frac{z^2}{\sigma^2}} \quad (\text{A.5})$$

From equation A.3, the expectation could be written as

$$\frac{E\{z(n)f(z(n))\}}{\sigma^2} = \frac{1}{\sigma^2} \int_0^\infty zf(z)P(z)dz \quad (\text{A.6})$$

$$= \frac{1}{\sigma^2} \left(\int_0^A zf(z)P(z)dz + \int_A^\infty zf(z)P(z)dz \right) \quad (\text{A.7})$$

solving equation A.7, taking first part

$$= \int_0^A zf(z)P(z)dz \quad (\text{A.8})$$

Putting in $f(z)$ and $P(z)$ into the equation from A.4 and A.5

$$= \int_0^A z \frac{2z}{\sigma^2} e^{-\frac{z^2}{\sigma^2}} dz \quad (\text{A.9})$$

$$= \int_0^A \frac{z^2}{\sigma^2} e^{-\frac{z^2}{\sigma^2}} 2z dz \quad (\text{A.10})$$

evaluating integral

$$\text{suppose, } t = \frac{-z^2}{\sigma^2} \quad (\text{A.11})$$

$$dt = \frac{-2z}{\sigma^2} dz \quad (\text{A.12})$$

$$-\sigma^2 dt = 2z dz \quad (\text{A.13})$$

$$= \sigma^2 \int_0^A t e^t dt \quad (\text{A.14})$$

Evaluating integral by parts now

$$u = t, v = e^t \quad (\text{A.15})$$

$$du = 1 \cdot dt, dv = e^t \cdot dt \quad (\text{A.16})$$

$$uv - \int v du \quad (\text{A.17})$$

$$= \left(t \cdot e^t - \int e^t dt \right) \quad (\text{A.18})$$

$$= (t \cdot e^t - e^t) \quad (\text{A.19})$$

$$= e^t (t - 1)$$

putting this evaluation back in to A.14

$$\int_0^A z f(z) P(z) dz = [\sigma^2 e^t (t - 1)]_0^A \quad (\text{A.20})$$

$$= \left[\sigma^2 e^{-\frac{z^2}{\sigma^2}} \left(-\frac{z^2}{\sigma^2} - 1 \right) \right]_0^A \quad (\text{A.21})$$

$$= \left[-e^{-\frac{z^2}{\sigma^2}} (z^2 + \sigma^2) \right]_0^A \quad (\text{A.22})$$

$$\int_0^A z f(z) P(z) dz = -e^{-\frac{A^2}{\sigma^2}} (A^2 + \sigma^2) + \sigma^2 \quad (\text{A.23})$$

Solving the second part from A.7

$$\int_A^\infty z f(z) P(z) dz = \int_A^\infty z \cdot A \cdot \frac{2z}{\sigma^2} e^{-\frac{z^2}{\sigma^2}} dz \quad (\text{A.24})$$

$$= 2A \int_A^\infty \frac{z^2}{\sigma^2} e^{-\frac{z^2}{\sigma^2}} dz \quad (\text{A.25})$$

$$t^2 = \frac{z^2}{\sigma^2} \quad (\text{A.26})$$

$$t = \frac{z}{\sigma} \quad (\text{A.27})$$

$$\sigma dt = dz \quad (\text{A.28})$$

$$= 2A\sigma \int_A^\infty t^2 e^{-t^2} dt \quad (\text{A.29})$$

evaluating the integral by parts

$$u = t, v = \int e^{-t^2} t \cdot dt \quad (\text{A.30})$$

$$du = 1 \cdot dt, dv = e^{-t^2} t \cdot dt \quad (\text{A.31})$$

$$uv - \int v du \quad (\text{A.32})$$

$$t \int e^{-t^2} t \cdot dt - \int \int e^{-t^2} t \cdot dt \cdot dt \quad (\text{A.33})$$

solving integral

$$\int t \cdot e^{-t^2} dt = -\frac{1}{2} e^{-t^2} \quad (\text{A.34})$$

using Equation A.34 in A.33 gives

$$= -t \frac{1}{2} e^{-t^2} + \int \frac{1}{2} e^{-t^2} dt \quad (\text{A.35})$$

Substituting the solution back to the equation A.29,

$$= 2A\sigma \left(\left[-t \frac{1}{2} e^{-t^2} \right]_A^\infty + \frac{1}{2} \int_A^\infty e^{-t^2} dt \right) \quad (\text{A.36})$$

Using the definition of error function

$$erfc(x) = \frac{2}{\sqrt{\pi}} \int_x^\infty e^{-t^2} dt \quad (\text{A.37})$$

Using Equation A.37 in Equation A.36

$$= 2A\sigma \left(\left[-\frac{t}{2} e^{-t^2} \right]_A^\infty + \frac{\sqrt{\pi}}{4} erfc(t) \right) \quad (\text{A.38})$$

Replacing variables back and putting limits

$$= 2A\sigma \left(\left[-\frac{z}{2\sigma} e^{-\frac{z^2}{\sigma^2}} \right]_A^\infty + \frac{\sqrt{\pi}}{4} \operatorname{erfc}\left(\frac{A}{\sigma}\right) \right) = A^2 e^{-\frac{A^2}{\sigma^2}} + A\sigma \frac{\sqrt{\pi}}{2} \operatorname{erfc}\left(\frac{A}{\sigma}\right) \quad (\text{A.39})$$

Using Equation A.23 and Equation A.39 in Equation A.7

$$\alpha = \frac{1}{\sigma^2} \left(-e^{-\frac{A^2}{\sigma^2}} (A^2 + \sigma^2) + \sigma^2 + A^2 e^{-\frac{A^2}{\sigma^2}} + A\sigma \frac{\sqrt{\pi}}{2} \operatorname{erfc}\left(\frac{A}{\sigma}\right) \right) \quad (\text{A.40})$$

$$= 1 - e^{-\frac{A^2}{\sigma^2}} + \frac{\sqrt{\pi}}{2} \operatorname{erfc}\left(\frac{A}{\sigma}\right) \frac{A}{\sigma} \quad (\text{A.41})$$

As clipping ratio $\gamma = A/\sigma$

$$\alpha = 1 - e^{-\gamma^2} + \frac{\sqrt{\pi}}{2} \operatorname{erfc}(\gamma) \gamma \quad (\text{A.42})$$

Equation A.42 shows the distortion factor for clipping.

A.1.2 Alpha for IWRAP Limiting

The limiting function $f(z(n))$ for IWRAP could be written as follows:

$$f(z(n)) = \begin{cases} z, & \text{if } 0 \leq z < A \\ 2A - z, & A \leq z < \infty \end{cases} \quad (\text{A.43})$$

Using the Equations A.3 and A.43, calculation of α for IWRAP is as follows:

$$\alpha = \frac{E \{z(n)f(z(n))\}}{\sigma^2} = \frac{1}{\sigma^2} \left(\int_0^A z f(z) P(z) dz + \int_A^\infty z f(z) P(z) dz \right) \quad (\text{A.44})$$

Pdf of the OFDM signal is the same as in Equation A.5. As $f(z)$ is the same for first part, so the integral evaluation will be taken from Equation A.23

$$\int_0^A z f(z) P(z) dz = -e^{-\frac{A^2}{\sigma^2}} (A^2 + \sigma^2) + \sigma^2 \quad (\text{A.45})$$

Now taking second part from Equation A.44

$$\int_A^\infty z f(z) P(z) dz = \int_A^\infty z (2A - z) \frac{2z}{\sigma^2} e^{-\frac{z^2}{\sigma^2}} dz \quad (\text{A.46})$$

$$= \int_A^\infty 2Az \frac{2z}{\sigma^2} e^{\frac{-z^2}{\sigma^2}} dz - \int_A^\infty z^2 \frac{2z}{\sigma^2} e^{\frac{-z^2}{\sigma^2}} dz \quad (\text{A.47})$$

Evaluating Equation A.47 gives

$$= 2A^2 e^{\frac{-A^2}{\sigma^2}} + A\sigma\sqrt{\pi}\text{erfc}\left(\frac{A}{\sigma}\right) - e^{\frac{-A^2}{\sigma^2}} (A^2 + \sigma^2) \quad (\text{A.48})$$

Using Equation A.45 and Equation A.48 in Equation A.44

$$\alpha = \frac{1}{\sigma^2} \left(-e^{\frac{-A^2}{\sigma^2}} (A^2 + \sigma^2) + \sigma^2 + 2A^2 e^{\frac{-A^2}{\sigma^2}} + A\sigma\sqrt{\pi}\text{erfc}\left(\frac{A}{\sigma}\right) - e^{\frac{-A^2}{\sigma^2}} (A^2 + \sigma^2) \right) \quad (\text{A.49})$$

$$\alpha = 1 - 2e^{\frac{-A^2}{\sigma^2}} + \frac{A}{\sigma}\sqrt{\pi}\text{erfc}\left(\frac{A}{\sigma}\right) \quad (\text{A.50})$$

Using $\gamma = A/\sigma$,

$$\alpha = 1 - 2e^{-\gamma^2} + \gamma\sqrt{\pi}\text{erfc}(\gamma) \quad (\text{A.51})$$

Equation A.51 is the distortion factor for IWrap.

Appendix B

Calculating output power of IWRAP limiter

Taking Equation A.5 and Equation A.43, the output power of the IWRAP limiter can be expressed as:

$$P_{limit} = E \{x^2(n)\} = \int_0^{\infty} x^2(n) P(x) dx \quad (B.1)$$

$$\int_0^A x^2 \frac{2x}{\sigma^2} e^{-\frac{x^2}{\sigma^2}} dx + \int_A^{\infty} (2A - x) \frac{2x}{\sigma^2} e^{-\frac{x^2}{\sigma^2}} dx \quad (B.2)$$

Evaluating the first term of the above equations gives:

$$\int_0^A x^2 \frac{2x}{\sigma^2} e^{-\frac{x^2}{\sigma^2}} dx = -e^{-\frac{A^2}{\sigma^2}} (A^2 + \sigma^2) + \sigma^2 \quad (B.3)$$

Now taking the second term of the Equation B.2 gives:

$$\int_A^{\infty} (2A - x)^2 \frac{2x}{\sigma^2} e^{-\frac{x^2}{\sigma^2}} dx = \int_A^{\infty} (4A^2 - 4Ax + x^2) \frac{2x}{\sigma^2} e^{-\frac{x^2}{\sigma^2}} dx \quad (B.4)$$

$$\int_A^{\infty} (2A - x)^2 \frac{2x}{\sigma^2} e^{-\frac{x^2}{\sigma^2}} dx = \int_A^{\infty} (4A^2 - 4Ax + x^2) \frac{2x}{\sigma^2} e^{-\frac{x^2}{\sigma^2}} dx \quad (B.5)$$

$$= e^{-\frac{A^2}{\sigma^2}} (A^2 + \sigma^2) - 2A\sigma\sqrt{\pi} \operatorname{erfc}\left(\frac{A}{\sigma}\right) \quad (B.6)$$

where $erfc$ is the error function as follows:

$$erfc(x) = \frac{2}{\sqrt{\pi}} \int_x^{\infty} e^{-t^2} dt \quad (\text{B.7})$$

Using Equation B.3 and Equation B.6 in Equation B.2

$$P_{limit} = -e^{-\frac{A^2}{\sigma^2}} (A^2 + \sigma^2) + \sigma^2 + e^{-\frac{x^2}{\sigma^2}} (A^2 + \sigma^2) - 2A\sigma\sqrt{\pi}erfc\left(\frac{A}{\sigma}\right) \quad (\text{B.8})$$

$$= \sigma^2 - 2A\sigma\sqrt{\pi}erfc\left(\frac{A}{\sigma}\right) \quad (\text{B.9})$$

$$= \sigma^2 \left(1 - 2\frac{A}{\sigma}\sqrt{\pi}erfc\left(\frac{A}{\sigma}\right) \right) \quad (\text{B.10})$$

$$= \sigma^2 \left(1 - 2\frac{A}{\sigma}\sqrt{\pi}erfc\left(\frac{A}{\sigma}\right) \right) \quad (\text{B.11})$$

where $\gamma = A/\sigma$, and σ^2 is the average power of the input signal.

$$P_{limit} = \sigma^2(1 - 2\gamma\sqrt{\pi}erfc(\gamma)) \quad (\text{B.12})$$